

**Reconstruction of upwelling and productivity in the southern part
of the Peru-Chile Current: A multi parameter approach**

**Dissertation zur Erlangung des Doktorgrades
am Fachbereich Geowissenschaften der Universität Bremen**

vorgelegt von

**Mahyar Mohtadi
Bremen, Februar 2004**

Tag des Kolloquiums:

15.03.2004

Gutachter:

PD. Dr. Dierk Hebbeln
Prof. Dr. Gerhard Bohrmann

Prüfer:

Prof. Dr. Gerold Wefer
PD. Dr. Matthias Zabel

Contents

Abstract	1
Zusammenfassung	3
Chapter 1. Introduction	5
1.1. Motivation and main objectives	5
1.2. Study area	7
1.2.1. Modern oceanography of the Southeast Pacific	7
1.2.2. Atmospheric circulation	8
1.2.3. Regional climate of Chile	9
1.3. Planktic foraminifera as a proxy for oceanic (paleo) environments	11
1.4. Bulk sediment-biogenic compounds as proxy for (paleo) productivity	12
1.4.1. Calcium carbonate (CaCO ₃)	13
1.4.2. Biogenic silica (opal)	13
1.4.3. Organic carbon (C _{org})	14
1.5. Material and methods	15
1.5.1. Samples	15
1.5.2. Methods	15
1.5.2.1. Planktic foraminifera analyses	15
1.5.2.2. Stable oxygen and carbon isotopes	15
1.5.2.3. AMS ¹⁴ C dating	16
1.5.2.4. Bulk sediment analyses	16
1.5.2.5. Siliceous plankton analyses	16
1.6. Overview of own research	17
1.7. References	19
Chapter 2. Publications	28
Manuscript I	28
Upwelling and productivity along the Peru-Chile Current derived from faunal and isotopic compositions of planktic foraminifera in surface sediments	

Manuscript II	52
Changing marine productivity off northern Chile during the last 19,000 years: a multiparameter approach	
Manuscript III	84
Mechanisms and variations of the paleoproductivity off northern Chile (24°S – 33°S) during the last 40,000 years	
Chapter 3. Conclusion and perspectives	112
Conclusion and perspectives	112
References	114
Danksagung	115

Abstract

Surface sediments and sediment cores were investigated with the aim to reconstruct the present and past regional upwelling and productivity variations in the southern part of the Peru-Chile Current (PCC). Several parameters such as organic carbon, calcium carbonate, opal, isotopic and faunal composition of planktic foraminifera, and the siliceous plankton assemblage served as proxies for the production and sedimentation of organic matter.

To assess the present-day productivity pattern, variations in the isotopic and faunal compositions of planktic foraminifera in 91 surface sediment samples were observed. The results revealed a distinct latitudinal segmentation of the hydrological regime off the Chilean coast, i.e., high productivity under upwelling conditions north of 39°S with two centers at 30°S - 33°S and north of 25°S, and highest productivity in a non-upwelling system south of 39°S. It could be shown that the planktic foraminifera species *Globigerina bulloides*, *Neogloboquadrina pachyderma* and *Globigerinita glutinata* can be used as upwelling indicators in this region, whereas *Globorotalia inflata*, and *Neogloboquadrina incompta* are instead associated with high nutrient supply. Also the isotopic compositions of *G. bulloides* and *N. incompta* appear to be reliable proxies for reconstructing upper water column properties in this region.

In order to reconstruct the paleoproductivity during the last 40,000 years, five sediment cores were investigated off central and northern Chile. Geochemical and micropaleontological observations reveal generally higher productivities during the last glacial compared to the Early and Middle Holocene. During the Late Holocene, productivity increased again regardless of the position of the investigated cores. In addition, the observed predominantly southward increase in paleoproductivity, as recorded under present-day conditions, points to the same driving mechanisms of productivity in the last 40,000 years. During the last glacial, however, significant discrepancies can be observed between the record at 33°S and other records further north. Highest productivities at 33°S occurred around the Last Glacial Maximum (LGM, 21,000 ± 1000 yr BP), whereas further north, the productivity was highest before and after the LGM, and decreased slightly during the LGM.

The applied productivity proxies showed that next to latitudinal position and strength of the zonal systems, i.e. the Southern Westerlies and the Antarctic Circumpolar Current (ACC), other processes such as the strength of the South Pacific subtropical gyre, El Niño Southern Oscillation (ENSO) events, and the hemispheric thermal gradient have been strongly affecting the upwelling intensity and paleoproductivity in this region during the last 40,000 years. In

spite of the strong coupling of the above mentioned processes, for paleoclimate reconstructions it is important to quantify the northward migration of the climate zones. It could be distinguished between the regions influenced by the Southern Westerlies south of 33°S, and the areas north of 33°S with no significant fingerprint of the zonal wind system through the last 40,000 years. In addition, other episodic events such as flooding of the shelf during Termination I (18,000 – 10,000 yr BP), as well as humid phases onshore prior to the LGM and during Termination I, may have increased the nutrient supply into the upwelling area north of 33°S resulting in enhanced paleoproductivity.

Zusammenfassung

Um den Verlauf des Küstenauftriebs und der marinen Produktivität im südlichen Teil des Peru-Chile-Stroms (PCC) rekonstruieren zu können, wurden Oberflächensedimente und Sedimentkerne untersucht. Die Produktion und die Sedimentation des organischen Materials wurden anhand von verschiedenen Parametern wie organischem Kohlenstoff, Kalziumkarbonat, Opal, isotopischer und faunischer Zusammensetzung der planktischen Foraminiferen sowie des kieseligen Planktons erforscht.

Um das heutige Verteilungsmuster der Produktivität abzuschätzen, wurden Veränderungen in der isotopischen und der faunischen Zusammensetzung der planktischen Foraminiferen in 91 Sedimentoberflächenproben untersucht. Die Ergebnisse zeigen eine deutliche N-S Segmentierung des hydrologischen Regimes vor der chilenischen Küste, nämlich hohe Produktivitäten unter Auftriebsbedingungen nördlich von 39°S, besonders in den Auftriebszentren zwischen 30°S und 33°S sowie nördlich von 25°S, und höchste Produktivitäten in einer Region ohne Auftrieb südlich von 39°S. Es konnte gezeigt werden, dass die planktischen Foraminiferen *Globigerina bulloides*, *Neogloboquadrina pachyderma* und *Globigerinita glutinata* als Auftriebsindikatoren benutzt werden können, während *Globorotalia inflata* und *Neogloboquadrina incompta* überwiegend mit hohem Nährstoffeintrag assoziiert sind. Es erscheint ferner, dass die isotopische Zusammensetzung von *G. bulloides* und *N. incompta* als ein zuverlässiger Proxy benutzt werden kann, um die Eigenschaften der oberen Wassersäule zu rekonstruieren.

Um die Paläoproduktivität während der letzten 40.000 Jahre zu rekonstruieren, wurden fünf Sedimentkerne vor Zentral- und Nordchile untersucht. Geochemische und mikropaläontologische Untersuchungen lassen generell höhere Produktivitäten während der letzten Kaltzeit im Vergleich zum Frühen und Mittleren Holozän erkennen. Unabhängig von der Position der untersuchten Kerne stieg die Produktivität während des Spätholozäns an. Ferner deutet der kontinuierlich zu beobachtende Anstieg der Produktivität nach Süden, wie er unter heutigen Bedingungen zu verzeichnen ist, auf die gleichen Steuermechanismen der Produktivität während der letzten 40.000 Jahre hin. Während des letzten Glazials sind jedoch signifikante Unterschiede zwischen den Daten von 33°S und anderen Daten weiter nördlich zu beobachten. Höchste Produktion bei 33°S trat während des Letzten Glazialen Maximums (LGM, 21.000 ± 1000 yr BP) auf, wobei weiter nördlich die Produktion vor und nach dem LGM am höchsten war und während des LGM leicht zurückging.

Die angewandten Produktivitätsindikatoren zeigen, dass neben der geographischen Breite und der Strömungsintensität der südlichen Westwinde und des Antarktischen Zirkumpolarstroms (ACC), andere Prozesse wie die Intensität der subtropischen Gyre im Südpazifik, der El Niño Southern Oscillation (ENSO) Ereignisse sowie der hemisphärischen Thermalgradienten, die Auftriebsintensität und Paläoproduktivität in dieser Region während der letzten 40.000 Jahre stark beeinflusst haben. Für die paläoklimatischen Rekonstruktionen ist es trotz der starken Kopplung der oben genannten Prozesse wichtig, die nordwärts gerichtete Migration der Klimazonen zu quantifizieren. Für die letzten 40.000 Jahre konnte zwischen den von den südlichen Westwinden beeinflussten Regionen südlich von 33° und den von diesem zonalen Windsystem nicht wesentlich geprägten Gebieten nördlich von 33°S unterschieden werden. Zusätzlich könnten andere episodische Ereignisse, wie das Fluten der Schelfe während der Termination I (18.000 – 10.000 yr BP) sowie die festländischen Humidphasen in Nordchile vor dem LGM und während der Termination I, die Nährstoffzufuhr in die Auftriebsgebiete und dadurch die Produktivität nördlich von 33°S erhöht haben.

Part 1. Introduction

1.1. Motivation and main objectives

The climate on Earth is strongly coupled with the content of carbon dioxide, one of the most important greenhouse gases in the atmosphere. Measurements of gas bubbles trapped in ice cores indicate that cold and warm periods of the Earth's climate are associated with changes in the CO₂ concentration (Barnola et al., 1987; Jouzel et al., 1996), which varies between ~ 200 ppmV during glacial and ~ 280 ppmV during interglacial periods (Petit et al., 1999).

One of the major sources and sinks for the atmospheric CO₂ is the world's ocean (Broecker and Peng, 1993b; Broecker, 1982). Among other processes, fluctuations in deep-water formation and water stratification are proposed to make a large contribution to changing atmospheric CO₂ concentration (Archer and Johnson, 2000; Moore et al., 2000). This so-called "physical pump" describes the burial of CO₂ to depth by formation of deep-water masses on one hand, and the outgassing of CO₂ by upwelling of cold, CO₂-rich deep-water masses on the other hand (Archer et al., 2000b). Another potential sink is the primary production of phytoplankton in the photic zone, and the export production in the underlying water masses (Broecker and Peng, 1993a). This so-called "biological pump" describes the carbon biologically fixed in the organic matter and exported to the deep sea (Broecker and Henderson, 1998).

Over 50% of marine productivity takes place in only 15% of the global ocean area, namely in the high productivity regions of the equatorial and subpolar divergence zones and of the Eastern Boundary Currents (EBCs, Berger et al., 1989). In addition, these upwelling regions act as sources for the outgassing of CO₂ through the "physical pump". Among other EBCs, the PCC (or Humboldt current) stands out with a strong continuous upwelling regime resulting in a very high biological productivity making the PCC one of the most productive marine environments and an important part of the global carbon cycle (Berger et al., 1987).

Little data performed on marine sediments exist from the southern part of the PCC between 22 °S and 45°S. Recent paleoclimatic and paleoceanographic studies based on terrigenous sediment and continental rainfall reconstructions (Lamy et al., 1998a; 1999; 2001), paleotemperature reconstructions (Kim et al., 2002), and paleoproductivity derived from biogenic barium (Klump et al., 2001), and from planktic foraminifera and geochemical compounds (Marchant et al., 1999; Hebbeln et al., 2002) have shown significant variations during the last 33,000 years. Periods of high marine productivity seem to be associated with lower temperatures and higher continental rainfall suggesting a strong connection between

oceanographic and atmospheric processes off central and south Chile. Latitudinal shifts in the position of the Southern Westerlies, as the main onshore precipitation source, in line with the migration of the ACC as the main macronutrient source, have been proposed to drive the paleoproductivity variations off central and south Chile (Lamy et al., 1998a; 1999; Marchant et al., 1999; Hebbeln et al., 2002). However, all these data are obtained from only three sediment cores located at 27.5°S, 33°S and 41°S. To date, the limited downcore paleoceanographic data in general, and off north Chile between 22° and 33°S in particular, hamper paleoceanographic and paleoclimatic reconstructions on a regional scale.

Numerous continental paleoclimate reconstructions based on different proxies exist for northern Chile and subtropical South America (e.g. Heusser, 1990; Grosjean, 1994; 2001; Grosjean et al., 1995; 1997; Thompson et al., 1995; Ammann et al., 2001; Jenny et al., 2002; Latorre et al., 2002; 2003; Abbott et al., 2003). Results from these studies indicate that beside the southern westerlies, additional phenomena, e.g. extra-tropical cyclones, ENSO events, and the South Atlantic convergence zone affect the humidity in this region. However, the continental paleoclimate reconstructions for the LGM and the Early and Middle Holocene are controversial (Grosjean et al., 2003 and references therein). In addition, results from a number of studies do not support the hypothesis of a glacial – interglacial latitudinal migration of the Southern Westerlies (e.g. Fox and Strecker, 1991; Veit, 1992; 1996; Ammann et al., 2001; Grosjean et al., 2001).

One goal of this thesis is to generate a better understanding of the present-day driving mechanisms and spatial distribution patterns of productivity in this region by investigating surface sediments from different water depths and latitudes. To address this issue, investigations on the faunal and isotopic composition of planktic foraminifera were carried out. The obtained information should reveal the response of the marine productivity to different hydrographic regimes in this region as well as to the onshore latitudinal precipitation gradient. Previous studies on surface sediments are based on other proxies (Romero and Hebbeln, 2003), or do not cover some oceanographically important areas due to uneven distribution of the available samples (Ingle et al., 1980; Hebbeln et al., 2000a; Romero et al., 2001; Feldberg and Mix, 2002). The results reported here together with other studies can serve as a baseline data set for the paleoclimatic and paleoceanographic reconstructions along the Chilean continental margin.

Another objective of this thesis is the assessment of the productivity variation in this part of the world's ocean through the late Quaternary glacial-interglacial cycles, especially by comparing LGM and Holocene conditions. The main topics to be addressed by using a multi-

parameter investigation are: a) a large-scale estimation of the paleoproductivity during the last glacial and the Holocene; b) the related paleoceanographic and paleoclimatic conditions; c) a better understanding of the response and the correlation of different proxies; and d) the link between the marine and terrestrial climate allowing a better comparison between marine and continental time series.

1.2. Study area

The study area extends along the Chilean continental slope and adjacent areas between 24°S and 44°S (Fig. 1-1). Within this area, significant latitudinal changes occur in the continental climate and in the hydrographic and atmospheric circulations.

1.2.1. Modern oceanography of the Southeast Pacific

The PCC mainly controls the oceanic circulation in the SE Pacific. It is the largest eastern boundary current in the world, with an extension of more than 40° of latitude making the eastern portion of the southern Pacific subtropical gyre (Fig. 1-1). It originates between 40°S and 45°S, where the west wind drift transports the cold surface waters of the ACC eastward. After approaching the South American continent, the ACC deflects into the northward flowing PCC and the southward flowing Cape Horn Current (Strub et al., 1998). The PCC flows with a velocity of $\sim 2 \text{ cm s}^{-1}$ between 0 and 100 m depth (Shaffer et al., 1995), with an average transport of 15 – 20 Sv ($1 \text{ Sv} = 10^6 \text{ m}^3 \text{ s}^{-1}$) (Wooster and Reid, 1963). At $\sim 5^\circ\text{S}$, it is deflected away from the coast and becomes part of the westward flowing South Equatorial Current (SEC, Strub et al., 1998).

Inshore of the PCC and near the shelf break $\sim 200 \text{ km}$ offshore, the low-latitude surface waters of the Peru-Chile Counter Current (PCCC) flow poleward. This water mass transports relatively warm waters southwards and separates the PCC from its coastal branch, the Peru-Chile Coastal Current ($\text{PCC}_{\text{coast}}$), a minor current transporting cold, nutrient-rich waters upwelled along the Chilean coast northward. The $\text{PCC}_{\text{coast}}$ extends up to 100 km off the coast and is influenced by the low-salinity waters of the South Chilean fjord region (Strub et al., 1998).

Beneath these surface water masses between 100 and 400 m depth, the poleward flowing Gunther Undercurrent (GUC) is located, with a velocity of max. 25 cm s^{-1} (Johnson et al., 1980). Subsurface waters from the SW Pacific flow northeastward, transit in the lower part of the eastward flowing Equatorial Undercurrent (EUC), and initiate the GUC when they flow

again southward along the South American continent (Toggweiler et al., 1991). The GUC originates near the Galapagos Islands and is characterized by high salinities and low dissolved oxygen (Strub et al., 1998). Between 400 and 1200 m depth, the Antarctic Intermediate Water (AAIW) flows equatorward, underlain by sluggish southward flowing Pacific Deep Water (PDW, Shaffer et al., 1995; Strub et al., 1998). The deepest parts of the Peru-Chile trench are filled with equatorward flowing Antarctic Bottom Water (Ingle et al., 1980).

Close to the coast, cold (11° - 14° C) waters of the GUC are brought to the surface by upwelling. Coastal upwelling is driven by persistent southeastern winds resulting in offshore Ekman flow of the surface waters and consequent upward flow of the subsurface waters (Shaffer et al., 1995), and is generally limited to within 50 – 60 km of the shoreline (Strub et al., 1998). Coastal upwelling results in cold Sea Surface Temperatures (SSTs) along the Chilean coast and high productivity in this region. Five main upwelling cells are presently observed off central and northern Chile, at 23° , 27° , 30° , 33° and 35° - 38° S (Strub et al., 1998). The position of these upwelling cells is determined by the topography and hence, they do not move along the coast with changes of the wind field.

1.2.2 Atmospheric circulation

Three main features dominate the atmospheric circulation and the precipitation regime in the study area.

1. The area of intense summer convection, known as the “Bolivian High” producing summer precipitation in the Andes north of 27° S (Lenters and Cook, 1999). Moisture brought onto the continent from the Atlantic by the Tropical Easterlies produces summer precipitation in the tropics and subtropics of South America (Fig. 1-2). The amount of moisture that reaches the crest of the Andes and the western edge of the Altiplano appears to be related to the strength of the Southern Westerlies: when Westerlies are strong, moist air from the east fails to reach the Andean crest (Aravena et al., 1999; Garreaud, 1999).
2. The Southeast Pacific anticyclone off central and northern Chile producing seasonal upwelling-favorable winds along the coast, and dry conditions onshore (Aceituno and Monticinos, 1993).
3. The Southern Westerlies south of 38° S producing downwelling and high winter precipitations onshore (Miller, 1976; Strub et al., 1998).

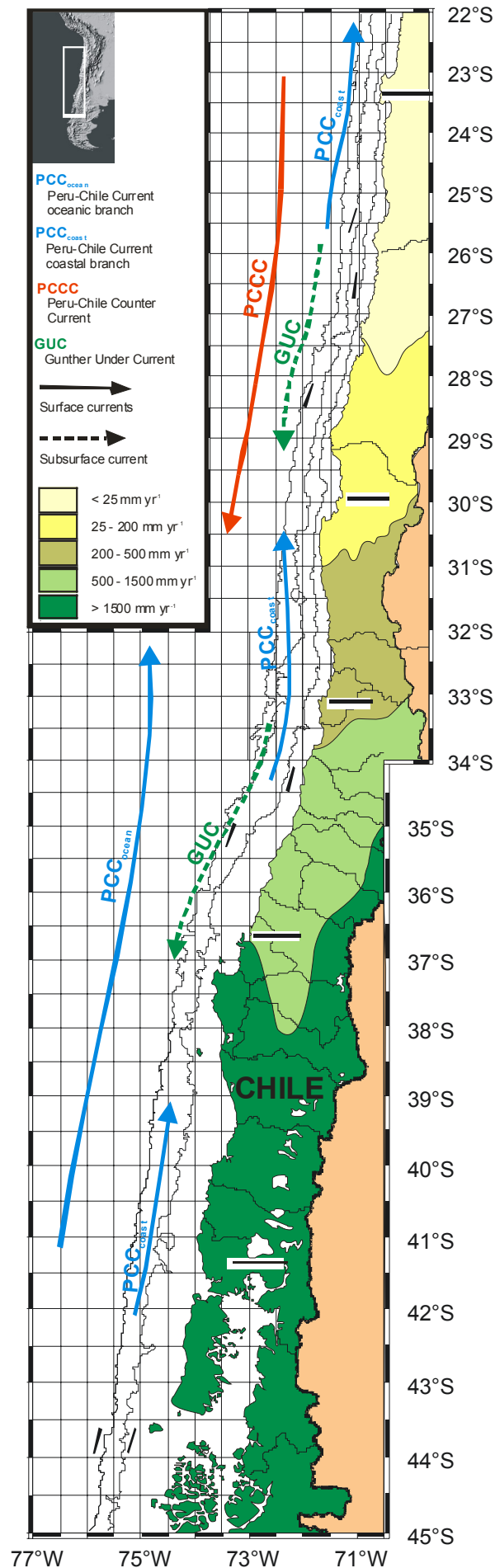


Fig. 1-1 Schematic map of the study area with the present-day main oceanographic features after Strub et al. (1998), and the climate zonation of Chile after Veit (1996) and Weischet (1996).

Precipitation in central and southern Chile is strongly related to the Westerly circulation belt (Aceituno, 1988). The Westerlies intensify when the Southeast Pacific high-pressure cell is weakened, or the hemispheric thermal gradient increases (Fig. 1-2). Under such conditions, more frontal systems of the Southern Westerlies reach further north resulting in an increased precipitation in central Chile between 32°S and 35°S. Also, during warm phases of ENSO when the Hadley cell is weakened and abnormally warm conditions prevail in the equatorial Pacific, the South Pacific high-pressure cell weakens and a positive rainfall anomaly can be observed in central Chile between 30°S and 35°S (Montecinos et al., 2000).

1.2.3 Regional climate of Chile

The climate of Chile shows a strong meridional segmentation. North of 27°S, the Atacama Desert with precipitation values below 50 mm yr⁻¹ stands for one of the driest regions worldwide (Fig. 1-1, 1-2). One of the reasons for the existence of such hyper-arid conditions is the coastal upwelling, which causes fog to precipitate above the coastal waters and thus removes

moisture from the air (Miller, 1976). Perennial rivers are absent, with only episodic flash-floods occurring during ENSO events (Garleff et al., 1991; Rutland and Fuenzalida, 1991).

In the arid region between 27°S and 31°S, the winter precipitation which is brought by the fronts of the Westerlies increases southward to max. 200 mm yr⁻¹. The precipitation promotes vegetation cover and soil development and sustains relict forests in this region (Aravena et al., 1989). Generally, the sediments derived from the Andes do not reach the ocean. Central Chile between 31°S and 37°S is characterized by a semi-arid Mediterranean climate and winter precipitation up to 1000 mm yr⁻¹ brought by the Southern Westerlies. Precipitation is higher in the Andes than in the Coastal Range, sufficient to evolve a perennial river system, and increases southward (Miller, 1976). South of 37°S, the humid climate is affected by the Southern Westerlies year-round, with precipitations >1500 mm yr⁻¹ and evergreen parkland vegetations (Miller, 1976; Heusser, 1983).

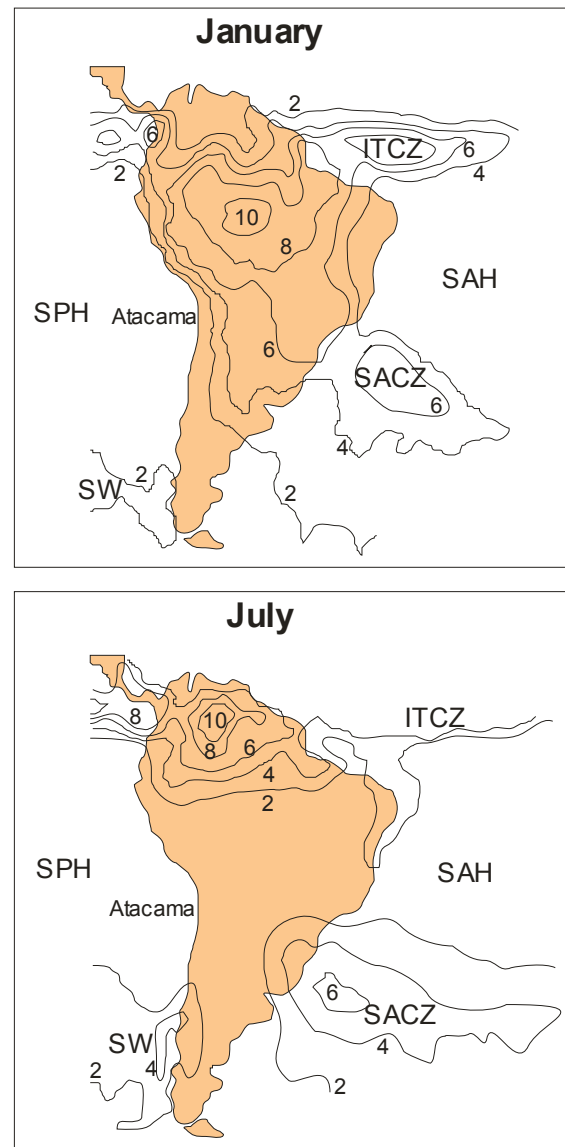


Fig. 1-2 The satellite derived data of a 20-year average (1979 – 1998) precipitation field (PSG CLIM) for South America for January and July. Contours are in mm per day. ITCZ: Inter tropical convergence zone; SACZ: South Atlantic convergence zone; SAH: South Atlantic high; SPH: South Pacific high; SW: Southern Westerlies. Modified after Godfrey et al. (2003).

1.3. Planktic foraminifera as a proxy for oceanic (paleo) environments

Planktic foraminifera are one of the most important organism groups for paleoceanographic reconstructions. Their sensitivity to environmental variations and their distribution through passive transport, as well as their high relative abundances and good preservation potential make them ideal proxies for interpreting marine sediments and provide a good tool for the reconstruction of (past) oceanic conditions (e.g. Bé and Tolderlund, 1971; Thiede, 1975; Hemleben et al., 1989; Mix et al., 1999). Among planktic foraminifera, most spinose species live in the upper 50 m of the water column (e.g. *Globigerinoides* spp.), whereas non-spinose species, such as *Globorotalia* spp., preferably live between 50 m and 300 m, or even below 300 m (Mortyn and Charles, 2003). Some species such as *Neogloboquadrina dutertrei* and *Globorotalia menardii* follow the thermocline depth (Fairbanks et al., 1982; Faul et al., 2000); other species such as *G. glutinata* and *G. bulloides* are associated with high nutrient supply (Thiede, 1975).

Planktic foraminifera can be grouped in five zoogeographic provinces (Bé, 1977; Hemleben et al., 1989). Most of the species occur in different zoogeographic zones, but each zoogeographic province is represented by at least one principal species (Fig. 1-3, Bé and Tolderlund, 1971). The distinct depth habitat and spatial distribution of planktic foraminifera species can be used to reconstruct discrete hydrographic settings in the past (e.g. Imbrie and Kipp, 1971).

Several studies have examined the isotopic geochemistry of planktic foraminifera (Fairbanks et al., 1982; Kohfeld et al., 1996; Spero and Williams, 1988; 1989; Spero and Lea, 1993; 1996; Spero et al., 1997; Mortyn and Charles, 2003). The basic idea behind these observations is that the isotopic composition of planktic foraminifera shells primarily reflects physical properties of the ambient water such as temperature, salinity and stable carbon isotope composition of dissolved inorganic carbon (DIC). More simply, the $\delta^{18}\text{O}$ of shell calcite increases with salinity, depth and decreasing temperatures. In contrast, shell $\delta^{13}\text{C}$ decreases with depth because phytoplankton elevate surface ^{13}C by preferential uptake of ^{12}C , and heterotrophic organisms reintroduce ^{12}C via respiration at depth (Kroopnick, 1974).

Consequently, the isotopic composition of the planktic foraminifera species can be used to reconstruct the physical and geochemical structure of surface and subsurface waters (e.g. Spero et al., 2003). However, environmental parameters such as PH and carbonate ion concentration or physiological processes such as symbiont photosynthesis and foraminiferal respiration may offset this pattern (Spero and Williams, 1989; Spero et al., 1997; Bemis et al., 2000).






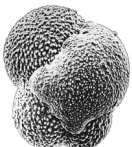
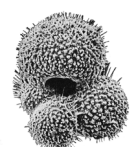




Tropical	Subtropical	Transitional	Subpolar	Polar	
 <i>Globigerinoides sacculifer</i>		 <i>Globigerinoides ruber</i>		 <i>Turbotalita quinqueloba</i>	Surface water
	 <i>Pulleniatina obliquiloculata</i>	 <i>Neogloboquadrina duterrei</i>	 <i>Globigerinita glutinata</i>	 <i>Globigerina bulloides</i>	Thermocline
		 <i>Globorotalia truncatulinoides</i>	 <i>Globorotalia inflata</i>	 <i>Neogloboquadrina incompta</i>	Sub-thermocline
				 <i>Neogloboquadrina pachyderma</i>	

Fig. I-2 Sketch on some planktic foraminiferal species with respect to their zoogeographic provinces and habitats. Note that most of the species may occur in different zoogeographic zones.

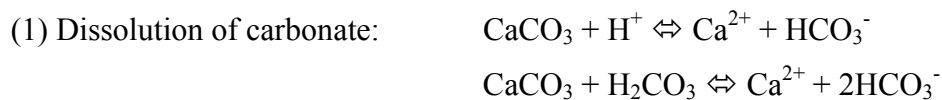
1.4. Bulk sediment-biogenic compounds as proxy for (paleo) productivity

The photosynthetic fixation of carbon per unit area and per unit time is termed “primary production”, which is limited by sunlight and nutrient availability. The principle idea of paleoproductivity reconstructions is the assumption that spatial variations in any biogenic component of marine sediments reflect spatial variations in the production of these components in the overlying surface waters. Accumulation of biogenic components, such as calcium carbonate, biogenic opal and organic carbon has been used to reconstruct changes in past oceanic primary production (e.g. Pedersen, 1983; Lyle et al., 1988; Sarnthein et al., 1988; Charles et al., 1991; Mortlock et al., 1991). However, examples of inconsistencies are given for organic carbon (e.g. Jahnke, 1996), for biogenic opal (e.g. Nelson et al., 1995), and for calcium carbonate (e.g. Rühlemann et al., 1999). Lateral advection of water masses, sediment redistribution and most importantly, spatial variations in the preservation efficiency of the biogenic matter all affect the relationship between surface water processes and burial in underlying sediments. In the following, a brief introduction to some aspects of each proxy is given.

1.4.1. Calcium carbonate (CaCO₃)

The carbonate shells of phytoplankton (coccolithophorids, dinoflagellates) and zooplankton (mainly planktic and benthic foraminifera, pteropods) comprise a significant portion of marine sediments, especially in tropical and temperate climates. Thus, the combined accumulation rates of carbonate test producers in sediment may reflect carbonate production in the upper water column and thus, act as a proxy for primary production (Berger, 1977; 1985; Bender and Graham, 1978; Van Kreveld et al., 1996; Catubig et al., 1998). The ratio between the primary and secondary producers is important since, in general, coccolithophorids are the main contributors of carbonate in areas of low productivity whereas planktic foraminifera are the most important carbonate producers when nutrient concentration is high (Berger, 1976). However, studies from various oligotrophic and mesotrophic areas show that the ratio between calcium carbonate and organic carbon is nearly the same, and thus, the application of carbonate accumulation rates to detect changing climatic conditions appears to be reasonable (Van Kreveld et al., 1996).

Variations in the carbonate accumulation rate, however, may also reflect carbonate dissolution which can overprint the productivity signal (Berger, 1975a; 1975b; Milliman, 1993; Berelson et al., 1994). From the estimated present-day carbonate production of 5.3 billion tons per year in the world's ocean, 3.2 billion tons are supposed to accumulate in marine sediments, whilst the remainder is dissolved in the water column or at the sea floor (Milliman, 1993). As an effect of pressure, calcite solubility increases with depth. The dissolution of calcite starts at the depth at which the carbonate ion concentration [CO₃²⁻] of the water equals the [CO₃²⁻] of calcite saturation. Below this depth, termed the lysocline, the water is calcite-undersaturated and calcareous particles dissolve (equation 1). Carbonate dissolution occurs particularly in the deep sea below the lysocline, and in high-productivity continental margins as a result of organic matter oxidation by benthic organisms (Jahnke et al., 1994).



1.4.2. Biogenic silica (opal)

Opal is an important paleoproductivity proxy because of the significant role of the opal producers in the biological pump and its overall good preservation. Almost all the biogenic silica produced in the oceans is precipitated by planktic organisms in the surface layers, especially by diatoms, with a global production of $240 \times 10^{12} \text{ mol yr}^{-1}$ (Nelson et al., 1995;

Tréguer et al., 1995). The global overall preservation efficiency of biogenic silica is close to 3% (Tréguer et al., 1995). Diatoms are one of the major contributors to ocean primary production in temperate and cold waters of diverging surface currents and EBCs (Tréguer et al., 1995). Radiolarians contribute less than diatoms to the production of biogenic silica, with higher contributions in areas of lower primary production (Takahashi, 1991).

It is important to note that both the equatorial and coastal upwelling areas in the Pacific Ocean provide a higher opal export rate than that in the Atlantic Ocean (Ragueneau et al., 2000 and references therein). The dissolution rate of biogenic silica depends on the silicic acid concentration in the ambient water (Ragueneau et al., 2000), seasonality of export production (Berger and Wefer, 1990), rapid sinking of diatoms through formation of large fecal pellets (Goldman, 1988) or aggregation (Smetacek, 1985), and diatom sexual phase (Crawford, 1995).

1.4.3. Organic carbon (C_{org})

Organic carbon is widely used as paleoproductivity indicator since it is the basic element of all organisms (Müller and Suess, 1979; Sarnthein et al., 1987; 1988; Rühlemann et al., 1999). The distribution of organic carbon in marine sediments is proportional to its production in surface waters and hence, changes in its accumulation rates on glacial-interglacial timescales have been used to reconstruct paleoproductivity based on empirical equations (Müller and Suess, 1979; Stein, 1991; Sarnthein et al., 1992).

The preservation efficiency of C_{org} depends on several factors, such as the quantity of organic matter exported to the deep sea (the amount and the seasonality of C_{org} flux), remineralization processes in the water column and at sediment-water interface (the oxygenation of bottom water, water depth), exposure time of the biogenic matter (sedimentation rate), and on molecular composition of organic material (fresh or reworked, marine or terrestrial origin) (e.g. Canfield, 1994; Mayer, 1994; Hartnett et al., 1998). Therefore, glacial-interglacial changes in C_{org} accumulation rates also reflect different hydrological or sedimentological conditions. For paleoproductivity estimations it is essential to ascertain the contribution of terrestrial organic carbon to the marine environment e.g. by determination of the $\delta^{13}C_{org}$ of total organic carbon (Fry and Sherr, 1989).

1.5. Material and methods

1.5.1. Samples

The samples studied were collected during the three R/V Sonne cruises SO-80 (Stoffers et al., 1992), SO-102 (CHIPAL, Hebbeln et al., 1995), and SO-156 (PUCK, Hebbeln et al., 2001) along the Chilean coast. Surface sediment samples were retrieved using a multicorer (MUC). Sediment cores were recovered by a gravity corer (SL). The samples were obtained mainly from the Chilean continental slope, with few samples gained from the shelf and the deep sea. Core locations and further descriptions are presented in the respective manuscripts (Chapter 2). From each gravity core, two sample-series of approx. 10 cm³ were taken at 5-cm intervals, one set for geochemical analyses, another set for stable isotope and micropaleontological analyses. Archived core materials are kept at the Department of Geosciences, University of Bremen, Germany.

1.5.2. Methods

1.5.2.1. Planktic foraminifera analyses

The sediment sample set for foraminiferal analyses was freeze-dried, weighed and washed through a 150µm sieve. All specimens were individually picked and identified following the taxonomy of planktic foraminifera proposed by Parker (1962), Kennett and Srinivasan (1983), and Hemleben et al. (1989). For *N. pachyderma*, the relative abundances of right (dex, also known as *N. incompta*) and left (sin) coiling individuals were determined, and the two forms were treated as individual species. *N. dutertrei* was distinguished from *N. incompta* primarily by the presence of an umbilical tooth, presence of more than four chambers, and a more pitted texture based on the description of Parker (1962).

1.5.2.2. Stable oxygen and carbon isotopes

A Finnigan MAT 251 mass spectrometer (with an automated carbonate preparation at the University of Bremen) has been used to measure the stable oxygen ($\delta^{18}\text{O}$) and carbon ($\delta^{13}\text{C}$) isotope compositions of the planktic foraminifera species *G. bulloides* and *N. incompta* for surface samples, and *N. pachyderma* and *N. incompta*. for gravity cores, respectively. Each measurement was performed on 10-20 individuals >212 µm of one species. For all stable oxygen isotope measurements a working standard was used (Burgbrohl CO₂ gas), which has been calibrated against PDB by using the NBS 18, 19 and 20 standards.

1.5.2.3. AMS ^{14}C dating

Accelerator mass spectrometry (AMS) dating were determined at the Leibniz Laboratory for Age Determinations and Isotope Research at the University of Kiel (Nadeau et al., 1997), and at the Center for Isotope Research in Groningen, the Netherlands. The ^{14}C AMS dates were obtained from approx. 10 mg calcium carbonate from tests of mixed planktic foraminifera. All ages were corrected for ^{13}C and a mean ocean reservoir age of 400 years (Bard, 1988). The ^{14}C ages were converted to calendar years using the CALPAL software and are reported as cal yr BP (Jöris and Weninger, 1998, updated 2003).

1.5.2.4. Bulk sediment analyses

The sediment sample set for bulk analyses was freeze-dried and homogenized prior to processing. After decalcification of the samples by 6 N HCl, total organic carbon (TOC) was obtained by combustion at 1050°C using a Heraeus CHN-O-Rapid elemental analyzer as described by Müller et al. (1994). Carbonate content was calculated from the difference between total carbon (TC), measured with the CHN analyzer on untreated samples, and TOC:

$$(2) \quad \text{CaCO}_3 = (\text{TC} - \text{TOC}) * 8.33$$

All samples for analysis of biogenic silica (opal) were freeze-dried and ground in an agate mortar. Opal was determined at 10 cm resolution (except for GeoB 7112-5 at 5 cm resolution) with a sequential leaching technique proposed by De Master (1981), and modified by Müller and Schneider (1993).

1.5.2.5. Siliceous plankton analyses

For the study of siliceous plankton, samples were prepared following the method proposed by Schrader and Gersonde (1978). Qualitative and quantitative analyses were done at x400 magnifications using a Zeiss-Axioscope with phase-contrast illumination (Mohtadi et al., in press). Counts were carried out on permanent slides of acid-cleaned material (Mountex mounting medium). Several traverses across each cover-slip were examined, depending on microorganism abundances. At least two cover slips per sample were scanned in this way. The counting procedure and definition of counting units for diatoms followed those of Schrader and Gersonde (1978).

1.6. Overview of own research

1. Mohtadi, M., Hebbeln, D., and Marchant, M. (submitted). Upwelling and productivity along the Peru-Chile Current derived from faunal and isotopic compositions of planktic foraminifera in surface sediments. *Marine Geology*

The first manuscript aims to provide a present-day picture of the productivity pattern along the southern part of the PCC between 24°S and 44°S. Using the present-day distribution pattern of planktic foraminifera species and their isotopic composition, this study shows that beside the ACC, coastal upwelling controls the productivity north of 39°S, while south of 39°S, the high marine production is promoted additionally by riverine input from the continent.

2. Mohtadi, M., Romero, O.E., and Hebbeln, D. (in press). Changing marine productivity off northern Chile during the last 19,000 years: a multiparameter approach. *Journal of Quaternary Science*

This paper deals with the history of productivity off northern Chile during the deglaciation and the Holocene using the qualitative and quantitative variations in geochemical and micropaleontological parameters. By comparing our results with terrestrial and marine studies, we refer to other controlling mechanisms of productivity in this area beside the lateral advection of the ACC, such as mechanisms controlling the upwelling intensity (position and intensity of the South Pacific anticyclone, ENSO, hemispheric thermal gradient) and onshore precipitation (ENSO, trade winds).

3. Mohtadi, M., and Hebbeln, D. (submitted). Mechanisms and variations of the Paleoproductivity off northern Chile (24°S - 33°S) during the last 40,000 years. *Paleoceanography*

The third manuscript addresses the various late Quaternary controlling mechanisms of productivity by the comparison of different geochemical and micropaleontological parameters in five sediment cores from central and northern Chile. This study shows that the influence of the Southern Westerlies never exceeded 31°S, since data from 30°S and farther north show a common but different pattern than that recorded at 33°S. The productivity was highest at 33°S during the LGM caused by maximal intensity and northward extension of the Southern Westerlies. North of 33°S, highest productivities were recorded prior to the LGM and during the deglaciation. The productivity was controlled by variations in the upwelling intensity

caused by ENSO and strength of the South Pacific anticyclone, as well as episodic events such as flooding of the shelf and enhanced continental runoff.

1.7. References

- Abbott, M.B., Wolfe, B.B., Wolfe, A.P., Seltzer, G.O., Aravena, R., Mark, B.G., Polissar, P.J., Rodbell, D.T., Rowe, H.D. and Vuille, M., 2003. Holocene paleohydrology and glacial history of the central Andes using multiproxy lake sediment studies. *Palaeogeography, Palaeoclimatology, Palaeoecology*, 194(1-3): 123-138.
- Aceituno, P., 1988. On the functioning of the Southern Oscillation in the South American Sector. Part 1: Surface Climate. *Monthly Weather Review*, 116: 505-524.
- Aceituno, P. and Monticinos, A., 1993. Análisis de la estabilidad de la relación entre la oscilación del sur y la precipitación en América del Sur. *Bull. Inst. fr. études andines*, 22(1): 53-64.
- Ammann, C., Jenny, B., Kammer, K. and Messerli, B., 2001. Late Quaternary Glacier response to humidity changes in the arid Andes of Chile (18-29°S). *Palaeogeography, Palaeoclimatology, Palaeoecology*, 172: 313-326.
- Aravena, R., Suzuki, O. and Pollastri, A., 1989. Coastal fog and its relation to groundwater in the IV region of northern Chile. *Chemical Geology*, 79: 83-91.
- Aravena, R., Suzuki, O., Peña, H., Pollastri, A., Fuenzalida, H. and Gilli, A., 1999. Isotopic composition and origin of the precipitation in Northern Chile. *Appl. Geochem.*, 14: 411-422.
- Archer, D., Winguth, A., Lea, D. and Mahowald, N., 2000b. What caused the Glacial/Interglacial Atmospheric $p\text{CO}_2$ Cycles? *Reviews of Geophysics*, 38(2): 159-189.
- Archer, D.E. and Johnson, K., 2000. A model of the iron cycle in the ocean. *Global Biogeochemical Cycles*, 14(1): 269-279.
- Bard, E., 1988. Correction of accelerator mass spectrometry ^{14}C ages measured in planktonic foraminifera: Paleoceanographic implications. *Paleoceanography*, 3: 635-645.
- Barnola, J.M., Raynaud, D., Korotkevich, Y.S. and Lorius, C., 1987. Vostok ice core provides 160,000 year record of atmospheric CO_2 . *Nature*, 329: 408-414.
- Bé, A.W.H. and Tolderlund, D.S., 1971. Distribution and ecology of living planktonic foraminifera in surface water of the Atlantic and Indian Oceans. In: B.M. Turnell and W.R. Riedel (Editors), *The Micropaleontology of the Ocean*. Cambridge University Press, pp. 105-149.
- Bé, A.W.H., 1977. An ecological, zoogeographic and taxonomic review of recent planktonic foraminifera. In: A.T.S. Ramsey (Editor), *Oceanic Micropaleontology*. Academic Press, London.
- Bemis, B.E., Spero, H.J., Lea, D.W. and Bijma, J., 2000. Temperature influence on the carbon isotopic composition of *Globigerina bulloides* and *Orbulina universa* (planktonic foraminifera). *Marine Micropaleontology*, 38: 213-228.

- Bender, M.L. and Graham, D.W., 1978. Long term constraints on the global marine carbonate system. *J. Mar. Res.*, 36(3): 551-567.
- Berelson, Hammond, McManus and Kilgore, 1994. Dissolution kinetics of calcium carbonate in equatorial Pacific sediments. *Global Biogeochemical Cycles*, 8: 219-235.
- Berger, W.H., 1975a. Deep-sea carbonates: dissolution profiles from foraminiferal preservation. In: C.F.f.F. Research (Editor), *Dissolution of deep-sea carbonates*. Cushman Foundation for Foraminiferal Research, Ithaca, NY, United States, pp. 82-86.
- Berger, W.H., 1975b. Dissolution of deep-sea carbonates: an introduction. In: C.F.f.F. Research (Editor), *Dissolution of deep-sea carbonates*. Cushman Foundation for Foraminiferal Research, Ithaca, NY, United States, pp. 7-10.
- Berger, W.H., 1976. Biogenous deep sea sediments: Production, preservation, and interpretation. In: J.P. Riley and R. Chester (Editors), *Chemical Oceanography*. Academic Press, London, pp. 266-388.
- Berger, W.H., 1977. Deep-sea carbonate and the deglaciation preservation spike in pteropods and foraminifera. *Nature*, 269: 301-304.
- Berger, W.H., 1985. CO₂ Increase and climate prediction: clues from deep-sea carbonates. *Episodes*, 8-3: 163-167.
- Berger, W.H., Fischer, K., Lai, C. and Wu, G., 1987. Ocean productivity and organic carbon flux. (Part I: Overview and maps of primary productivity and export production). University of California: San Diego: SIO ref. 87-30.
- Berger, W.H., Smetacek, V.S. and Wefer, G., 1989. Ocean productivity and paleoproductivity -an overview. In: W.H. Berger, V.S. Smetacek, and G. Wefer (Editor), *Productivity of the oceans: present and past*. John Wiley & Sons, New York, pp. 1-34.
- Berger, W.H. and Wefer, G., 1990. Export production: seasonality and intermittency, and paleoceanographic implications. *Palaeogeography Palaeoclimatology Palaeoecology*, 89: 245-254.
- Broecker, W. and Peng, J., 1993a. What caused the glacial to interglacial CO₂ to change? In: M. Heimann (Editor), *The global carbon cycle*. Springer, Berlin, pp. 95-115.
- Broecker, W.S., 1982. Glacial to interglacial changes in ocean chemistry. *Progress in Oceanography*, 11: 151-197.
- Broecker, W.S. and Peng, T.H., 1993b. Evaluation of the ¹³C constraint on the uptake of fossil fuel CO₂ by the ocean. *Paleoceanography*, 7: 619-626.
- Broecker, W.S. and Henderson, G.M., 1998. The sequence of events surrounding Termination II and their implications for the cause of glacial-interglacial CO₂ changes. *Paleoceanography*, 13(4): 352-364.
- Canfield, D.E., 1994. Factors influencing organic carbon preservation in marine sediments. *Chemical Geology*, 114: 315-329.

- Catubig, N.R., Archer, D.E., Francois, R. and DeMenocal, P., 1998. Global deep-sea burial rate of calcium carbonate during the last glacial maximum. *Paleocenography*, 13(3): 298-310.
- Charles, C.D., Froelich, P.N., Zibello, M.A., Mortlock, R.A. and Morley, J.J., 1991. Biogenic opal in Southern Ocean sediments over the last 450,000 years: Implications for surface water chemistry and circulation. *Paleoceanography*, 6(6): 697-728.
- Crawford, R.M., 1995. The role of sex in the sedimentation of a marine diatom bloom. *Limnology and Oceanography*, 40(1): 200-204.
- De Master, D.J., 1981. The supply and accumulation of silica in the marine environment. *Geochimica Cosmochimica Acta*, 45: 1715-1732.
- Fairbanks, R.G., Sverdrlove, M., Free, R., Wiebe, P.H. and Bé, A.W.H., 1982. Vertical distribution and isotopic fractionation of living planktonic foraminifera from the Panama Basin. *Nature*, 298: 841-844.
- Faul, K.L., Ravelo, A.C. and Delaney, M.L., 2000. Reconstructions of upwelling, productivity, and photic zone depth in the eastern equatorial Pacific Ocean using planktonic foraminiferal stable isotopes and abundances. *Journal of Foraminiferal Research*, 30(2): 110-125.
- Feldberg, M.J. and Mix, A.C., 2002. Sea-surface temperature estimates in the Southeast Pacific based on planktonic foraminiferal species; modern calibration and Last Glacial Maximum. *Marine Micropaleontology*, 44(1-2): 1-29.
- Fox, A.N. and Strecker, M.R., 1991. Pleistocene and modern snowlines in the Central Andes (24-28°S). *Bamberger Geographische Schriften*, 11: 169-182.
- Fry, B. and Sherr, E.B., 1989. $\delta^{13}\text{C}$ measurements as indicators of carbon flow in marine and freshwater ecosystems. In: P.W. Rundel, J.R. Ehleringer and K.A. Nagy (Editors), *Stable isotopes in ecological research*. Ecological studies. Springer, New York, pp. 196-229.
- Garleff, K., Schäbitz, F., Stingl, H. and Veit, H., 1991. Jungquartäre Landschaftsentwicklung beiderseits der Ariden Diagonale Südamerikas. *Bamberger Geographische Schriften*, 11: 359-394.
- Garreaud, R., 1999. Multiscale analysis of summertime precipitation over the central Andes. *Monthly Weather Review*, 127: 901-921.
- Godfrey, L.V., Jordan, T.E., Lowenstein, T.K. and Alonso, R.L., 2003. Stable isotope constraints on the transport of water to the Andes between 22[deg] and 26[deg]S during the last glacial cycle. *Palaeogeography, Palaeoclimatology, Palaeoecology*, 194(1-3): 299-317.
- Goldman, J.G., 1988. Spatial and temporal discontinuities of biological processes in pelagic surface waters. In: B.J. Rothschild (Editor), *Toward a Theory of Biological-Physical Interactions in the World Ocean*. Kluwer Academic Publishing, Dordrecht, pp. 273-296.

- Grosjean, M., 1994. Paleohydrology of the Laguna Lejia (north Chilean Altiplano) and climatic implications for late-glacial times. *Palaeogeography, Palaeoclimatology, Palaeoecology*, 109: 89-100.
- Grosjean, M., Geyh, M.A., Messerli, B. and Schotterer, U., 1995. Late-glacial and early Holocene lake sediments, ground water formations and climate in the Atacama Altiplano. *Journal of Paleolimnology*, 14: 241-252.
- Grosjean, M., Nuñez, L., Cartajena, I. and Messerli, B., 1997. Mid-Holocene Climate and Culture Change in the Atacama Desert, Northern Chile. *Quaternary Research*, 48: 239-246.
- Grosjean, M., 2001. Mid-Holocene climates in the South-Central Andes: humid or dry? *Science*, 292: 2391.
- Grosjean, M., van Leeuwen, J.F.N., van der Knaap, W.O., Geyh, M.A., Ammann, B., Tanner, W., Messerli, B., Nunez, L.A., Valero-Garces, B.L. and Veit, H., 2001. A 22,000 ¹⁴C year BP sediment and pollen record of climate change from Laguna Miscanti (23°S), northern Chile. *Global and Planetary Change*, 28(1-4): 35-51.
- Grosjean, M., Cartajena, I., Geyh, M.A. and Nunez, L., 2003. From proxy data to paleoclimate interpretation: the mid-Holocene paradox of the Atacama Desert, northern Chile. *Palaeogeography, Palaeoclimatology, Palaeoecology*, 194(1-3): 247-258.
- Hartnett, H.E., Keil, R.G., Hedges, J.I. and Devol, A.H., 1998. Influence of oxygen exposure time on organic carbon preservation in continental margin sediments. *Nature*, 391: 572-574.
- Hebbeln, D., Wefer, G. and cruise participants, 1995. Cruise Report of R/V SONNE Cruise 102, Valparaiso-Valparaiso, 9.5.-28.6.95. *Berichte aus dem Fachbereich Geowissenschaften*, 68. Universität Bremen, Bremen, 126 pp.
- Hebbeln, D., Marchant, M., Freudenthal, T. and Wefer, G., 2000a. Surface sediment distribution along the Chilean continental slope related to upwelling and productivity. *Marine Geology*, 164(3-4): 119-137.
- Hebbeln, D. and cruise participants, 2001. PUCK, report and preliminary results of R/V Sonne cruise SO 156, Valparaiso (Chile) - Talcahuano (Chile), March 29 - May 14, 2001. *Berichte aus dem Fachbereich Geowissenschaften der Universität Bremen*, 182. Universität Bremen, Bremen, 195 pp.
- Hebbeln, D., Marchant, M. and Wefer, G., 2002. Paleoproductivity in the southern Peru-Chile Current through the last 33000 yr. *Marine Geology*, 186(3-4): 487-504.
- Hemleben, C., Spindler, M. and Anderson, O.R., 1989. *Modern planktonic foraminifera*. Springer, New York, 363 pp.
- Heusser, C.J., 1983. Quaternary palynology of Chile. In: J. Rabassa (Editor), *Quaternary of South America and Antarctic Peninsula*. Balkema, Rotterdam, pp. 5-22.
- Heusser, C.J., 1990. Ice age vegetation and climate of subtropical Chile. *Palaeogeography, Palaeoclimatology, Palaeoecology*, 80: 107-127.

- Imbrie, J. and Kipp, N.G., 1971. A new micropaleontological method for quantitative paleoclimatology: application to a late Pleistocene Caribbean core. In: K.K. Turekian (Editor), *The Late Cenozoic Glacial Ages*. Yale Univ. Press, New Haven, pp. 71-181.
- Ingle, J.C., Keller, G. and Kolpack, R.L., 1980. Benthic foraminiferal biofacies, sediments and water masses of the southern Peru-Chile Trench area, southeastern Pacific Ocean. *Micropaleontology*, 26: 113-150.
- Jahnke, R.A., Craven, D.B. and Gaillard, J.F., 1994. The influence of organic matter diagenesis on CaCO₃ dissolution at the deep-sea floor. *Geochimica et Cosmochimica Acta*, 58: 2799-2809.
- Jahnke, R.A., 1996. The global ocean flux of particulate organic carbon: Areal distribution and magnitude. *Global Biogeochemical Cycles*, 10(1): 71-88.
- Jenny, B., Valero-Garces, B.L., Villa-Martinez, R., Urrutia, R., Geyh, M. and Veit, H., 2002. Early to Mid-Holocene Aridity in Central Chile and the Southern Westerlies: The Laguna Aculeo Record (34°S). *Quaternary Research*, 58(2): 160-170.
- Johnson, D.R., Fonseca, T. and Sievers, H., 1980. Upwelling in the Humboldt Coastal Current near Valparaiso, Chile. *Journal of Marine Research*, 38(1): 1-15.
- Jöris, O. and Weninger, B., 1998. Extension of the ¹⁴C calibration curve to ca. 40,000 cal BC by synchronizing Greenland ¹⁸O/¹⁶O ice core records and North Atlantic foraminifera profiles: A comparison with U/Th coral data. *Radiocarbon*, 40(1): 495-504.
- Jouzel, J. et al., 1996. Climatic interpretations of the recently extended Vostok ice record. *Climate Dynamics*, 12: 513-521.
- Kennett, J.P. and Srinivasan, M., 1983. *Neogene planktonic foraminifera - A Phylogenetic atlas*. Hutchinson Ross Publishing, Stroudsburg, 265 pp.
- Kim, J., Schneider, R.R., Hebbeln, D., Müller, P.J. and Wefer, G., 2002. Last deglacial sea-surface temperature evolution in the southeast Pacific compared to climate changes on the South American continent. *Quaternary Science Reviews*, 21: 2085-2097.
- Klump, J., Hebbeln, D. and Wefer, G., 2001. High concentrations of biogenic barium in Pacific sediments after Termination I - A signal of changes in productivity and deep water chemistry. *Marine Geology*, 177: 1-11.
- Kohfeld, K.E., Fairbanks, R.G., Smith, S.L. and Walsh, I.D., 1996. *Neogloboquadrina pachyderma* (sinistral coiling) as paleoceanographic tracers in polar oceans: Evidence from Northeast Water Polynya plankton tows, sediment traps, and surface sediments. *Paleoceanography*, 11(6): 679-699.
- Kroopnick, P., 1974. The dissolved O₂-CO₂-¹³C system in the eastern equatorial Pacific. *Deep-Sea Research*, 21: 211-227.
- Lamy, F., Hebbeln, D. and Wefer, G., 1998a. Late Quaternary precessional cycles of terrigenous sediment input off the Norte Chico, Chile (27.5°S) and paleoclimatic implications. *Palaeogeography, Palaeoclimatology, Palaeoecology*, 141(3-4): 233-251.

- Lamy, F., Hebbeln, D. and Wefer, G., 1999. High resolution marine record of climatic change in mid-latitude Chile during the last 28,000 years based on terrigenous sediment parameters. *Quaternary Research*, 51: 83-93.
- Lamy, F., Hebbeln, D., Rohl, U. and Wefer, G., 2001. Holocene rainfall variability in southern Chile: a marine record of latitudinal shifts of the Southern Westerlies. *Earth and Planetary Science Letters*, 185(3-4): 369-382.
- Latorre, B.A., Spadaro, I. and Rioja, M.E., 2002. Occurrence of resistant strains of *Botrytis cinerea* to *Anilinopyrimidine fungicides* in table grapes in Chile. *Crop Protection*, 21(10): 957-961.
- Latorre, C., Betancourt, J.L., Rylander, K.A., Quade, J. and Matthei, O., 2003. A vegetation history from the arid prepuna of northern Chile (22-23°S) over the last 13500 years. *Palaeogeography, Palaeoclimatology, Palaeoecology*, 194(1-3): 223-246.
- Lenters, J.D. and Cook, K.H., 1999. Summertime precipitation variability over South America: Role of the large-scale circulation. *Monthly Weather Review*, 127: 409-431.
- Lyle, M., Murray, D.W., Finney, B.P., Dymond, J., Robbins, J.M. and Brooksforce, K., 1988. The record of Late Pleistocene biogenic sedimentation in the eastern tropical Pacific Ocean. *Paleoceanography*, 3(1): 39-59.
- Marchant, M., Hebbeln, D. and Wefer, G., 1999. High resolution planktic foraminiferal record of the last 13,300 years from the upwelling area off Chile. *Marine Geology*, 161: 115-128.
- Mayer, L.M., 1994. Surface area control of organic carbon accumulation in continental shelf sediments. *Geochimica et Cosmochimica Acta*, 58(4): 1271-1284.
- Miller, A., 1976. The climate of Chile. In: W. Schwerdtfeger (Editor), *World Survey of Climatology Vol. 12*. Elsevier, Amsterdam, pp. 113-145.
- Milliman, J.D., 1993. Production and accumulation of calcium carbonate in the ocean: budget of a non-steady state. *Global Biogeochemical Cycles*, 7(4): 927-957.
- Mix, A.C., Morey, A.E., Pisias, N.G. and Hostetler, S.W., 1999. Foraminiferal fauna estimates of paleotemperature: Circumventing the no-analog problem yields cool ice age tropics. *Paleoceanography*, 14(3): 350-359.
- Mohtadi, M., Romero, O.E. and Hebbeln, D., in press. Changing marine productivity off northern Chile during the last 19,000 years: a multiparameter approach. *Journal of Quaternary Science*.
- Montecinos, A., Díaz, A. and Aceituno, P., 2000. Seasonal diagnostic and predictability of rainfall in subtropical South America based on tropical Pacific SST. *Journal of Climate*, 13: 746-758.
- Moore, J.K., Abbott, M.R., Richman, J.G. and Nelson, D.M., 2000. The Southern Ocean at the last glacial maximum: A strong sink for atmospheric carbon dioxide. *Global Biogeochemical Cycles*, 14(1): 455-475.

- Mortlock, R.A., Charles, C.D., Froehlich, P.N., Zibello, M.A., Saltzman, J., Hays, J.D. and Burckle, L.H., 1991. Evidence for lower productivity in the Antarctic Ocean during the last glaciation. *Nature*, 351: 220-223.
- Mortyn, P.G. and Charles, C.D., 2003. Planktic foraminiferal depth habitat and $\delta^{18}\text{O}$ calibrations: Plankton tow results from the Atlantic sector of the Southern Ocean. *Paleoceanography*, 18(2): 1037, doi: 10.1029/2001PA000637.
- Müller, P.J. and Suess, E., 1979. Productivity, sedimentation rate and sedimentary organic matter in the oceans-I. organic carbon preservation. *Deep-Sea Research*, 26 A: 1347-1362.
- Müller, P.J. and Schneider, R., 1993. An automated leaching method for the determination of opal in sediments and particulate matter. *Deep-Sea Research I*, 40(3): 425-444.
- Müller, P.J., Schneider, R. and Ruhland, G., 1994. Late Quaternary PCO_2 variations in the Angola Current: Evidence from organic carbon $\delta^{13}\text{C}$ and alkenone temperature. In: R. Zahn, T.F. Pedersen, M.A. Kaminski and L. Labeyrie (Editors), *Carbon cycling in the glacial ocean: Constraints on the ocean's role in global change*. NATO ASI Series I. Springer-Verlag, Berlin, pp. 343-366.
- Nadeau, M.J., Schleicher, M., Grootes, P.M., Erlenkeuser, H., Gottolong, A., Mous, D.J.W., Sarnthein, J.M. and Willkomm, N., 1997. The Leibniz-Labor AMS facility at the Christian-Albrechts University, Kiel, Germany. *Nuclear Instruments and Methods in Physics Research*, 123: 22-30.
- Nelson, D.M., Tréguer, P., Brzezinski, M., Leynaert, A. and Quéguiner, B., 1995. Production and dissolution of biogenic silica in the ocean: revised global estimates, comparison with regional data and relationship to biogenic sedimentation. *Global Biogeochemical Cycles*, 9: 359-372.
- Parker, F., 1962. Planktic foraminifera species in Pacific sediments. *Micropaleontology*, 8: 219-254.
- Pedersen, T.F., 1983. Increased productivity in the eastern equatorial Pacific during the last glacial maximum (19,000 to 14,000 yr B.P.). *Geology*, 11: 16-19.
- Petit, J.R. et al., 1999. Climate and atmospheric history of the past 420,000 years from the Vostok ice core, Antarctica. *Nature*, 399: 429-436.
- Ragueneau, O. et al., 2000. A review of the Si cycle in the modern ocean: recent progress and missing gaps in the application of biogenic opal as a paleoproductivity proxy. *Global and Planetary Change*, 26: 317-365.
- Romero, O. and Hebbeln, D., 2003. Biogenic silica and diatom thanatocoenosis in surface sediments below the Peru-Chile Current: controlling mechanisms and relationship with productivity of surface waters. *Marine Micropaleontology*, 48(1-2): 71-90.
- Romero, O.E., Hebbeln, D. and Wefer, G., 2001. Temporal and spatial variability in export production in the SE Pacific Ocean: evidence from siliceous plankton fluxes and surface sediment assemblages. *Deep Sea Research I*, 48(12): 2673-2697.

- Rühlemann, C., Müller, P.J. and Schneider, R.R., 1999. Organic Carbon and Carbonate as Paleoproductivity Proxies: Examples from High and Low Productivity Areas of the Tropical Atlantic. In: G. Fischer and G. Wefer (Editors), *Use of Proxies in Paleoceanography: Examples from the South Atlantic*. Springer, Berlin, Heidelberg, pp. 315-344.
- Ruttland, J. and Fuenzalida, H., 1991. Synoptic aspects of the central Chile rainfall variability associated with the Southern Oscillation. *International Journal of Climatology*, 11: 63-76.
- Sarnthein, M., Winn, K. and Zahn, R., 1987. Paleoproductivity of oceanic upwelling and the effect on atmospheric CO₂ and climatic change during deglaciation times. In: W.H. Berger and L.D. Labeyrie (Editors), *Abrupt climatic change: evidence and implications*. NATO ASI Series. Series C: Mathematical and Physical Sciences. D. Reidel Publishing Company, pp. 311-337.
- Sarnthein, M., Winn, K., Duplessy, J.-C. and Fontugne, M.R., 1988. Global variations of surface ocean productivity in low and mid latitudes: Influence on CO₂ reservoirs of the deep ocean and atmosphere during the last 21,000 years. *Paleoceanography*, 3(3): 361-399.
- Sarnthein, M., Pflaumann, U., Ross, R., Tiedemann, R. and Winn, K., 1992. Transfer functions to reconstruct ocean palaeoproductivity: a comparison. In: C.P. Summerhayes, W.L. Prell and K.C. Emeis (Editors), *Upwelling Systems: Evolution Since the Early Miocene*. Geological Society Special Editions, pp. 411-427.
- Schrader, H. and Gersonde, R., 1978. Diatoms and silicoflagellates. In: W.J. Zachariasse et al. (Editors), *Micropaleontological counting methods and techniques - an exercise on an eight meter section of the Lower Pliocene of Capo Rosello, Sicily*. Utrecht Micropaleontology Bulletin, pp. 129-176.
- Shaffer, G., Salinas, S., Pizarro, O., Vega, A. and Hormazabal, S., 1995. Currents in the deep ocean off Chile (30°S). *Deep-Sea Research*, 42: 425-436.
- Smetacek, V., 1985. Role of sinking in diatom life-history cycles: ecological, evolutionary and geological significance. *Marine Biology*, 84: 239-251.
- Spero, H.J. and Williams, D.F., 1988. Extracting environmental information from planktonic foraminiferal $\delta^{13}\text{C}$ data. *Nature*, 335: 717-719.
- Spero, H.J. and Williams, D.F., 1989. Opening the carbon isotope "Vital Effect" black box, 1, seasonal temperatures in the euphotic zone. *Paleoceanography*, 4(6): 593-601.
- Spero, H.J. and Lea, D.W., 1993. Intraspecific stable isotope variability in the planktic foraminifera *Globigerinoides sacculifer*: Results from laboratory experiments. *Marine Micropaleontology*, 22: 221-234.
- Spero, H.J. and Lea, D.W., 1996. Experimental determination of stable isotope variability in *Globigerina bulloides*: implications for paleoceanographic reconstructions. *Marine Micropaleontology*, 28: 231-246.
- Spero, H.J., Bijma, J., Lea, D.W. and Bemis, B.E., 1997. Effect of seawater carbonate concentration on foraminiferal carbon and oxygen isotopes. *Nature*, 390: 497-500.

- Spero, H.J., Mielke, K.M., Kalve, E.M., Lea, D.W. and Pak, D.K., 2003. Multispecies approach to reconstructing eastern equatorial Pacific thermocline hydrography during the past 360 kyr. *Paleoceanography*, 18(1): 1022, doi: 10.1029/2002PA000814.
- Stein, R., 1991. Accumulation of organic carbon in marine sediments. *Lecture Notes in Earth Science*, 34. (Springer), Berlin, 217 pp.
- Stoffers, P., Hekinian, R. and Cruise Participants, 1992. Cruise report Sonne 80a - Midplate III oceanic volcanism in the Southeast Pacific. *Berichte. Universität Kiel, Kiel*, 128 pp.
- Strub, P.T., Mesías, J.M., Montecino, V., Rutllant, J. and Salinas, S., 1998. Coastal ocean circulation off western South America. In: A.R. Robinson and K.H. Brink (Editors), *The Global Coastal Ocean - Regional Studies and Synthesis. The Sea, ideas and observations on progress in the study of the seas.* John Wiley & Sons, Inc., New York, pp. 273-313.
- Takahashi, K., 1991. Radiolaria: flux, ecology, and taxonomy in the Pacific and Atlantic. *Ocean Biocoenosis*, 3: 1-303.
- Thiede, J., 1975. Distribution of foraminifera in surface waters of a coastal upwelling area. *Nature*, 253: 712-714.
- Thompson, L.G., Mosley-Thompson, E., Davis, M.E., Lin, P.N., Henderson, K.A., Cole-Dai, J., Bolzan, J.F. and Liu, K.B., 1995. Late Glacial Stage and Holocene tropical ice core records from Huascarán, Peru. *Science*, 269: 46-50.
- Toggweiler, J.R., Dixon, K. and Broecker, W.S., 1991. The Peru upwelling and the ventilation of the South Pacific thermocline. *Journal of geophysical Research*, 96(C11): 20,467-20,497.
- Tréguer, P., Nelson, D.M., Van Bennekom, A.J., De Master, D.J., Leynaert, A. and Quéguiner, B., 1995. The silica balance in the World ocean: a reestimate. *Science*, 268: 375-379.
- Van Kreveld, S.A., Knappertsbusch, M., Ottens, J., Ganseen, G.M. and Van Hinte, J.E., 1996. Biogenic carbonate and IRD (Heinrich Layer) accumulation in deep sea sediments from a northeast Atlantic piston core. *Marine Geology*, 131.
- Veit, H., 1992. Jungquartäre Landschafts- und Bodenentwicklung im chilenischen Andenvorland zwischen 27-33°S. *Bonner Geographische Abhandlungen*, 85: 196-208.
- Veit, H., 1996. Southern Westerlies during the Holocene deduced from geomorphological and pedological studies in the Norte Chico, Northern Chile (27-33°S). *Palaeogeography Palaeoclimatology Palaeoecology*, 123: 107-119.
- Weischet, W., 1996. Regionale Klimatologie. Teil 1. Die Neue Welt: Amerika, Neuseeland, Australien. *Teubner Studienbücher der Geographie*, I. Teubner, Stuttgart, 468 pp.
- Wooster, W.S. and Reid, J.L., 1963. Eastern boundary currents. In: M.N. Hill (Editor), *The Sea.* Nescience Publications, New York, pp. 253-280.

Upwelling and productivity along the Peru-Chile Current derived from faunal and isotopic compositions of planktic foraminifera in surface sediments

Mohtadi, M.^a, Hebbeln, D.^a, and Marchant, M.^b

^a *Geowissenschaften, Universität Bremen, Postfach 330440, 28334 Bremen, Germany*

^b *Depto. Zoología, Universidad de Concepción, Casilla 160-C, Concepción, Chile*

Submitted to Marine Geology

Abstract

We report on the spatial distribution of isotopic compositions of the two planktic foraminifera species *Globigerina bulloides* and *Neogloboquadrina incompta*, and the faunal assemblages of planktic foraminifera in 91 surface sediment samples along the Chilean continental slope between 24°S and 44°S. In contrast to *G. bulloides*, both $\delta^{13}\text{C}$ and $\delta^{18}\text{O}$ data of *N. incompta* show little variability in the study area. North of 39°S, the isotopic values of *N. incompta* are heavier than those of *G. bulloides*, whereas south of 39°S, this relation inverses and points to a change from a well-mixed, deep thermocline caused by coastal upwelling north of 39°S to well-stratified water masses in a non-upwelling environment south of 39°S. In addition, the faunal composition of planktic foraminifera marks this change by transition from an upwelling assemblage north of 39°S to a high-nutrient-non-upwelling assemblage south of 39°S, which is characterized by decreased contributions of upwelling indicators such as *G. bulloides*, *N. pachyderma* and *Globigerinita glutinata*. Our data point to higher marine productivity at upwelling centers north of 25°S and at 30° - 33°S. South of 39°S, significant supply of nutrients by fluvial input most likely boosts the productivity. This pattern is documented in the high $\delta^{13}\text{C}$ values of both *G. bulloides* and *N. incompta*.

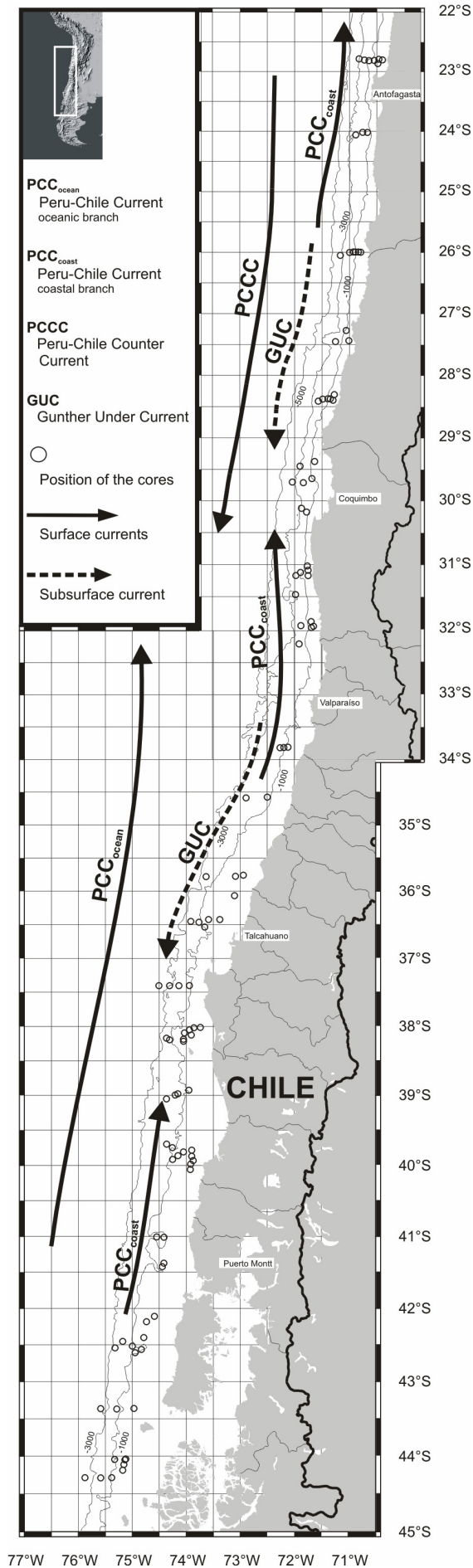
Keywords: Coastal upwelling, Productivity, Peru-Chile Current, Planktic foraminifera, Surface Sediments, Stable isotopes

1. Introduction

Marine sediments act as long-term sink for biogenic particles. Quantity as well as the biogeochemical characteristics of particle settling to the sea floor are related to the environmental conditions during their generation and may be used to trace present and past environmental and productivity conditions (Fischer and Wefer, 1999). Analyses of planktic foraminiferal assemblages and their isotopic composition form a key component of (pale) oceanographic and (paleo) productivity reconstructions (e.g. Labeyrie et al., 1992; Niebler et al., 1999; Lea et al., 2000; Meggers et al., 2002). Their sensitivity to environmental variations and their distribution through passive transport, as well as their high relative abundances and good preservation potential make them ideal proxies to interpret marine sediments and oceanic conditions (e.g. Bé and Tolderlund, 1971; Thiede, 1975; Hemleben et al., 1989; Mix et al., 1999).

The Peru-Chile Current (PCC) is one of the most productive marine environments worldwide (Berger et al., 1987). Previously published studies on surface sediments along the Chilean continental slope focused on the composition of the terrigenous sediment fraction (Krissek et al., 1980; Scheidegger and Krissek, 1982; Lamy et al., 1998b), siliceous plankton and biogenic silica (Romero et al., 2001; Romero and Hebbeln, 2003), barium contents (Klump et al., 2000), and sediment data together with benthic foraminifera (Bandy and Rodolfo, 1964; Ingle et al., 1980). Hebbeln et al. (2000a) and Feldberg and Mix (2002) provide the only studies on planktic foraminifera from the surface sediments beneath the southern part of the PCC. However, the spatial resolution of the data presented in Feldberg and Mix (2002) is very low (13 samples between 20°S and 50°S), and the sample distribution in Hebbeln et al. (2000a) is uneven (along six transects between 27°S and 43°S), and do not cover some oceanographically important areas off the Chilean coast.

Based on an unprecedented spatial resolution, this paper reports on regional distribution patterns of planktic foraminifera and the isotopic composition of two planktic foraminifera species in the surface sediments beneath the PCC between 23°S and 44°S. We intend to show that the qualitative variations in these signals correspond to the prevailing oceanographic and climatic conditions, such as water mass characteristics, thermocline depth, coastal upwelling, and hydrological regime of the continent. Present observations and previously published results serve as a baseline data set for the paleoclimatic and paleoceanographic reconstructions along the Chilean continental margin.

**Fig. 1**

Schematic map of the study area showing the position of the investigated surface sediment samples (open circles), and principal oceanographic features (arrows) after Strub et al. (1998).

2. Regional setting

Eastward flowing subantarctic surface waters of the Antarctic Circumpolar Current (ACC) approach the South American continent between 40° and 45°S and split into the northward flowing PCC (or Humboldt Current, Fig. 1) and the southward flowing Cape Horn Current (Strub et al., 1998; Shaffer et al., 1995). 100-300 km off the Chilean coast, the poleward flowing subtropical surface waters of the Peru-Chile Countercurrent (PCCC) divide the PCC into a coastal (PCC_{coast}) and an oceanic branch (PCC_{ocean}). Beneath these surface currents flow the equatorial subsurface waters of the Gunther Undercurrent (GUC, or Peru-Chile Undercurrent), located mainly between 100 and 400 m water depth. Below 400 m depth, the Antarctic Intermediate Water (AAIW) flows equatorward, underlain by the southward flowing Pacific Deep Water (PDW). The northward flowing Antarctic Bottom Water (AABW) fills the deepest parts of the Chile trench (Ingle et al., 1980).

North of 42°S, equatorial surface waters of the GUC reach the surface as a result of coastal upwelling (Morales et al., 1996). Upwelling occurs north of 35°S throughout

the year but is restricted to the austral summer between 35° and 42°S. South of 42°S, prevailing onshore blowing westerlies prevent coastal upwelling (Strub et al., 1998). Annual average pigment concentration north of 30°S lies below 0.3 mg cm⁻³ (Thomas et al., 1994; Thomas, 1999). South of 30°S, pigment concentration are on average higher and can exceed 6 mg m⁻³ during austral winter (Thomas et al., 1994).

A strong N-S segmentation can also be observed in the continental climate of Chile (Miller, 1976; Heusser, 1984; Garleff et al., 1991). Extremely low precipitation (<50 mm yr⁻¹) occurs in the hyper-arid area north of 27°S. Southward increasing rainfall (up to 1000 mm yr⁻¹) characterizes the semi-arid region between 27° and 39°S, while heavy precipitation (>2000 mm yr⁻¹) takes place in the humid zone south of 39°S. This gradient of the precipitation patterns has a pronounced effect on the river discharge, and subsequently, on the terrigenous sediment input to the study area, which increases significantly towards the south (Scholl et al., 1970; Milliman et al., 1995).

3. Material and methods

A total of 91 sediment samples were collected with a multicorer during the PUCK cruise of R/V Sonne in March-May 2001 (Hebbeln et al., 2001). For the analyses reported here, the uppermost centimeter of the undisturbed surface sediments has been used. The samples were retrieved from water depths ranging between 180 m and 3500 m and cover almost each degree of latitude between 23° and 44°S (Fig. 1, Table 1). The analyses of the planktic foraminifera fauna is based on the >150 µm fraction, which was separated by sieving. Each sample considered for this study contained at least 200 specimens, which were identified following the taxonomy of planktic foraminifera proposed by Parker (1962), Kennett and Srinivasan (1983), and Hemleben et al. (1989). Following the description of Parker (1962), *Neogloboquadrina dutertrei* was distinguished from *N. incompta* (also known as *N. pachyderma* dex.) by the occurrence of an umbilical tooth, and the presence of more than four chambers.

A Finnigan MAT 251 mass spectrometer with an automated carbonate preparation at the University of Bremen has been used to measure the stable oxygen ($\delta^{18}\text{O}$) and carbon ($\delta^{13}\text{C}$) isotope compositions of the planktic foraminifera species *G. bulloides* and *N. incompta*. Each measurement was performed on 15-20 individuals >212 µm of one species. The $\delta^{13}\text{C}$ of *N. incompta* remains basically invariant in respect of its shell mass (e.g. Kohfeld et al., 1996), although some size-dependent variability in the isotopic record has been reported in the Southern Ocean (Donner and Wefer, 1994). Size-related trends are reported also for the

isotopic composition of *G. bulloides* (e.g. Spero and Lea, 1996; Bemis et al., 1998). To avoid any potential bias, specimens of roughly equal size were selected for the isotopic measurements. Additionally, we include the isotopic data of *G. bulloides* and *N. incompta* from 36 surface sediments obtained by Hebbeln et al. (1995; 2000a) to give a more comprehensive picture from this region. For all stable carbon and oxygen isotope measurements a working standard (Burgbrohl CO₂ gas) was used, which has been calibrated against PDB by using the NBS 18, 19 and 20 standards. Consequently, all the isotope data given here are relative to the PDB standard. Analytical standard deviation is about ± 0.07 ‰ for $\delta^{18}\text{O}$, and ± 0.05 for $\delta^{13}\text{C}$ (Isotope Laboratory, Department of Geosciences, University of Bremen).

4. Results

4.1. Stable isotopes

The $\delta^{18}\text{O}$ data of *N. incompta* show relatively little variability (-0.06 to 1.56‰), with slightly heavier $\delta^{18}\text{O}$ values in the south of the study area (Table 1, Fig. 2b). In addition, the deeper samples (>1000 m, i.e., samples farther from the coast) have a broader range of the $\delta^{18}\text{O}$ values (1.6‰) than the shallower samples (1.1‰, Table 1, Fig. 2d). The $\delta^{13}\text{C}$ data of *N. incompta* display a narrow range as well, with a minor southward increase in the average values (Table 1, Fig. 2f, h). A prominent feature is the generally lighter isotopic data of the samples from Hebbeln et al. (2000a), possibly caused by differences in the size of the selected tests for the isotopic measurement (up to 400 μm in Hebbeln et al., 2000a).

The $\delta^{18}\text{O}$ data of *G. bulloides* display a much broader range than those of *N. incompta* (-0.48 to 3.87‰, Table 1), with a considerable bimodal latitudinal distribution (Fig. 2a). The $\delta^{18}\text{O}$ values in the samples north of 36°S are on average 1.2‰ lighter than in the samples south of 39°S. Among the samples south of 39°S, outliers with values >2‰ are mostly from 39°/40°S (Table 1). The $\delta^{18}\text{O}$ data in the deeper, farther offshore samples show a narrower range, and extend towards lighter values (Fig. 2c). The $\delta^{13}\text{C}$ data of *G. bulloides* vary between -1.06 and 2.32‰ (Fig. 2e, g), again with a clear bimodal latitudinal distribution. The values north of 36°S are on average much lighter (-0.25‰) than those recorded south of 39°S (1.13‰, Table 1, Fig. 2e). A pronounced distribution pattern of *G. bulloides* $\delta^{13}\text{C}$ versus depth cannot be observed (Fig. 2g).

Table 1

Position and depth of the investigated surface sediment samples from the Chilean continental slope between 24°S and 44°S, with the stable isotopic data of *N. incompta* and *G. bulloides* (vs. PDB), and the total amount of planktic foraminifera per cm⁻³.

GeoB No.	Latitude (°S)	Longitude (°W)	Depth (m)	<i>N. incompta</i>		<i>G. bulloides</i>		Total pl. forams (ind. cm ⁻³)
				$\delta^{18}\text{O}$ (‰)	$\delta^{13}\text{C}$ (‰)	$\delta^{18}\text{O}$ (‰)	$\delta^{13}\text{C}$ (‰)	
7115-1	24.00	70.36	523	1.48	0.1	1.11	-1.00	258
7121-1	26.00	70.54	1442	1.02	1.42	1.06	0.34	67
7122-2	26.00	70.50	673	1.3	0.9	1.99	-0.28	83
7116-1	26.00	71.00	1996					2
7123-1	27.17	71.03	557	0.35	0.91	0.09	-0.45	22
7131-1	28.23	71.30	1650	0.72	0.80	-0.15	-0.72	34
7127-1	28.23	71.28	1462	0.91	0.91	0.03	-0.84	63
7130-1	28.25	71.37	2080	0.86	1.37	0.12	-0.57	157
7129-1	28.25	71.20	476	0.99	1.23	0.78	-0.30	124
7133-1	29.23	71.39	635	0.91	1.17	0.02	-0.21	82
7132-1	29.28	71.54	3253	0.91	0.84	0.40	-0.48	16
7135-1	29.40	71.41	1432	0.96	1.15	1.47	-0.15	142
7136-1	29.43	72.10	3189	1.08	0.96	-0.36	-1.06	31
7134-1	29.43	71.46	1888	0.92	1.19	0.66	-0.29	131
7138-1	30.08	71.52	2733	1.04	1.04	-0.18	-0.99	39
7137-2	30.10	71.44	1199	1.11	0.97	0.81	0.32	31
7139-1	30.12	71.59	3267	0.87	1.22	0.71	1.36	16
7140-1	31.02	71.45	345	0.93	0.87	0.57	-0.14	598
7141-1	31.05	71.45	301	0.90	1.27	0.38	0.07	1200
7143-1	31.06	71.53	1371	0.88	1.31	2.08	-0.20	124
7144-1	31.10	71.58	1961	0.90	1.23	0.90	-0.02	126
7142-2	31.11	71.45	481	0.83	0.78	1.36	-0.66	520
7149-1	31.29	72.00	3086	0.97	1.28			8
7145-1	31.53	71.42	326	0.86	1.41	0.12	-0.77	655
7146-1	31.58	71.38	183	1.02	1.46	0.53	-0.09	246
7148-1	31.58	71.56	2289	0.86	1.29	-0.48	-0.94	13
7147-1	31.59	71.40	398	1.11	1.24	0.19	-0.64	316
7150-1	32.17	71.57	1591	0.94	1.06	0.88	0.32	128
7153-1	33.48	72.10	863	0.92	1.21	0.58	0.05	5
7154-2	33.48	72.16	1385	0.95	0.81	1.34	0.90	4
7152-1	33.48	72.07	420	0.62	0.48			3
7156-1	34.35	72.31	1247	1.02	1.37	2.84	0.57	4
7158-1	35.47	73.29	1563	0.88	-0.01			1
7198-1	38.10	74.23	2287	0.92	1.28			0.1
7199-2	38.12	74.20	1673	-0.06	1.19			0.5
7209-2	38.59	74.10	1525	0.88	1.76	3.87	0.83	7
7208-1	39.01	74.13	1794	1.18	1.35			2
7207-1	39.04	74.22	2236	1.01	1.38	0.86	1.60	5
7212-1	39.42	74.23	1469	0.80	1.43			9
7213-1	39.44	74.17	1190	0.96	1.52	0.93	1.85	19
7215-1	39.49	74.04	498	0.74	1.22			1
7214-1	39.53	74.10	772	1.12	1.78	2.85	1.58	79
7211-1	39.56	74.16	890	1.31	1.67	3.75	2.32	11
7197-1	41.00	74.33	816	1.26	1.59			6
7195-1	41.12	74.25	521	0.92	1.60	0.52	0.11	19
7194-1	41.25	74.26	308	1.21	1.37	2.50	1.24	8
7173-4	42.05	74.34	160	1.24	1.70			0.05
7193-1	42.11	74.43	209	0.99	1.58	1.05	0.42	17
7172-3	42.25	74.47	296	0.99	1.69	1.18	1.53	42
7175-4	42.27	75.13	1973	0.91	1.42	1.17	0.87	35
7174-2	42.33	75.00	1222	1.37	1.55	0.42	0.05	46
7179-1	42.34	75.20	2760	1.49	1.99	1.93	0.91	8
7177-2	42.35	74.50	905	1.07	1.62	2.14	1.39	9
7180-1	43.22	75.34	3485	1.56	2.05	0.87	1.10	6
7181-1	43.22	75.17	1212	1.09	1.50	2.66	1.57	10
7182-1	43.22	74.55	301	0.91	1.03	1.24	0.90	24
7183-1	44.03	75.08	443	0.80	1.29	1.60	1.41	46
7192-1	44.05	75.22	1014	0.82	1.27	1.74	1.09	24
7186-1	44.09	75.10	1171	0.89	1.29	1.38	0.83	4
7187-1	44.12	75.10	476	1.17	1.32	1.86	1.05	12
7191-1	44.17	75.36	1939	1.16	1.54	1.66	1.04	14
7189-1	44.17	75.23	868	0.76	1.11	1.7	1.08	20
7190-1	44.17	75.52	3285	1.21	1.35			3

Table 2 Faunal distribution of the most important planktic foraminifera species in the investigated surface sediment samples from the Chilean continental slope between 24°S and 44°S.

GeoB No.	<i>G. bulloides</i> %	<i>G. glutinata</i> %	<i>G. ruber</i> %	<i>G. crassaformis</i> %	<i>G. inflata</i> %	<i>G. hexagona</i> %	<i>N. duterrei</i> %	<i>N. incompta</i> %	<i>N. pachyderma</i> %	<i>O. universa</i> %	<i>P. obliquiloculata</i> %	<i>T. quinqueloba</i> %	others %
7115-1	24.05	3.80	0.63	0.00	1.90	0.00	0.63	31.96	30.06	0.00	0.63	0.00	6.33
7121-1	19.70	3.94	1.21	0.61	1.21	0.30	1.82	47.58	17.27	0.30	0.91	0.30	4.85
7122-2	22.00	4.89	1.22	0.00	3.91	0.00	1.96	36.19	21.52	0.49	2.20	0.00	5.62
7116-1	31.29	0.00	0.68	1.36	0.00	6.12	40.14	9.52	0.00	9.52	0.68	0.00	0.68
7123-1	27.93	4.23	0.47	0.00	0.00	0.23	0.70	50.70	9.86	0.47	0.23	0.23	4.93
7131-1	30.61	2.73	0.91	0.00	0.30	0.61	3.03	51.82	5.45	0.91	0.30	0.61	2.73
7127-1	23.79	2.57	0.96	0.00	0.96	0.32	1.61	55.63	9.00	0.64	0.32	0.00	4.18
7130-1	22.40	3.91	0.52	0.00	1.56	0.00	2.60	53.65	11.46	0.26	0.26	0.26	3.12
7129-1	32.46	5.90	0.33	0.33	3.61	0.66	1.97	35.74	15.08	0.33	0.66	0.00	2.95
7133-1	27.30	3.97	0.25	0.00	0.99	0.25	4.22	49.88	5.96	0.50	1.99	0.25	4.47
7132-1	17.41	3.16	0.00	0.00	0.63	0.00	6.33	61.39	6.01	0.95	0.63	0.32	3.16
7135-1	22.13	4.89	0.86	0.00	0.86	0.57	5.17	46.55	13.22	0.00	0.86	0.00	4.89
7136-1	14.33	3.33	0.33	0.00	1.33	0.00	6.67	61.33	6.33	0.33	1.00	0.67	4.33
7134-1	20.50	3.42	1.24	0.00	0.31	0.00	3.73	51.24	15.84	0.00	0.00	0.31	3.42
7138-1	15.04	3.17	0.00	0.00	0.53	0.26	5.01	62.27	8.44	0.53	0.26	1.32	3.17
7137-2	21.59	2.66	0.00	0.00	1.66	0.00	6.64	49.17	12.29	0.66	1.66	0.66	2.99
7139-1	11.64	5.35	0.31	0.31	1.89	0.00	9.75	56.92	8.49	1.57	1.57	0.00	2.20
7140-1	29.70	4.09	0.54	0.54	5.18	0.00	7.63	36.78	7.63	0.82	1.36	0.54	5.18
7141-1	32.61	3.26	0.00	1.09	3.53	0.27	4.62	41.03	6.52	0.00	0.82	0.54	5.71
7143-1	21.45	4.29	0.66	0.66	3.96	0.66	5.28	46.53	10.89	1.32	0.99	0.66	2.64
7144-1	14.56	5.83	0.97	0.00	3.24	0.32	4.85	52.43	11.00	0.65	0.32	1.62	4.21
7142-2	22.26	5.33	0.00	0.31	2.19	0.31	4.08	45.77	15.36	0.63	0.31	0.00	3.45
7149-1	7.24	2.63	1.64	0.00	0.66	0.00	4.93	75.00	3.95	0.99	1.32	0.00	1.64
7145-1	33.58	1.99	1.00	0.25	2.24	0.00	4.23	49.00	3.98	0.50	1.00	0.00	2.24
7146-1	31.46	2.98	0.00	0.00	0.33	0.99	3.97	50.99	6.29	0.99	0.33	0.00	1.66
7148-1	14.62	3.36	1.19	0.00	0.40	0.20	5.93	62.65	8.10	0.99	0.00	0.00	2.57
7147-1	27.91	2.84	0.78	0.00	0.26	0.26	1.81	54.26	7.75	0.26	0.52	0.00	3.36
7150-1	25.24	3.51	3.83	0.00	7.99	0.00	8.63	41.21	6.39	0.64	0.96	0.00	1.60
7153-1	19.39	1.94	1.39	0.00	2.77	0.00	4.43	60.66	5.26	0.83	2.77	0.00	0.55
7154-2	17.78	1.90	0.63	0.32	0.63	0.00	2.86	68.25	5.08	0.63	0.00	0.32	1.59
7152-1	19.54	2.32	1.32	0.00	0.99	0.00	3.64	63.91	5.96	0.99	0.33	0.00	0.99
7156-1	20.26	2.89	0.96	0.00	1.29	0.32	1.61	53.38	16.40	0.00	0.32	0.00	2.57
7209-2	9.38	3.36	0.35	0.53	3.89	0.53	7.79	53.63	18.76	1.06	0.00	0.71	0.00
7208-1	0.00	0.00	0.00	0.00	0.00	0.00	7.59	88.61	2.53	0.00	0.00	0.00	1.27
7207-1	5.83	1.67	0.28	0.00	0.00	0.28	18.89	65.56	2.78	3.06	0.00	0.56	1.11
7212-1	1.11	1.94	0.00	0.00	0.00	0.55	19.39	70.08	4.16	2.77	0.00	0.00	0.00
7213-1	3.01	0.00	0.00	0.00	0.00	0.00	26.58	58.36	5.48	6.58	0.00	0.00	0.00
7214-1	10.88	0.00	0.00	2.59	0.00	0.00	12.95	67.88	3.11	1.04	0.00	0.00	1.55
7211-1	2.87	5.26	0.00	0.48	5.26	0.48	17.22	60.77	3.83	3.83	0.00	0.00	0.00
7197-1	2.07	0.83	0.41	0.21	0.62	0.83	27.74	59.21	4.97	2.28	0.41	0.41	0.00
7195-1	5.19	0.00	0.00	0.00	0.27	0.27	13.93	64.21	10.93	1.91	0.00	3.28	0.00
7194-1	14.02	0.00	0.00	0.00	0.00	0.00	34.89	47.98	0.62	2.49	0.00	0.00	0.00
7193-1	14.87	1.75	0.00	0.58	4.66	1.17	7.58	60.06	7.00	2.33	0.00	0.00	0.00
7172-3	3.65	1.95	0.49	0.00	0.49	0.00	6.33	83.70	2.92	0.00	0.00	0.49	0.00
7175-4	3.18	2.89	0.00	0.58	1.16	0.29	2.60	79.77	6.36	0.29	0.00	2.31	0.58
7174-2	0.66	0.22	0.00	0.66	0.88	0.22	2.20	80.44	8.79	0.44	0.00	5.49	0.00
7179-1	3.02	2.68	0.00	0.00	0.34	2.01	10.40	71.14	10.07	0.00	0.00	0.00	0.34
7177-2	12.78	1.42	0.00	1.42	0.57	0.57	57.10	19.60	0.00	6.53	0.00	0.00	0.00
7180-1	1.90	0.42	0.00	0.84	0.42	0.00	11.39	82.28	0.42	2.32	0.00	0.00	0.00
7181-1	14.93	2.67	0.00	0.00	0.00	0.00	19.20	58.40	1.07	1.60	0.00	0.00	2.13
7182-1	3.35	1.46	0.00	0.63	2.72	0.00	0.84	91.00	0.00	0.00	0.00	0.00	0.00
7183-1	3.57	4.24	0.00	0.00	0.89	0.22	2.46	73.88	13.39	0.22	0.00	0.89	0.22
7192-1	7.05	1.92	0.00	1.92	5.34	2.14	9.19	66.67	3.63	0.00	0.00	1.07	1.07
7186-1	8.72	1.34	0.00	3.36	2.68	1.34	41.61	8.05	22.15	0.00	0.00	6.71	4.03
7187-1	5.91	1.75	0.00	0.88	1.09	0.00	2.63	82.71	4.60	0.00	0.00	0.44	0.00
7191-1	7.19	1.08	0.00	0.72	2.16	0.72	5.94	71.94	6.29	0.00	0.00	2.52	1.44
7189-1	4.80	1.01	0.00	2.53	0.00	1.01	13.13	69.95	5.05	0.00	0.00	2.02	0.51
7190-1	2.94	5.15	0.00	0.74	0.74	0.00	11.03	77.21	1.47	0.74	0.00	0.00	0.00

4.2. Faunal composition of planktic foraminifera

Among the 91 observed sediment samples, only 58 contained more than 200 specimens. Very low abundances of planktic foraminifera occur between 23° and 24° S, and 36° and 39° S, respectively, where nearly none of the samples passed the statistical limit. Generally, low abundances of planktic foraminifera occur south of 33°S. However, one should bear in mind that the increased fluvial input of terrigenous sediments towards the south causes an increased dilution of the biogenic signal (Scholl et al., 1970; Milliman et al., 1995). Highest planktic foraminiferal abundances are recorded between 30° and 33°S, with up to 1200 individuals per cm³. North of 25°S, the abundances are on relatively high levels (Table 1).

The most important species in the study area is *N. incompta* (57%), followed by *G. bulloides* (15%), *N. dutertrei* (~10%), and *N. pachyderma* (8%). Together with *Globigerinita glutinata* (~3%) and *Globorotalia inflata* (~2%), these species account on average for almost 95% of the total planktic foraminifera fauna (Table 2). Significant N-S distribution patterns of various species can be observed in the study area. The contributions of *N. incompta* increase from 30-70% north of 36°S to 40-90% south of 39°S (Table 2, Fig. 3). Also *N. dutertrei* shows enhanced contributions south of 39°S, with values up to 60% of the total fauna. In contrast, *G. bulloides*, *G. glutinata*, and *N. pachyderma* record decreased contributions south of 39°S. Among the less important species, highest contributions of *Globigerinoides ruber* and *Pulleniatina obliquiloculata* are displayed north of 36°S, whilst *Turborotalita quinqueloba*, *Orbulina universa*, and *Globorotalia crassaformis* show increased contributions south of 39°S (Table 2, Fig. 3). The remaining species do not show any significant latitudinal distribution pattern.

Assuming water depth as a proxy for distance to coast, the contributions of various planktic foraminifera species reveal distinct patterns. Regardless of their latitudinal position, the relative abundance of *N. incompta* increases in the offshore-samples, while the contributions of *G. bulloides*, *G. inflata*, and *N. pachyderma* decrease towards open ocean-samples (Fig. 4).

5. Discussion

5.1. Stable isotopes

The use of shell stable isotope composition of planktic foraminifera has been vigorously employed to estimate the chemical and physical properties of water masses (e.g. Berger, 1981; Vincent and Killingley, 1985). This method is based upon the presumption that the calcite composition of the stable isotopes of oxygen and carbon in planktic foraminiferal shells is determined by the chemical processes in the ambient water mass where planktic

foraminifera grew. However, complex biomineralizing processes in planktic foraminifera introduce vital effects overprinting the environmental signal (e.g. Erez, 1978; Spero and Williams, 1989).

Recent sediment trap and plankton tow studies from the Arctic Ocean and California Current have suggested that *N. incompta* calcifies mainly at the depth of the thermocline, between 50 and 200 m (Ortiz et al., 1995; 1996; Kohfeld et al., 1996). Within this range, *N. incompta* appears to prefer shallower waters, although the possibility exists that other nonbiological influences, such as advection, potentially influence its abundances in the water column. On the other hand, sediment trap data from the North and East Pacific suggest that *G. bulloides* thrives mainly in the surface mixed layer above the thermocline (Fairbanks et al., 1982; Sautter and Thunell, 1991). Since *N. incompta* lives and calcifies in deeper waters than *G. bulloides*, the difference of isotopic values between these species could serve as an effective monitor of the structure of the upper water column.

Generally, oxygen isotope values of planktic foraminifera specify the temperature of the ambient water mass (e.g. Mulitza et al., 1998; Niebler et al., 1999), although sea surface salinity (SSS) can effect the oxygen isotope signal as well (e.g. Wolff et al., 1999). The southward decreasing sea surface temperatures (SST) trend of $>6^{\circ}$ C in the study area anticipate a general southward increase in the $\delta^{18}\text{O}$ values of both species, which indeed can be observed and attributed to the temperature decrease (Fig. 2a, b). However, the rather slight increase in the *N. incompta* $\delta^{18}\text{O}$ values corresponds with a remarkable southward increase in the *G. bulloides* $\delta^{18}\text{O}$ values.

Coastal upwelling north of 39°S causes a mixing of the cold, subsurface waters with the surface waters and a deep thermocline. One result of this well-mixed upper water column is that the significance of different depth habitats of discrete planktic foraminiferal species becomes rather marginal and thus, a roughly identical $\delta^{18}\text{O}$ signal of these species occurs. This becomes obvious by looking at the $\delta^{18}\text{O}$ - difference of *G. bulloides* and *N. incompta* showing values around zero north of 39°S (Fig. 5b). South of 40°S , the prevailing Southern Westerlies prevent coastal upwelling and lead to a well-stratified water column, which is additionally consolidated by high fresh water input from the continent into the ocean (Strub et al., 1998). This situation results in differences between the oxygen isotopic data of either species in the south of the study area (Fig. 5b). Nevertheless, south of 39°S the expectedly surface dwelling *G. bulloides* tends to much heavier $\delta^{18}\text{O}$ values than *N. incompta*.

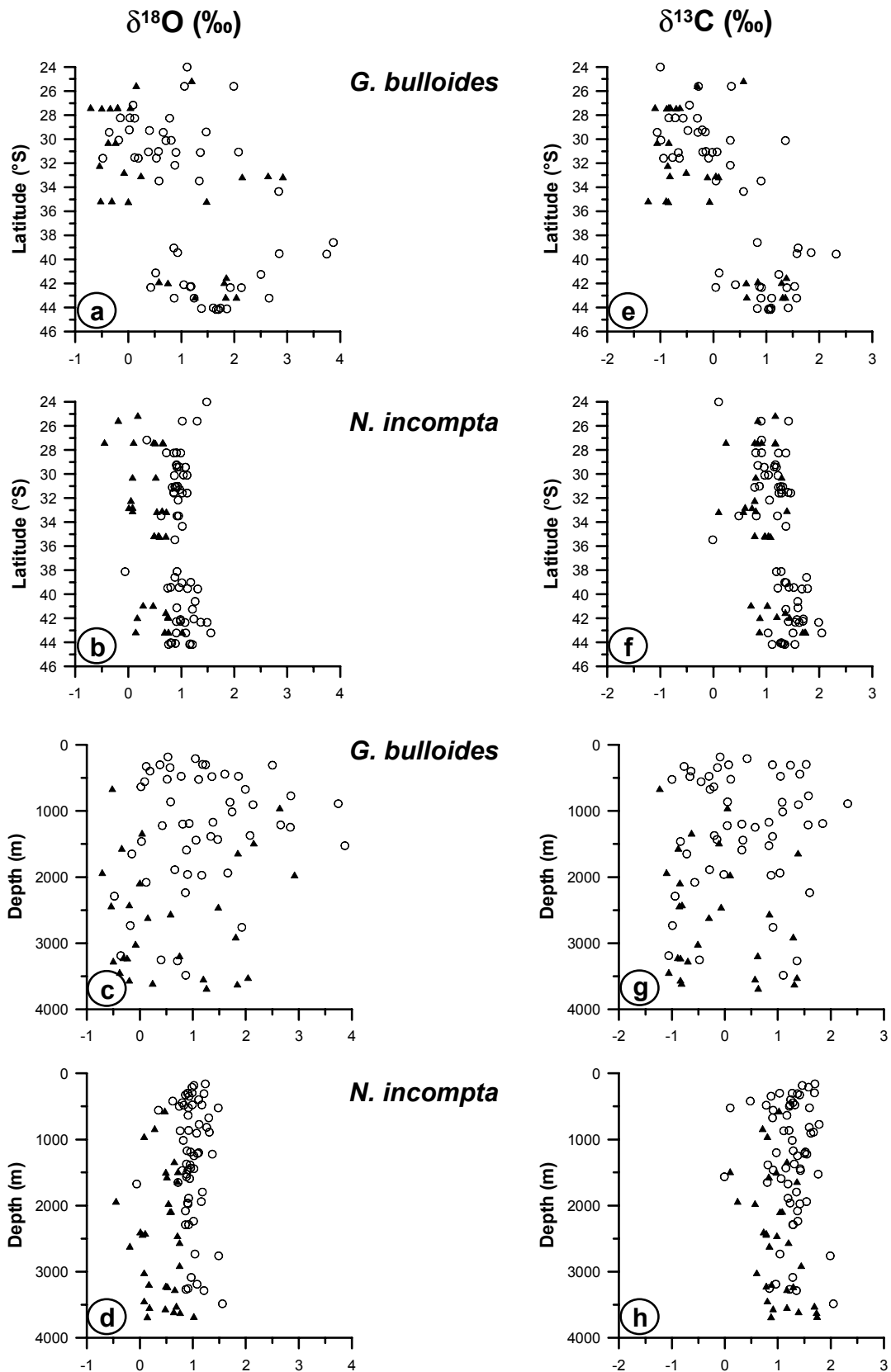


Fig. 2 Stable oxygen and carbon isotope data of *N. incompta* and *G. bulloides* in surface sediments along the Chilean continental slope. Open circles symbolize data from this study. Solid triangles represent data from Hebbeln et al. (2000a). a-d: $\delta^{18}\text{O}$ data (vs. PDB); e-h: $\delta^{13}\text{C}$ data (vs. PDB).

Recent studies from the Southern Ocean suggest that *G. bulloides* is not strictly surface dwelling, with core-top $\delta^{18}\text{O}$ values heavier from the predicted surface mixed layer (Mortyn and Charles, 2003). This feature in addition to different seasonal preferences of the two species may explain surprising high values of *G. bulloides* compared to *N. incompta*.

The $\delta^{13}\text{C}$ of planktic foraminifera could contain information about the composition of the $\delta^{13}\text{C}$ of the ambient water, which is controlled by several factors such as air-sea exchange (Broecker and Maier-Reimer, 1992; Charles et al., 1993), global ocean reservoir changes in $\delta^{13}\text{C}$ of CO_2 (Duplessy et al., 1988), and mixing of water masses (Lynch-Stieglitz et al., 1994). Oceanic $\delta^{13}\text{C}$ also varies with the nutrient concentrations and the preferential uptake of ^{12}C during photosynthesis (Broecker and Peng, 1982). The vital effects of a given planktic foraminifera species, specially symbiont-bearing foraminifera, additionally overprint any $\delta^{13}\text{C}$ changes (e.g. Billups and Spero, 1995; Ravelo and Fairbanks, 1995).

Both *N. incompta* and *G. bulloides* are symbiont-barren, and most abundant during periods of high phytoplankton productivity (Fairbanks et al., 1982; Reynolds and Thunell, 1985; Sautter and Thunell, 1991; Ortiz et al., 1995; Kohfeld et al., 1996). Following these authors, the information stored in the $\delta^{13}\text{C}$ data of these species could roughly reflect changes in the primary production in the uppermost 200 m. Both species show heavier $\delta^{13}\text{C}$ values south of 39°S indicating higher marine productivity in this part of the study area (Fig. 2e, f). The distance to the coast is apparently insignificant for the $\delta^{13}\text{C}$ composition of either species since almost all the samples lie within the high-productivity area off Chile (Fig. 2g, h).

Another prominent observation is that the *N. incompta* $\delta^{13}\text{C}$ values are much heavier compared to *G. bulloides* $\delta^{13}\text{C}$ values north of 39°S , whereas south of 39°S , the values are almost similar (Fig. 2e, f). This feature can be explained by the different habitats of these species under different hydrological regimes ruling off the Chilean coast, as mentioned above for the $\delta^{18}\text{O}$ data. The preferred absorption of ^{12}C by photosynthesis leads to ^{13}C enriched surface waters (Kroopnick, 1985), and causes relatively heavier $\delta^{13}\text{C}$ values of the surface dwelling *G. bulloides* south of 39°S (Fig. 5c, corrected for vital effect). This setting is disturbed by coastal upwelling and mixing of water masses north of 39°S , where $\delta^{13}\text{C}$ values of *N. incompta* show heavier values (Fig. 5c).

Fig. 5a shows the $\delta^{18}\text{O}$ - $\delta^{13}\text{C}$ relationship for *G. bulloides* and *N. incompta*. From these data it is evident that *G. bulloides* shows a broader range in its isotopic values with generally lighter $\delta^{13}\text{C}$ than *N. incompta*, which is reasonable considering the different vital effects of either species (e.g. Kohfeld et al., 1996; Spero and Lea, 1996). Furthermore, a group of *G. bulloides*

isotopic data with atypically heavy $\delta^{18}\text{O}$ values can be distinguished (marked with ellipse). The $\delta^{18}\text{O}$ of *N. incompta* as well as the $\delta^{13}\text{C}$ of both species in the same samples, however, are well inside the normal range. This appearance, also observed by Hebbeln et al. (2000a) in a few samples, cannot be explained at the moment. A better understanding of the variations and dynamics in the habitats and isotopic signals of these species requires a higher spatial coverage of field data such as plankton tow and sediment traps from this part of the world ocean.

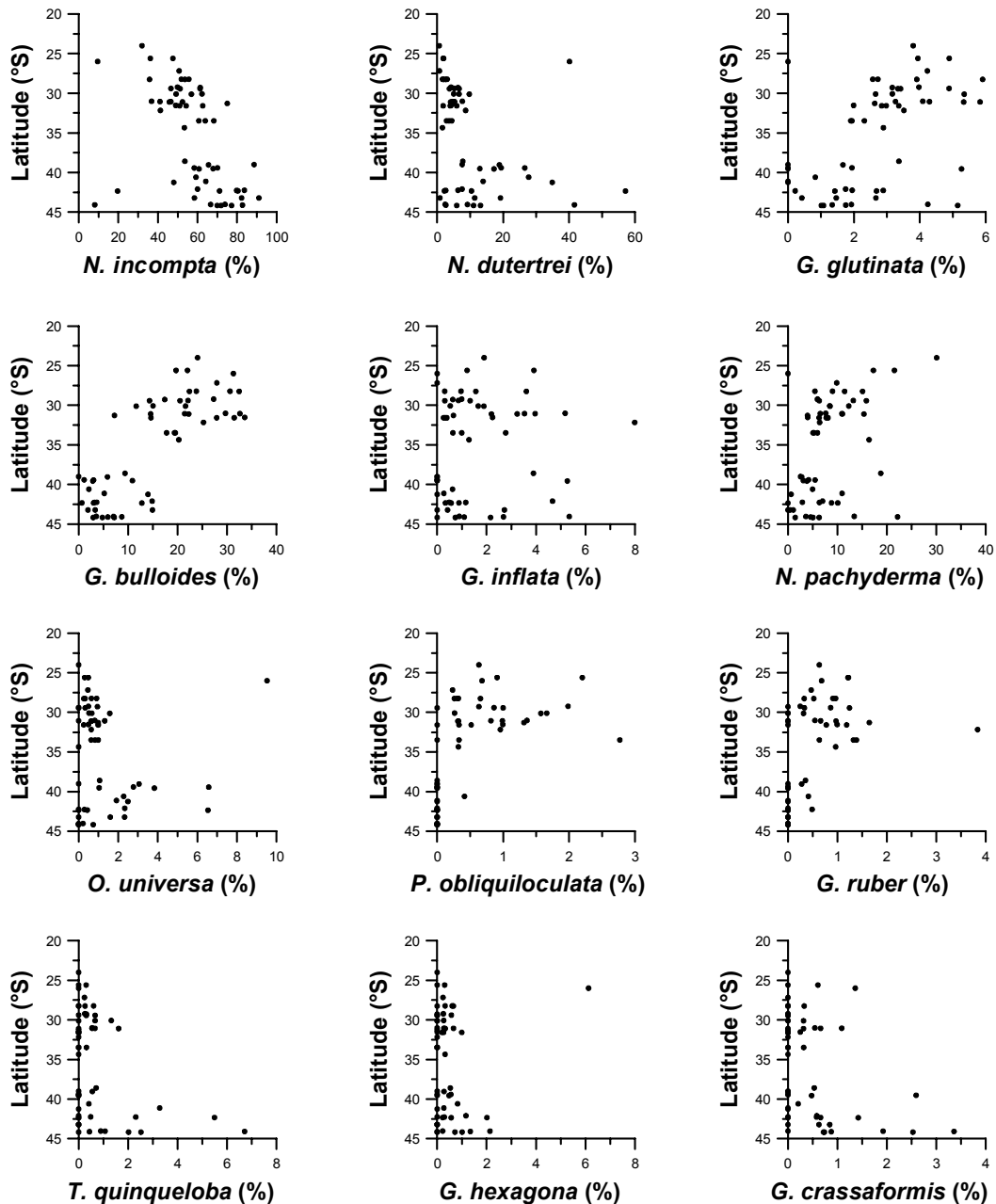


Fig. 3 Relative contributions of various species of planktic foraminifera (>150 μm) in surface sediments along the Chilean continental slope. Note the different scales for each panel.

5.2. Faunal composition of planktic foraminifera

An upwelling fauna, accompanied with tropical/subtropical species, dominates the planktic foraminiferal assemblage north of 39° S. From a number of recent studies it is evident that *G. bulloides* and *N. pachyderma* are principal upwelling indicators under upwelling conditions (e.g. Thiede, 1975; Reynolds and Thunell, 1985; Wefer et al., 1996; Little et al., 1997; Marchant et al., 1998; Ufkes et al., 1998; Ivanova et al., 1999; Hebbeln et al., 2000a). This is also indicated in our data, with relatively higher abundances of both species towards the coast, where the upwelling is strongest, and lower contributions towards the open ocean (Fig. 4), as well as in their latitudinal distribution with highest contribution in the upwelling areas north of 39°S (Fig. 3). Interestingly, contributions of *G. glutinata*, as another upwelling indicator off Chile (Thiede et al., 1975; Marchant et al., 1998), follow the same latitudinal distribution pattern recorded for *G. bulloides* and *N. pachyderma*, but are relatively independent of their distance to the coast (Fig. 3).

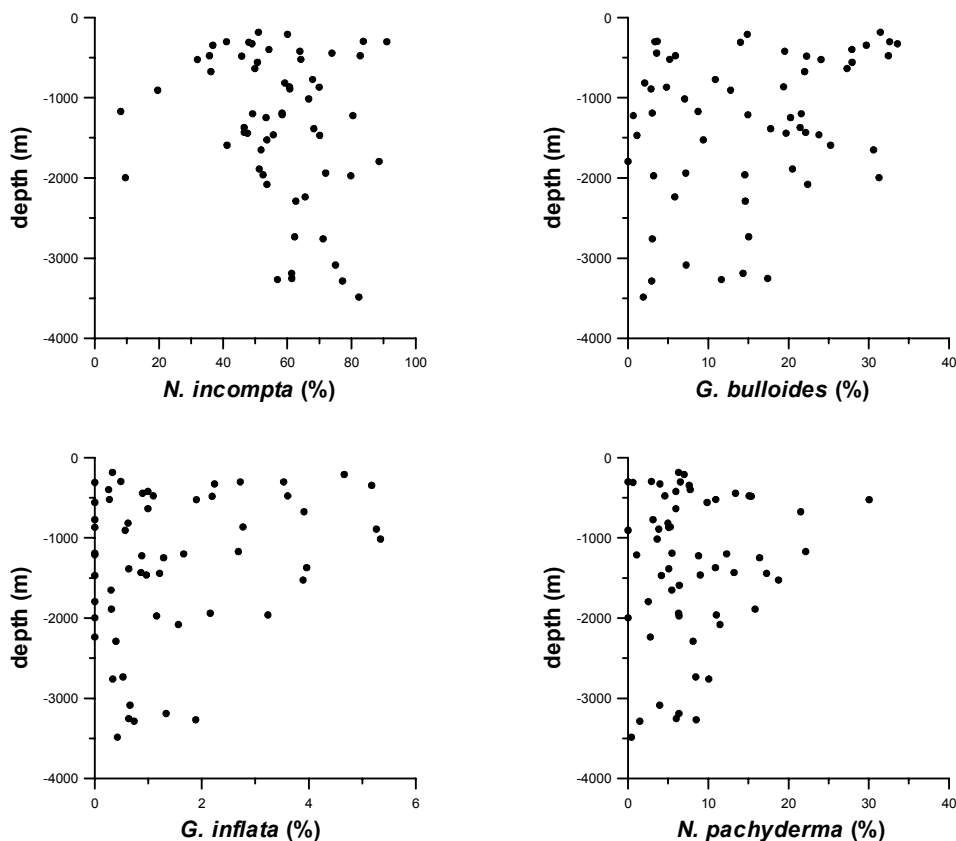


Fig. 4 Relative contributions of a few planktic foraminifera species versus depth as indicator of distance to coast.

The contributions of *G. inflata* with regard to distance to the coast draw the same pattern as observed for *G. bulloides* and *N. pachyderma* (Fig. 4). Surface samples and downcore investigations in the E and SE Pacific indicate that *G. inflata* is tightly coupled with the periods of strong upwelling and high productivity (Marchant et al., 1999; Hebbeln et al., 2000a; 2002; Feldberg and Mix, 2003; Martinez et al., 2003; Mohtadi et al., in press). Contributions of *G. inflata*, however, do not show a significant latitudinal trend, as recorded for *G. bulloides* and *N. pachyderma* suggesting that the abundance of this species in the study area is related rather to high productivity and food availability than to upwelling. This is true also for *N. incompta* with highest contributions in the south of the study area (south of 40°S), where data from planktic foraminifera as well as from other proxies do not give any hint to coastal upwelling (Hebbeln et al., 2000a; Romero and Hebbeln, 2003).

Enhanced contributions of transitional/subpolar species *T. quinqueloba* and *G. crassaformis* in the south, and of tropical/subtropical species *P. obliquiloculata* and *G. ruber* in the north fit in the general latitudinal temperature gradient of the study area (Fig. 3). Increased contributions of subtropical/transitional species *N. dutertrei* and *O. universa* in the south, however, suppose other distribution mechanisms such as advection beside temperature. If this is true, then most probably two different water masses are responsible for the delivery of these species. A southern source could be the southern limb of the South Pacific subtropical gyre transporting these species attached to the ACC into the study area. The northern source could be the warm surface waters of the PCCC transporting *N. dutertrei* into the study area, as inferred from sediment trap data by Marchant et al. (1998).

Plankton tow and sediment studies from the North Pacific demonstrate that *G. hexagona* is most abundant in subsurface waters below 400 m, that are not rapidly exchanged with the surface waters (Coulbourn et al., 1980; Ortiz et al., 1996). Hence, the rather invariable spatial abundance of this species can be explained by its deep habitat independent of hydrological changes in the surface waters of the study area (Fig. 3).

5.3. Productivity along the Chilean continental slope

Coastal Zone Color Scanner (CZCS) images show lowest pigment concentrations along the Chilean coast north of 33°S. South of 33°S, the pigment concentrations extend up continuously reaching their highest values between 37°S and 42°S (Thomas et al., 1994). These findings are generally corroborated by contents of organic carbon and biogenic opal, and diatom concentrations, of which lowest values appear between 26°S and 33°S, highest values at 34° - 38°S for opal and diatom and at 36° for organic carbon, and relatively high

values at 41° - 42°S (Fig. 6, Hebbeln et al., 2000a; Romero and Hebbeln, 2003). Between 38°-39°S, all values drop to much lower levels.

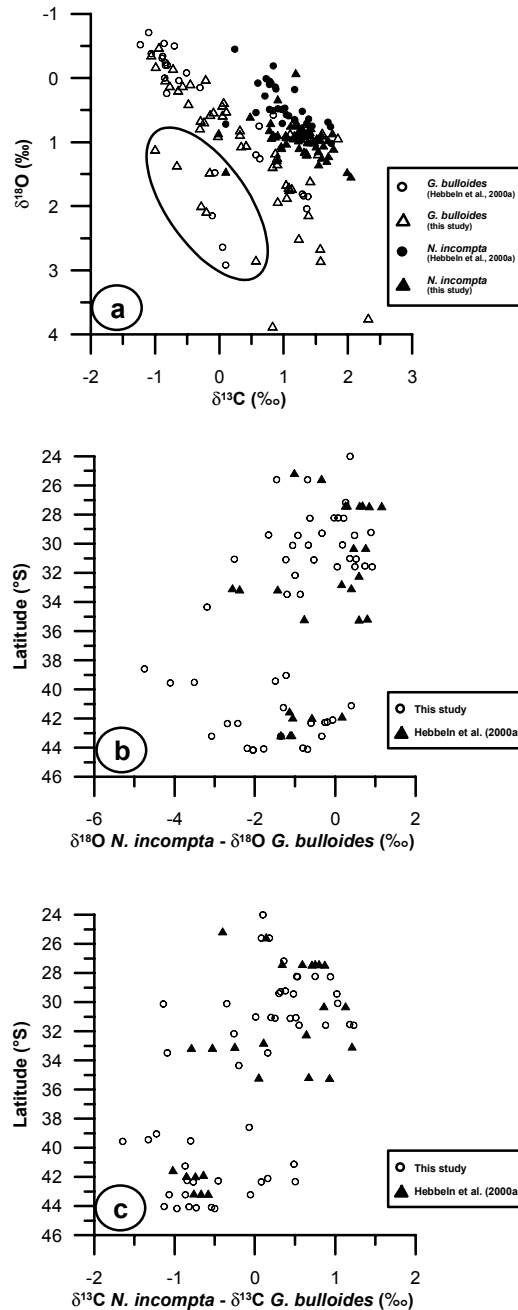


Fig. 5 a) Stable oxygen versus stable carbon isotopes of *N. incompta* (black dots and solid triangles) and *G. bulloides* (open circles and triangles) in the surface sediments along the Chilean continental slope. Samples with heavy $\delta^{18}\text{O}$ values are marked with the ellipse. b) Difference between the oxygen isotope values of *N. incompta* and *G. bulloides* as a proxy for the stratification of the water column. Values around zero suggest a deep thermocline and a well-mixed surface/subsurface layer. c) Difference between the carbon isotope values of *N. incompta* and *G. bulloides* (corrected for vital effect). Positive values north of 39°S indicate coastal upwelling, whereas negative values south of it represent stratified upper water column.

However, consistent with our planktic foraminiferal data, opal and diatom values are relatively high north of 26°S. Furthermore, high chlorophyll values have been recorded at 22° - 23°S almost year-round (Marin and Olivares, 1999). Possible explanation for the inconsistency between CZCS and biogenic phyto- and zooplankton data is that CZCS images are gained from the uppermost centimeters of the water column, while diatoms and planktic foraminifera thrive in a much wider range of depth, as proposed by Romero and Hebbeln (2003).

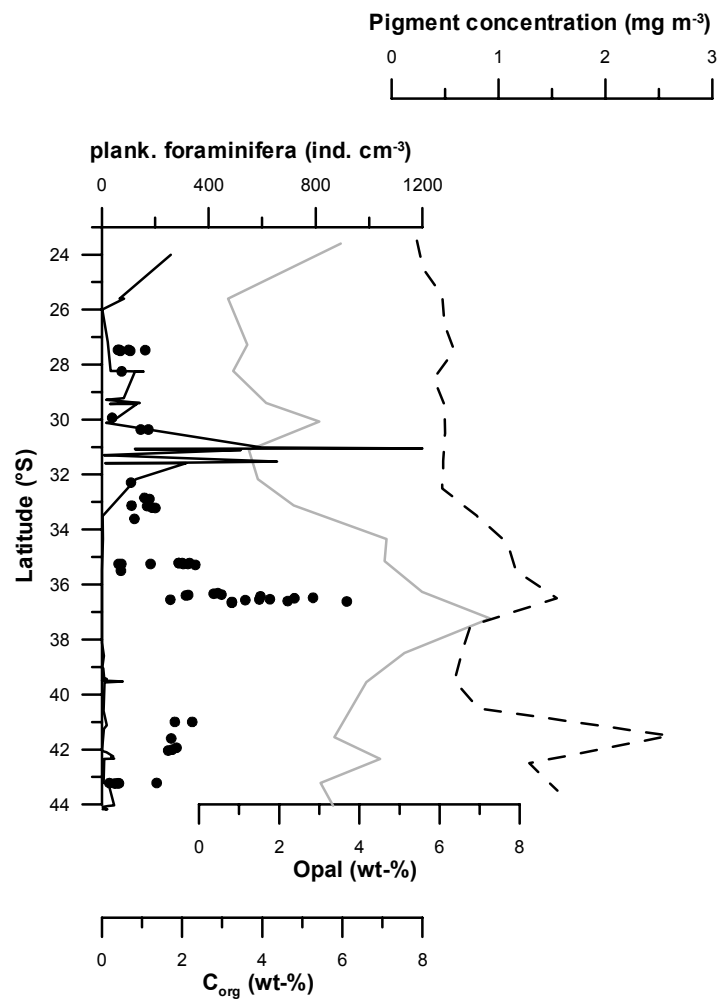


Fig. 6 Latitudinal distribution of different productivity proxies off Chile. Solid line: Absolute abundances of total planktic foraminifera in surface sediments from the Chilean continental margin, in individuals per cm⁻³. Dashed line: Pigment concentration in the surface waters derived from Coastal zone Color Scanner Data (CZCS), in mg m⁻³ (<http://daac.gsfc.nasa.gov>). Gray line: Opal contents in surface sediment samples from the Chilean continental slope, in wt% (Romero and Hebbeln, 2003). Black dots: Organic carbon (C_{org}) contents in surface sediment samples from the Chilean continental slope, in wt% (Hebbeln et al., 2000a).

Five main upwelling cells are presently observed off Chile (Strub et al., 1998). However, only three, at 23°S, at 30°S and at 33°S are indicated in our data (Fig. 6). Sediment samples beneath the upwelling cell at 36° - 38°S are almost free of planktic foraminifera, although the contents of other productivity proxies are highest (Fig. 6). This occurrence cannot be explained by dilution, as it should have affected the other data as well. Most probably the interference of carbonate dissolution at the sediment-water interface affects the contents of planktic foraminifera in the surface sediments. A better assessment of this issue requires detailed geochemical and hydrological investigations of water column and surface sediments from this area. South of 39°S, the concentrations of productivity proxies are diluted due to high terrigenous sediment input from the continent in this part of the study area. The accumulation rates of these proxies give a better estimation of marine productivity and mark highest values within the study area (Scholl et al., 1970; Lamy et al., 1999).

High marine productivity south of 39°S is most likely caused by higher continental runoff and supply of iron and other micronutrients into the coastal regions on one hand, and delivery of macronutrients such as phosphate and nitrate by the ACC (Levitus et al., 1994) on the other hand. The ACC is a high nutrient – low Chlorophyll water mass which is typically iron-depleted (de Baar et al., 1995; 1999). Hence, relatively lower productivities north of 39°S might be due to micronutrient depletion in the surface waters. There, coastal upwelling seems to be the main promoter for the high productivity by recycling of the nutrients which are transported northward by the PCC (Hebbeln et al., 2000a).

6. Conclusions

Spatial distribution of the isotopic signal preserved in shells of *G. bulloides* and *N. incompta* as well as the qualitative composition of the planktic foraminiferal fauna provide a comprehensive model of the main oceanographic processes off Chile. It also has implications for the interpretation of downcore analyses and thus, paleoenvironmental reconstructions within this area.

Our data suggest two different controlling mechanisms for the productivity along the PCC. North of 39°S, high marine productivity is caused by prevailing coastal upwelling with two centers north of 24°S and between 30°S and 33°S. High contributions of *G. bulloides*, *N. pachyderma* and *G. glutinata* characterize a typical upwelling fauna in this area. Contributions of the first two species are highest close to the coast, where upwelling is strongest. Almost similar $\delta^{18}\text{O}$ values of *G. bulloides* and *N. incompta* additionally point to a well-mixed upper water column caused by coastal upwelling.

South of 39°S, our data point to a predominant high-productivity environment under non-upwelling conditions. The $\delta^{13}\text{C}$ values of both *G. bulloides* and *N. incompta* record higher values south of 39°S suggesting that highest marine productivity off Chile takes place within this area. Different $\delta^{18}\text{O}$ values of the same species mirror a well-stratified upper water column, which is also documented in very low contributions of upwelling indicating species. The transition zone from coastal upwelling to non-upwelling setting between 36° S and 39° S cannot be precisely detected since statistically significant data on planktic foraminifera do not exist from this area.

Subtropical planktic foraminifera species such as *G. ruber* and *P. obliquiloculata* are most likely transported to the study area with the PCCC and record highest contributions in the north of the study area, whereas *N. dutertrei* and *O. universa* are probably advected with SE Pacific subtropical gyre into the ACC and show highest abundances in the south of the study area.

Acknowledgements

We thank M. Segl and B. Meyer-Schack for performing the stable isotope measurements. This study was supported by the German Bundesministerium für Bildung und Forschung through funding of the project “PUCK” (03G0156A). M. Marchant acknowledges financial support by the Deutscher Akademischer Austauschdienst (DAAD), the Chilean National Commission for Science and Technology for FONDAP-COPAS (project no. 150100007), and FONDECYT (projects no. 1040968 and 1010912). The Research Center Ocean Margins at the University of Bremen and Departamento de Zoología (Universidad de Concepción) provided technical support. The data presented in this paper are also available in digital format (www.pangaea.de/PangaVista). This is a RCOM publication Nr.

References

- Bandy, O.L. and Rodolfo, K.S., 1964. Distribution of foraminifera and sediments, Peru-Chile trench area. *Deep-sea Research*, 11: 817-837.
- Bé, A.W.H. and Tolderlund, D.S., 1971. Distribution and ecology of living planktonic foraminifera in surface water of the Atlantic and Indian Oceans. In: B.M. Turnell and W.R. Riedel (Editors), *The Micropaleontology of the Ocean*. Cambridge University Press, pp. 105-149.
- Bemis, B.E., Spero, H.J., Bijma, J. and Lea, D.W., 1998. Reevaluation of the oxygen isotopic composition of planktonic foraminifera: Experimental results and revised paleotemperature equations. *Paleoceanography*, 13(2): 150-160.
- Berger, W.H., 1981. Oxygen and carbon isotopes in foraminifera: an introduction. *Paleogeography, Paleoclimatology, Paleoecology*, 33: 3-7.
- Berger, W.H., Fischer, K., Lai, C. and Wu, G., 1987. Ocean productivity and organic carbon flux. (Part I: Overview and maps of primary productivity and export production). University of California: San Diego: SIO ref. 87-30.
- Billups, K. and Spero, H.J., 1995. Relationship between shell size, thickness and stable isotopes in individual planktonic foraminifera from two Equatorial Atlantic cores. *Journal of Foraminiferal Research*, 25(1): 24-37.
- Broecker, W.S. and Peng, T.H., 1982. *Tracers in the Sea*. Lamont Doherty Geol. Obs. Publications, New York, 689 pp.
- Broecker, W.S. and Maier-Reimer, E., 1992. The influence of air and sea exchange on the carbon isotope distribution in the sea. *Global Biogeochemical Cycles*, 6: 315-320.
- Charles, C.D., Wright, J.D. and Fairbanks, R.G., 1993. Thermodynamic influences on the marine carbon isotope record. *Paleoceanography*, 8(6): 691-697.
- Coulbourn, W.T., Parker, F.L. and Berger, W.H., 1980. Faunal and solution patterns of planktonic foraminifera in surface sediments of the North Pacific. *Marine Micropaleontology*, 5: 329-399.
- de Baar, H.J.W., de Jong, J.T.M., Bakker, D.C.E., Löscher, B.M., Veth, C., Bathmann, U. and Smetacek, V., 1995. Importance of iron for plankton blooms and carbon dioxide drawdown in the Southern Ocean. *Nature*, 373: 412-415.
- de Baar, H.J.W., de Jong, J.T.M., Nolting, R.F., Timmermanns, K.R., van Leeuwe, M.A., Bathmann, U., van der Loeff, M.R. and Sildam, J., 1999. Low dissolved Fe and the absence of diatom blooms in remote Pacific waters of the Southern Ocean. *Marine Chemistry*, 66: 1-34.
- Donner, B. and Wefer, G., 1994. Flux and stable isotope composition of *Neogloboquadrina pachyderma* and other planktonic foraminifers in the Southern Ocean (Atlantic sector). *Deep Sea Research Part I: Oceanographic Research Papers*, 41(11-12): 1733-1743.

- Duplessy, J.C., Shackleton, N.J., Fairbanks, R.G., Labeyrie, L., Oppo, D. and Kallel, N., 1988. Deepwater source variations during the last climatic cycle and their impact on the global deepwater circulation. *Paleoceanography*, 3(3): 343-360.
- Erez, J., 1978. Vital effect on stable-isotope composition seen in foraminifera and coral skeletons. *Nature*, 273: 199-202.
- Fairbanks, R.G., Sverdrlove, M., Free, R., Wiebe, P.H. and Bé, A.W.H., 1982. Vertical distribution and isotopic fractionation of living planktonic foraminifera from the Panama Basin. *Nature*, 298: 841-844.
- Feldberg, M.J. and Mix, A.C., 2002. Sea-surface temperature estimates in the Southeast Pacific based on planktonic foraminiferal species; modern calibration and Last Glacial Maximum. *Marine Micropaleontology*, 44(1-2): 1-29.
- Feldberg, M.J. and Mix, A.C., 2003. Planktonic foraminifera, sea surface temperatures, and mechanisms of oceanic change in the Peru and south equatorial currents, 0-150 ka BP. *Paleoceanography*, 18(1): 1016, doi: 10.1029/2001PA000740.
- Fischer, G. and Wefer, G., 1999. Use of proxies in paleoceanography: examples from the South Atlantic. Springer, Berlin, 727 pp.
- Garleff, K., Schäbitz, F., Stingl, H. and Veit, H., 1991. Jungquartäre Landschaftsentwicklung beiderseits der Ariden Diagonale Südamerikas. *Bamberger Geographische Schriften*, 11: 359-394.
- Hebbeln, D., Wefer, G. and cruise participants, 1995. Cruise Report of R/V SONNE Cruise 102, Valparaiso-Valparaiso, 9.5.-28.6.95. *Berichte aus dem Fachbereich Geowissenschaften*, 68. Universität Bremen, Bremen, 126 pp.
- Hebbeln, D., Marchant, M., Freudenthal, T. and Wefer, G., 2000a. Surface sediment distribution along the Chilean continental slope related to upwelling and productivity. *Marine Geology*, 164(3-4): 119-137.
- Hebbeln, D. et al., 2001. PUCK, report and preliminary results of R/V Sonne cruise SO 156, Valparaiso (Chile) - Talcahuano (Chile), March 29 - May 14, 2001. *Berichte aus dem Fachbereich Geowissenschaften*, 182. Universität Bremen, 195 pp.
- Hebbeln, D., Marchant, M. and Wefer, G., 2002. Paleoproductivity in the southern Peru-Chile Current through the last 33000 yr. *Marine Geology*, 186(3-4): 487-504.
- Hemleben, C., Spindler, M. and Anderson, O.R., 1989. *Modern planktonic foraminifera*. Springer, New York, 363 pp.
- Heusser, C.J., 1984. Late Quaternary climates of Chile. In: J.C. Vogel (Editor), *Late Cenozoic Palaeoclimates of the Southern Hemisphere*. Balkema, Rotterdam, pp. 59-83.
- Ingle, J.C., Keller, G. and Kolpack, R.L., 1980. Benthic foraminiferal biofacies, sediments and water masses of the southern Peru-Chile Trench area, southeastern Pacific Ocean. *Micropaleontology*, 26: 113-150.

- Ivanova, E.M., Conan, S.M.-H., Peeters, F.J.C. and Troelstra, S.R., 1999. Living *Neogloboquadrina pachyderma* sin and its distribution in the sediments from Oman and Somalia upwelling areas. *Marine Micropaleontology*, 36(2-3): 91-107.
- Kennett, J.P. and Srinivasan, M., 1983. Neogene planktonic foraminifera - A Phylogenetic atlas. Hutchinson Ross Publishing, Stroudsburg, 265 pp.
- Klump, J., Hebbeln, D. and Wefer, G., 2000. The impact of sediment provenance on barium-based productivity estimates. *Marine Geology*, 169: 259-271.
- Kohfeld, K.E., Fairbanks, R.G., Smith, S.L. and Walsh, I.D., 1996. *Neogloboquadrina pachyderma* (sinistral coiling) as paleoceanographic tracers in polar oceans: Evidence from Northeast Water Polynya plankton tows, sediment traps, and surface sediments. *Paleoceanography*, 11(6): 679-699.
- Krissek, L.A., Scheidegger, K.F. and Kulm, L.D., 1980. Surface sediments of the Peru-Chile continental margin and the Nazca plate. *Geological Society of America Bulletin*, 91: 321-331.
- Kroopnick, P., 1985. The distribution of ^{13}C of ΣCO_2 in the world oceans. *Deep-Sea Research*, 32: 57-84.
- Labeyrie, L.D., Duplessy, J.-C., Duprat, J., Juillet-Leclerc, A., Moyes, J., Michel, E., Kallel, N. and Shackleton, N.S., 1992. Changes in the vertical structure of the North Atlantic Ocean between glacial and modern times. *Quaternary Science Reviews*, 11: 401-413.
- Lamy, F., Hebbeln, D. and Wefer, G., 1998b. Terrigenous sediment supply along the Chilean continental slope: modern regional patterns of texture and composition. *Geologische Rundschau*, 87: 477-494.
- Lamy, F., Hebbeln, D. and Wefer, G., 1999. High resolution marine record of climatic change in mid-latitude Chile during the last 28,000 years based on terrigenous sediment parameters. *Quaternary Research*, 51: 83-93.
- Lea, D.W., Pak, D.K. and Spero, H.J., 2000. Climate impact of late Quaternary Equatorial Pacific sea surface temperature variations. *Science*, 289: 1719-1724.
- Levitus, S., Burgett, R. and Boyer, T.B., 1994. World Ocean Atlas 1994, 3: Nutrients. NOAA, US Department of Commerce, Washington, DC.
- Little, M.G., Schneider, R.R., Kroon, D., Price, B., Bickert, T. and Wefer, G., 1997. Rapid paleoceanographic changes in the Benguela Upwelling System for the last 160,000 years as indicated by abundances of planktonic foraminifera. *Palaeogeography, Palaeoclimatology, Palaeoecology*, 130: 135-161.
- Lynch-Stieglitz, J., Fairbanks, R.G. and Charles, C.D., 1994. Glacial-interglacial history of Antarctic Intermediate Water: Relative strengths of Antarctic versus Indian Ocean sources. *Paleoceanography*, 9(1): 7-29.
- Marchant, M., Hebbeln, D. and Wefer, G., 1998. Seasonal flux patterns of planktic foraminifera in the Peru-Chile Current. *Deep-Sea Research I*, 45: 1161-1185.

- Marchant, M., Hebbeln, D. and Wefer, G., 1999. High resolution planktic foraminiferal record of the last 13,300 years from the upwelling area off Chile. *Marine Geology*, 161: 115-128.
- Marin, V.H. and Olivares, G.R., 1999. Estacionalidad de la productividad primaria en Bahía Mejillones del Sur (Chile): una aproximación proceso-funcional. *Revista Chilena de Historia Natural*, 72: 629-641.
- Martinez, I., Keigwin, L.D., Barrows, T.T., Yokoyama, Y. and Southon, J., 2003. La Niña-like conditions in the eastern equatorial Pacific and a stronger Choco jet in the northern Andes during the last glaciation. *Paleoceanography*, 18(2): 1033, doi: 10.1029/2002PA000877.
- Meggers, H., Freudenthal, T., Nave, S., Targarona, J., Abrantes, F. and Helmke, P., 2002. Assessment of geochemical and micropaleontological sedimentary parameters as proxies of surface water properties in the Canary Islands region. *Deep Sea Research Part II*, 49(17): 3631-3654.
- Miller, A., 1976. The climate of Chile. In: W. Schwerdtfeger (Editor), *World Survey of Climatology Vol. 12*. Elsevier, Amsterdam, pp. 113-145.
- Milliman, J.D., Rutkowski, C. and Meybeck, M., 1995. River discharge to the sea: a global river index (GLORI). LOICZ reports and studies. NIOZ, Texel, The Netherlands, 125 pp.
- Mix, A.C., Morey, A.E., Pisias, N.G. and Hostetler, S.W., 1999. Foraminiferal fauna estimates of paleotemperature: Circumventing the no-analog problem yields cool ice age tropics. *Paleoceanography*, 14(3): 350-359.
- Mohtadi, M., Romero, O.E. and Hebbeln, D., in press. Changing marine productivity off northern Chile during the last 19,000 years: a multiparameter approach. *Journal of Quaternary Science*.
- Morales, C.E., Blanco, J.L., Braun, M., Reyes, H. and Silva, N., 1996. Chlorophyll-a distribution and associated oceanographic conditions in the upwelling region off northern Chile during the winter and spring 1993. *Deep Sea Research Part I*, 43(3): 267-289.
- Mortyn, P.G. and Charles, C.D., 2003. Planktic foraminiferal depth habitat and $\delta^{18}\text{O}$ calibrations: Plankton tow results from the Atlantic sector of the Southern Ocean. *Paleoceanography*, 18(2): 1037, doi: 10.1029/2001PA000637.
- Mulitza, S., Wolff, T., Pätzold, J., Hale, W. and Wefer, G., 1998. Temperature sensitivity of planktic foraminifera and its influence on the oxygen isotope record. *Marine Micropaleontology*, 33: 223-240.
- Niebler, H.-S., Hubberten, H.-W. and Gersonde, G., 1999. Oxygen isotope values of planktic foraminifera: a tool for the reconstruction of surface water stratification. In: G. Fischer and G. Wefer (Editors), *Use of Proxies in Paleoceanography: Examples from the South Atlantic*. Springer-Verlag, Berlin, Heidelberg, pp. 165-189.

- Ortiz, J.D., Mix, A.C. and Collier, R.W., 1995. Environmental control of living symbiotic and asymbiotic foraminifera of the California Current. *Paleoceanography*, 10(6): 987-1009.
- Ortiz, J.D., Mix, A.C., Rugh, W., Watkins, J.M. and Collier, R.W., 1996. Deep-dwelling planktonic foraminifera of the northeastern Pacific Ocean reveal environmental control of oxygen and carbon isotopic disequilibria. *Geochimica et Cosmochimica Acta*, 60(22): 4509-4523.
- Parker, F., 1962. Planktic foraminifera species in Pacific sediments. *Micropaleontology*, 8: 219-254.
- Ravelo, A.C. and Fairbanks, R.G., 1995. Carbon isotopic fractionation in multiple species of planktonic foraminifera from core-tops in the tropical Atlantic. *Journal of Foraminiferal Research*, 25(1): 53-74.
- Reynolds, L.A. and Thunell, R.C., 1985. Seasonal succession of planktonic foraminifera in the subpolar North Pacific. *Journal of Foraminiferal Research*, 15: 282-301.
- Romero, O. and Hebbeln, D., 2003. Biogenic silica and diatom thanatocoenosis in surface sediments below the Peru-Chile Current: controlling mechanisms and relationship with productivity of surface waters. *Marine Micropaleontology*, 48(1-2): 71-90.
- Romero, O.E., Hebbeln, D. and Wefer, G., 2001. Temporal and spatial variability in export production in the SE Pacific Ocean: evidence from siliceous plankton fluxes and surface sediment assemblages. *Deep Sea Research I*, 48(12): 2673-2697.
- Sautter, L.R. and Thunell, R.C., 1991. Seasonal variability in the $\delta^{18}\text{O}$ and $\delta^{13}\text{C}$ of planktonic foraminifera from an upwelling environment; Sediment trap results from the San Pedro Basin, Southern California. *Paleoceanography*, 6(3): 307-34.
- Scheidegger, K.F. and Krissek, L.A., 1982. Dispersal and deposition of eolian and fluvial sediments off Peru and northern Chile. *Geological Society of America Bulletin*, 93: 150-162.
- Scholl, D.W., Christensen, M.N., Von Huene, R. and Marlow, M., S, 1970. Peru-Chile Trench. Sediments and sea-floor spreading. *Geological Society of America Bulletin*, 81: 1339-1360.
- Shaffer, G., Salinas, S., Pizarro, O., Vega, A. and Hormazabal, S., 1995. Currents in the deep ocean off Chile (30°S). *Deep-Sea Research*, 42: 425-436.
- Spero, H.J. and Williams, D.F., 1989. Opening the carbon isotope "Vital Effect" black box, 1, seasonal temperatures in the euphotic zone. *Paleoceanography*, 4(6): 593-601.
- Spero, H.J. and Lea, D.W., 1996. Experimental determination of stable isotope variability in *Globigerina bulloides*: implications for paleoceanographic reconstructions. *Marine Micropaleontology*, 28: 231-246.
- Strub, P.T., Mesías, J.M., Montecino, V., Rutllant, J. and Salinas, S., 1998. Coastal ocean circulation off western South America. In: A.R. Robinson and K.H. Brink (Editors), *The Global Coastal Ocean - Regional Studies and Synthesis*. The Sea, ideas and

- observations on progress in the study of the seas. John Wiley & Sons, Inc., New York, pp. 273-313.
- Thiede, J., 1975. Distribution of foraminifera in surface waters of a coastal upwelling area. *Nature*, 253: 712-714.
- Thomas, A.C., Huang, F., Strub, P.T. and James, C., 1994. Comparison of the seasonal and interannual variability of phytoplankton pigment concentrations in the Peru and California Current systems. *Journal of Geophysical Research*, 99: 7355-7370.
- Thomas, A.C., 1999. Seasonal distributions of satellite-measured phytoplankton pigment concentration along the Chilean coast. *Journal of Geophysical Research*, 104(C11): 25,877-25,890.
- Ufkes, E., Jansen, J.H.F. and Brummer, G.A., 1998. Living planktonic foraminifera in the eastern South Atlantic during spring: indicators of water masses, upwelling and the Congo (Zaire) River plume. *Marine Micropaleontology*, 33: 27-53.
- Vincent, E. and Killingley, J.S., 1985. Oxygen and carbon isotope record for the early and middle Miocene in the central equatorial Pacific (Leg 85) and paleoceanographic implications. *Initial Reports of the Deep Sea Drilling Project*, 85: 749-769.
- Wefer, G. et al., 1996. Late Quaternary surface circulation of the South Atlantic: The stable isotope record and implications for heat transport and productivity. In: G. Wefer, W.H. Berger, G. Siedler and D.J. Webb (Editors), *The South Atlantic: present and past circulation*. Springer, Berlin Heidelberg, pp. 461-502.
- Wolff, T., Mulitza, S., Rühlemann, C. and Wefer, G., 1999. Response of the tropical Atlantic thermocline to late Quaternary trade wind changes. *Paleoceanography*, 14(3): 374-383.

Changing marine productivity off northern Chile during the last 19,000 years: a multiparameter approach

Mohtadi, M., Romero, O. E., and Hebbeln, D.

*Department of Geosciences, University of Bremen, P.O. Box 330440, 28334 Bremen,
Germany*

Journal of Quaternary Science, in press

Abstract

A multiparameter approach including bulk sediment, planktic foraminifera, and siliceous phytoplankton was used to reconstruct rapid variations of paleoproductivity in the Peru-Chile Current System off northern Chile for the last 19 cal kyr. During the early deglaciation (19-16 cal kyr BP), our data point to strongest upwelling intensity and highest productivity of the last 19 cal kyr. The late deglaciation (16-13 cal kyr BP) is characterized by a major change in the oceanographic setting, warmer water masses and weaker upwelling ruling at the study site. Lowest productivity and weakest upwelling intensity are observed from the Early to the Middle Holocene (13-4 cal kyr BP), while the beginning of the Late Holocene (<4 cal kyr BP) is marked by increasing productivity, mainly driven by silicate-producing organisms. Changes in the productivity and upwelling intensity in our record may have resulted from a large-scale compression and/or displacement of the South Pacific subtropical gyre during more productive periods, in line with a northward extension of the Antarctic Circumpolar Current and increased advection of Antarctic water masses with the Peru-Chile Current. The corresponding increase in hemispheric thermal gradient and wind stress induced stronger upwelling. During the periods of lower productivity, this scenario probably reversed.

Keywords: Peru-Chile Current, paleoproductivity, upwelling, South Pacific, Holocene

1. Introduction

The carbon biologically fixed in the surface layer of the oceans and exported to the deep sea (the biological pump of CO₂) is one of the major factors controlling CO₂ partial pressure in the atmosphere through the Late Quaternary climatic cycles (Sarmiento and Sundquist, 1992; Broecker and Henderson, 1998). Accurate determination of this flux and its controlling factors are therefore important for understanding global carbon cycling and its response to climate change. Nowadays, 50% of the global ocean export production are produced within only 15% of the ocean area, namely in upwelling areas and in the coastal seas (Berger et al., 1989). Thus, these regions are of greatest importance for the reconstruction of paleoproductivity and its relation to climate through the Late Quaternary climatic cycles.

The central part of the Peru–Chile Current (PCC, or Humboldt Current) is among the least studied regions of the world oceans. The PCC stands out as an Eastern Boundary Current (EBC) with the longest N–S extension (over 40° of latitude), a strong continuous upwelling regime resulting in a very high biological productivity (>200 g C m⁻² yr⁻¹), and an intense cycling of carbon (Berger et al., 1987). All this makes the PCC an important part of the global carbon cycle.

Little information about the history of the productivity exists from the southern part of the PCC between ~ 20°S and 45°S. Previous studies are based on marine records located southward at 33°S (Marchant et al., 1999; Klump et al., 2001; Hebbeln et al., 2002), and at 41°S (Lamy et al., 2001; 2002). Hebbeln et al. (2000a; 2002) propose for the Chilean upwelling system that productivity is strongly related to the distance of a given site to the main nutrient source, namely the Antarctic Circumpolar Current (ACC). Thus, changes in the productivity most likely reflect the displacement of that nutrient source. Lamy et al. (1998; 1999) relate variations of grain size distribution and clay minerals in marine sediments to changes in the onshore-humidity caused by the latitudinal displacement of the Southern Westerlies. In conclusion, recent observations of marine records suggest that paleoproductivity changes off central and south Chile were caused by latitudinal displacement of both ACC and Southern Westerlies during the last 33 kyr (Lamy et al., 1998; 1999; 2001; Marchant et al., 1999; Hebbeln et al., 2002).

Contrary to the other marine records off central and south Chile, the marine sediments off north Chile contain a significant portion of terrigenous material of aeolian origin. The climate north of 30°S in Chile is hyper-arid with precipitation values <50 mm/a (Garleff et al., 1991). Numerous continental paleoclimate reconstructions based on different proxies exist for northern Chile and subtropical South America (e.g. Heusser, 1990; Grosjean, 1994; 2001;

Grosjean et al., 1995; 1997; Thompson et al., 1995; Ammann et al., 2001; Jenny et al., 2002; Latorre et al., 2002; 2003; Abbott et al., 2003). Results from these studies indicate that beside the southern westerlies, additional phenomena, e.g. extra-tropical cyclones, El Niño Southern Oscillation (ENSO) events, and the South Atlantic convergence zone affect the humidity in this region. As yet, the lack of high resolution marine records from the northern part off Chile has been a significant obstacle of tracing the Late Quaternary glacial/interglacial variability of climate–ocean interactions.

Here we present a multiparameter study based on bulk components, planktic foraminifera, and siliceous plankton, to assess the intensity of upwelling and productivity off northern Chile at $\sim 24^\circ$ S during the last deglaciation and the Holocene. We examine possible processes responsible for productivity variations by comparing our data with marine records from farther south along the Chilean coast, and continental records, in order to give a more comprehensive picture of the paleoproductivity and paleoclimate from this part of the world ocean.

2. Regional setting

The present-day hydrography north of 45° S in the SE Pacific is dominated by the northward flowing PCC (Subantarctic Surface Water, Fig. 1). The PCC originates from the ACC, when it approaches the South American continent between 40° and 45° S (Strub et al., 1998). Off the Chilean coast the PCC can be occasionally divided into an oceanic (PCC_{ocean}) and a coastal (PCC_{coast}) branch, separated by the poleward flowing Peru-Chile Counter current (PCCC, Subtropical Surface Water). The coastal branch of the PCC, also termed Chilean Coastal Current, is characterized by a significant admixture of low salinity surface waters derived from the Chilean fjord region. It extends to ~ 100 km off the coast followed by the PCCC, 100-300 km offshore, while further to the west the oceanic branch of the PCC prevails. Close to the coast these surface water masses are underlain by the poleward flowing Gunther Undercurrent (Equatorial Subsurface Water), mainly located between 100 and 400 m water depth over the shelf and the continental slope. Between 400 and 1700 m water depth Antarctic Intermediate Water (AAIW) flows equatorward, underlain by sluggishly southward flowing Pacific Deep Water (PDW) (Shaffer et al., 1995).

Perennial southerly winds result in Ekman drift-induced upwelling of cool, nutrient-rich waters along the Chilean coast (Brandhorst, 1963). Although the winds are upwelling-favorable throughout the year (Strub et al., 1998), the physical and the biological settings display distinct seasonal patterns. Between 18° S and 24° S farther offshore off northern Chile,

present-day primary productivity is highest during the austral winter (Thomas et al., 1994; Blanco et al., 2001) when sea surface temperatures are lowest. During this time the wind direction shifts from predominantly southeasterly to southwesterly directions. This seasonal pattern is reflected by the particle flux in the central PCC, with highest fluxes in late austral winter (September), intermediate fluxes until January and low fluxes between January and July (Hebbeln et al., 2000b; Romero et al., 2001).

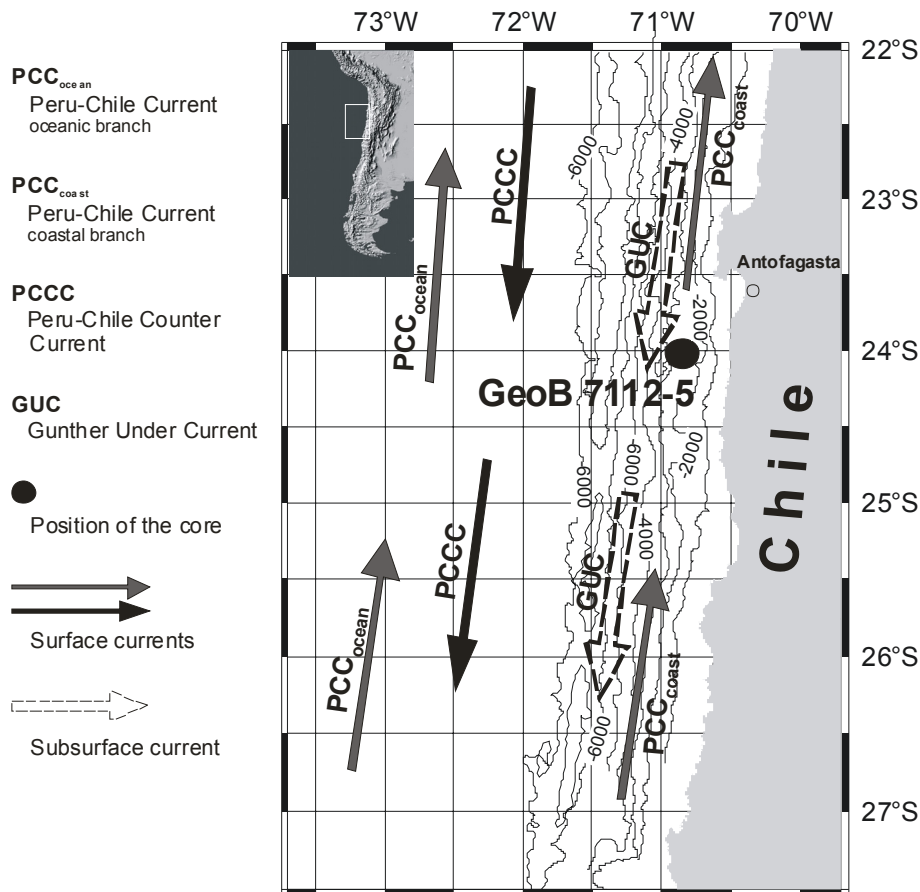


Fig. 1 Schematic map of the study area showing the location of the core and the principal oceanographic features (after Strub et al., 1998).

3. Sampling and analysis

3.1. Location

Gravity core GeoB7112-5 was collected during R/V SONNE Cruise 156 from a water depth of 2507 m on the continental slope off Antofagasta (core length 324 cm; 24°01.99'S, 70°49.41'W, Fig. 1). Lithology description and further core characteristics are given in the cruise report (Hebbeln et al., 2001).

3.2 Sampling

For this study, three sample-series of approx. 10 cm³ were taken at 5-cm intervals allowing geochemical, stable isotopic, and micropaleontological analysis to be carried out at an average sample interval of approximately 300 years. Archived core material is kept at the Department of Geosciences, University of Bremen, Germany.

3.3. Bulk geochemical analyses

The sediment sample set for bulk analyses was freeze-dried and ground in an agate mortar. Total carbon contents (TC) were measured on untreated samples. After decalcification of the samples by 6 N HCl, total organic carbon contents (TOC) were obtained by combustion at 1050°C using a Heraeus CHN-O-Rapid elemental analyzer as described by Müller et al. (1994). Carbonate was calculated from the difference between TC and TOC, and expressed as calcite ($\text{CaCO}_3 = (\text{TC} - \text{TOC}) * 8.33$). Opal was determined with a sequential leaching technique proposed by De Master (1981), modified by Müller and Schneider (1993). Accumulation rates (AR) were calculated by applying Van Andel et al. (1975) equation:

$$\text{AR}_{\text{Bulk}} (\text{g cm}^{-2} \text{ kyr}^{-1}) = \text{LSR} * \text{DBD} \quad (1)$$

with LSR = linear sedimentation rate in cm kyr⁻¹, and DBD = Dry Bulk Density in g cm⁻³. DBD was generated after the samples were freeze-dried, as:

$$\text{DBD} = \text{M}_{\text{dry}} / \text{V}_{\text{wet}} \quad (2)$$

with M_{dry} = mass of the dried sample in g, and V_{wet} = volume of the sample before freeze-drying in cm³. The AR of each component was calculated by multiplying their wt% with the AR_{Bulk} (Thiede et al., 1982).

3.4. Siliceous plankton analysis

For the study of siliceous plankton, samples were prepared following the method proposed by Schrader and Gersonde (1978). Qualitative and quantitative analyses were done at x400 magnifications using a Zeiss-Axioscope with phase-contrast illumination. Counts were carried out on permanent slides of acid-cleaned material (Mountex mounting medium). Several traverses across the cover-slip were examined, depending on microorganism abundances. At

least two cover slips per sample were scanned in this way. Diatom counting of replicate slides indicated that the analytical error of the concentration estimates is $\leq 15\%$. The counting procedure and definition of counting units for diatoms followed those of Schrader and Gersonde (1978). Diatoms and silicoflagellates were identified to the lowest taxonomic level possible. Accumulation rate of diatoms is expressed as valves per square cm per thousand years ($\text{valves cm}^{-2} \text{ kyr}^{-1}$), and of silicoflagellates as skeletons per square cm per thousand years ($\text{skeletons cm}^{-2} \text{ kyr}^{-1}$).

3.5. Planktic foraminifera analyses

The sediment sample set for foraminiferal analyses was freeze-dried, weighed and washed through a $63\mu\text{m}$ sieve. The analyses of the planktic foraminiferal fauna are based on the $>150\mu$ fraction, separated by sieving from the $>63\mu\text{m}$ fraction. This fraction was divided by using a microsplitter. All the counted sub-samples contained at least 300 individuals. All specimens were individually picked and identified following the taxonomy of planktic foraminifera proposed by Parker (1962), Kennett and Srinivasan (1983), and Hemleben et al. (1989). For *Neogloboquadrina pachyderma* the relative abundances of right (dex.) and left (sin.) coiling individuals were determined, and the two forms were treated as individual species. *Neogloboquadrina dutertrei* was distinguished from *N. pachyderma* primarily by the presence of an umbilical tooth, presence of more than four chambers, and a more pitted texture based on the description of Parker (1962). Accumulation rates of foraminifera are expressed as individuals per square cm per thousand years ($\text{ind. cm}^{-2} \text{ kyr}^{-1}$).

3.6. Stable oxygen isotope measurements

Stable oxygen isotopes were measured on shells of the planktic foraminifera species *N. pachyderma* sin. and *N. pachyderma* dex., with a Finnigan MAT 251 mass spectrometer at the isotope laboratory of Department of Geosciences, University of Bremen. Twenty individual shells were picked for each measurement. The isotopic composition of the carbonate sample was measured on the CO_2 gas evolved by treatment with phosphoric acid at a constant temperature of 75°C . For all stable oxygen isotope measurements a working standard (Burgbrohl CO_2 gas) was used, which has been calibrated against PDB by using the NBS 18, 19 and 20 standards. Consequently, all $\delta^{18}\text{O}$ data given here are relative to the PDB standard. Analytical standard deviation is about 0.07‰ PDB.

3.7. AMS-dating

Five ^{14}C AMS (accelerator mass spectrometry) dates for core GeoB7112-5 were determined on ca. 10 mg carbonate at the Leibniz laboratory for age determinations and isotope research

at the University of Kiel (Nadeau et al., 1997). All ages are corrected for ^{13}C and for a reservoir age of 400 yr after Bard (1988). In upwelling areas, such as off Chile, reservoir ages might be likely higher. However, since no information is available for this region, the mean ocean reservoir age proposed by Bard (1988) has been used (Fig. 2A). The ^{14}C ages were converted into calendar years using the Calib 4.3 software (modified version 2002, Stuiver and Reimer, 1993).

Core depth (cm)	^{14}C AMS raw age (yr BP)	\pm Err.	Calendar age (yr BP)	sedimentation rate (cm kyr $^{-1}$)
23	2680	30	2341	14.53
128	7855	55	8328	11.03
178	11,010	55	12,406	17.24
253	13,970	80	16,180	15.21
308	16,260	110	18,815	

Table 1 Conventional radiocarbon ages and converted calendar ages for core GeoB 7112-5, after Stuiver & Reimer (1993, modified 2000), with the estimated sedimentation rates.

4. Results

4.1. Age model

The age model is based on AMS ^{14}C dates (Tab. 1). Ages between dated levels were obtained by linear interpolation between the nearest AMS dating points. The time span covered by the record is about 18 kyr, derived from the calculated age for the oldest (19.14 cal kyr BP) and the youngest (1.26 cal kyr BP) parts of the core (Fig. 2A). The age model is additionally supported by the correlation of the stable oxygen isotope measurements of the record with the SPECMAP $\delta^{18}\text{O}$ stack (Imbrie et al., 1984). The generated average sedimentation rate is ~ 15.5 cm kyr $^{-1}$ (range = 11.0 – 17.2 cm kyr $^{-1}$).

4.2. Bulk components

The biogenic sedimentation is dominated by calcium carbonate (CaCO_3), followed by biogenic silica (opal) and organic carbon (C_{org}). The relative content of CaCO_3 fluctuated between ~ 5.4 and 27.3 %, biogenic silica varied between ~ 2.5 and 7.5%, while organic carbon content ranged between 1.8 and ~ 2.6 % (Fig. 2B-D).

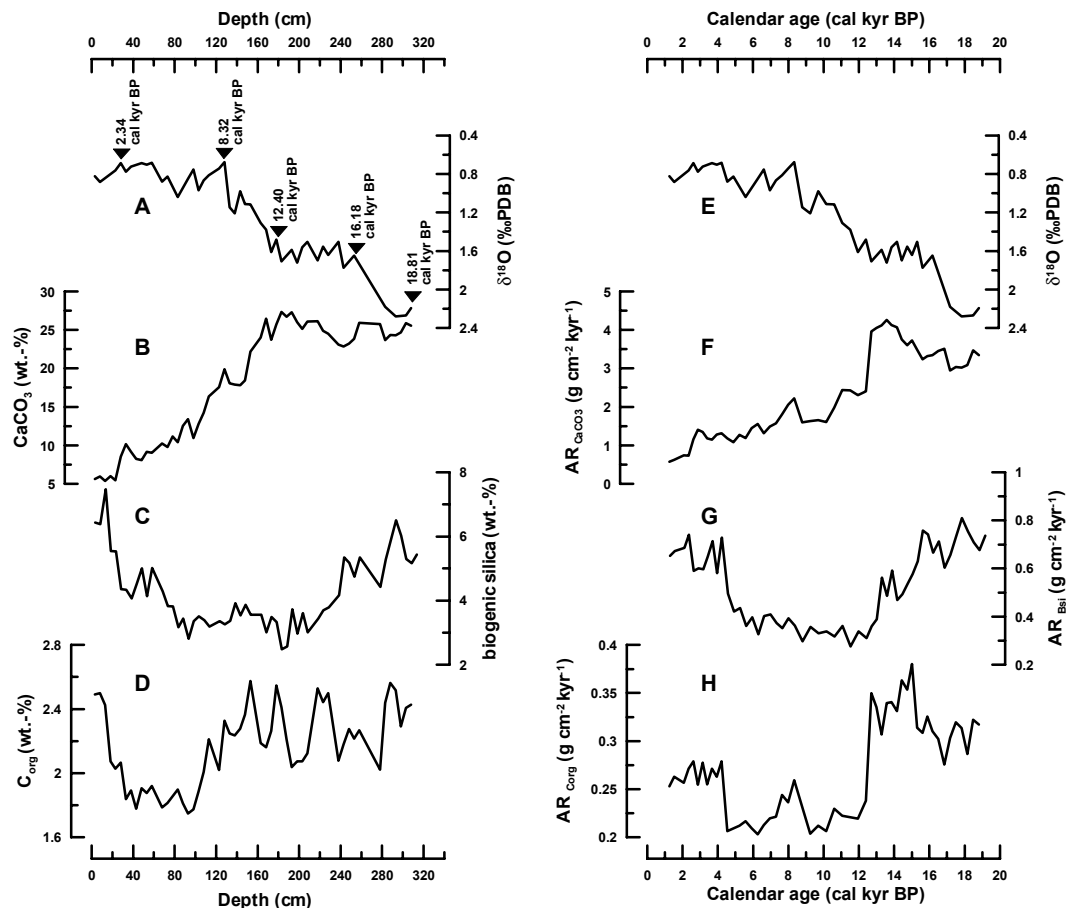


Fig. 2 Depth record of A) Stable oxygen isotopes with AMS ^{14}C data (triangles), B) CaCO_3 contents, C) Biogenic silica contents, D) Organic carbon (C_{org}) contents, and time record of E) Stable oxygen isotopes, accumulation rates of F) Calcium carbonate ($\text{AR}_{\text{CaCO}_3}$), G) Biogenic silica (AR_{Bsi}), and H) Organic carbon (AR_{Corg}), in $\text{g cm}^{-2} \text{ kyr}^{-1}$ in core GeoB 7112-5 at 24°S off northern Chile. Note the different scales for each panel.

The accumulation rate of calcium carbonate ($\text{AR}_{\text{CaCO}_3}$) ranges between ~ 0.5 and $4.2 \text{ g cm}^{-2} \text{ kyr}^{-1}$ (Fig. 2F). The highest $\text{AR}_{\text{CaCO}_3}$ occurred between ~ 14 and 13 cal kyr BP , and was followed by an abrupt diminution, and a tendency to decline towards the Early Holocene. In the study area, Carbonate Compensation Depth (CCD) and the lysocline lie presently at $\sim 4500 \text{ m}$, and $\sim 3700 \text{ m}$, respectively (Hebbeln et al., 2000a). Our core has been collected from a depth clearly above the lysocline (2500 m) and hence, should not be seriously affected by carbonate dissolution. In addition, the planktic foraminifera shells show a generally good preservation without considerable occurrence of fragmentation or species specific dissolution, as expressed in high abundances of species sensitive to carbonate-dissolution, such as *Globigerina bulloides* and *Globigerinita glutinata* (Vincent and Berger, 1981).

The AR of opal (AR_{Bsi}) decreases stepwise from 19 cal kyr BP towards the Early Holocene: two very sharp decreases are observed, after 14.8 cal kyr BP , and around $\sim 13 \text{ cal kyr BP}$ (Fig. 2G). After reaching the lowest values between ~ 12.5 and 11.5 cal kyr BP , the AR_{Bsi}

increased again. This increase was moderate during the Early (12-8 cal kyr BP) and Middle Holocene (8-4 cal kyr BP), but abrupt around 5 cal kyr BP. From 4.3 cal kyr BP towards the present, the AR_{Bsi} reached pre-Holocene values.

The AR of organic carbon (AR_{Corg}) is highest before the Holocene (>12 cal kyr BP, Fig. 2H). As already described for calcium carbonate and opal, a strong decrease occurred between 13 and 12.5 cal kyr BP. During the Holocene, the AR_{Corg} remains almost always below the average ($0.28 \text{ g cm}^{-2} \text{ kyr}^{-1}$). However, important fluctuations occurred. A sharp, minor increase is seen prior to ~8 cal kyr BP, followed by decreasing values. A second sharp increase is recorded at ~4.5 cal kyr BP.

4.3. Siliceous phytoplankton

4.3.1. Accumulation rates

The siliceous plankton community is numerically dominated by diatoms, followed by silicoflagellates. Phytoliths (silica bodies of epidermic grass cells) and the dinoflagellate *Actiniscus pentasterias* occurred in several samples. The accumulation rate of diatoms ($AR_{diatoms}$) ranges between $1.6 * 10^8$ and $6.2 * 10^6$ valves $\text{cm}^{-2} \text{ kyr}^{-1}$ (Fig. 3A). AR of silicoflagellates ($AR_{silicofl.}$) was between two and four orders of magnitude lower than the $AR_{diatoms}$ (range = $1.7 * 10^6$ - $4.7 * 10^4$ skeletons $\text{cm}^{-2} \text{ kyr}^{-1}$, Fig. 3A).

Diatoms mostly followed the downcore variations already described for opal ($r = 0.68$). The pattern of $AR_{diatoms}$ presents clearly two main phases (Fig. 3A): between ca. 19 and ~13 cal kyr BP almost all values were relatively high (~ between $1.6 * 10^8$ and $6.2 * 10^7$). At ~13 cal kyr BP an abrupt decrease occurred: the $AR_{diatoms}$ diminished by one order of magnitude in less than 1000 years. After ~12.5 cal kyr BP, the $AR_{diatoms}$ remained relatively low (~ between $5.9 * 10^7$ and $6.2 * 10^6$). A secondary abrupt, albeit minor increase occurred in the late Holocene, approximately at 3 cal kyr BP.

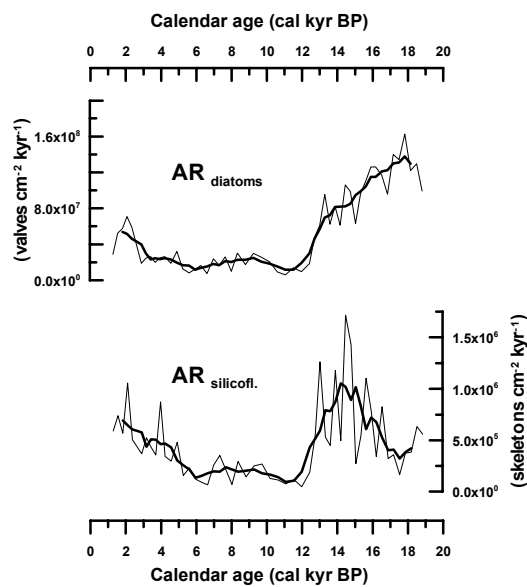
Silicoflagellates show stronger variations than diatoms. The distribution pattern is somehow similar, although highest $AR_{silicofl.}$ are observed between 16 and 13 cal kyr BP (Fig. 3A). As described for diatoms, an abrupt decrease in $AR_{silicofl.}$ occurred at ~13 cal kyr BP. Following rather low values, $AR_{silicofl.}$ started to increase to moderate values again at ~5 cal kyr BP, with two peaks at 3.9 and 2.0 cal kyr BP.

4.3.2. Diatom association

The diatom assemblage is highly diverse. A total of 167 marine species were found (Appendix). In addition, at least 17 freshwater diatoms also occurred, reflecting either eolian or fluvial input. The relative contribution of freshwater diatoms, however, never exceeded 0.18% of the total diatom assemblage.

The diatom thanatocoenosis is strongly dominated by the coastal upwelling assemblage (average relative contribution $\sim 83\%$, range of contribution is 98.8-66.4%, Fig. 3B). Dominant components are resting spores (RS) of *Chaetoceros affinis*, with *Chaetoceros* sp. 1, *C. coronatus*, *C. debilis*, and *C. diadema* as secondary contributors (Appendix). Highest relative contributions are recorded from ~ 19 till 13 cal kyr BP. At this time, a significant reduction to 75-80% in the contribution of upwelling-associated *Chaetoceros* spores parallels well the decrease in AR_{diatoms} and AR_{Bsi} . After ~ 7 cal kyr BP, the contribution of upwelling diatoms varied at a rather stable level of ~ 80 -85%.

A) Accumulation rate of siliceous phytoplankton



B) Relative abundance of diatom groups

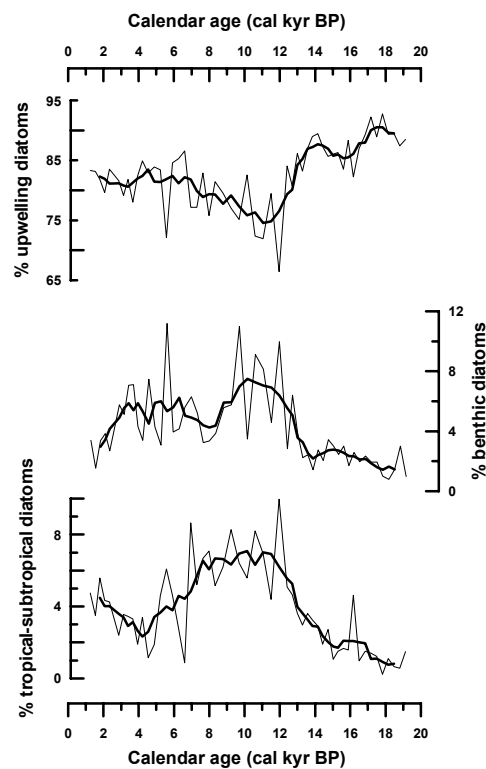


Fig. 3 Variability in the AR of siliceous phytoplankton and relative abundances of three diatom groups in core GeoB 7112-5 from 24° S off northern Chile. A) Downcore accumulation rates of siliceous plankton, from top to bottom: diatoms (AR_{diatoms} , valves $\text{cm}^{-2} \text{kyr}^{-1}$), and silicoflagellates ($AR_{\text{silicofl.}}$, skeletons $\text{cm}^{-2} \text{kyr}^{-1}$). B) Relative abundance of the three main diatom groups in percent, from top to bottom: upwelling diatoms, benthic diatoms, and tropical-subtropical diatoms. The bold line represents the 5-point running average. Note the different scales for each panel.

Accompanying members of the diatom thanatocoenosis are benthic and tropical/subtropical species (Appendix). *Actinoptychus senarius* and *A. vulgaris* contribute the most to the benthic community, with *Grammatophora marina* and *Paralia sulcata* as secondary components. The

average contribution of benthic and tropical/subtropical diatoms remained below 4% till ~13 cal kyr BP, to abruptly increase afterward. Subsequently, the benthic members show two maxima of ~7% between 12 and 9 cal kyr BP, and of 6% between 7 and 3 cal kyr BP. Both periods are characterized by very strong variations in the percentage contribution of benthic species. The highly diversified, tropical/subtropical diatom community is dominated by *Fragilariopsis doliolus*, and *Azpetia tabularis*, accompanied by *A. barronii*, *Thalassiosira ferelineata*, and *Roperia tessellata*. Downcore distribution of warm water diatoms shows highest average contribution of 7% between ~13 and 6 cal kyr BP. During the Late Holocene, a slight increase is observed towards the present.

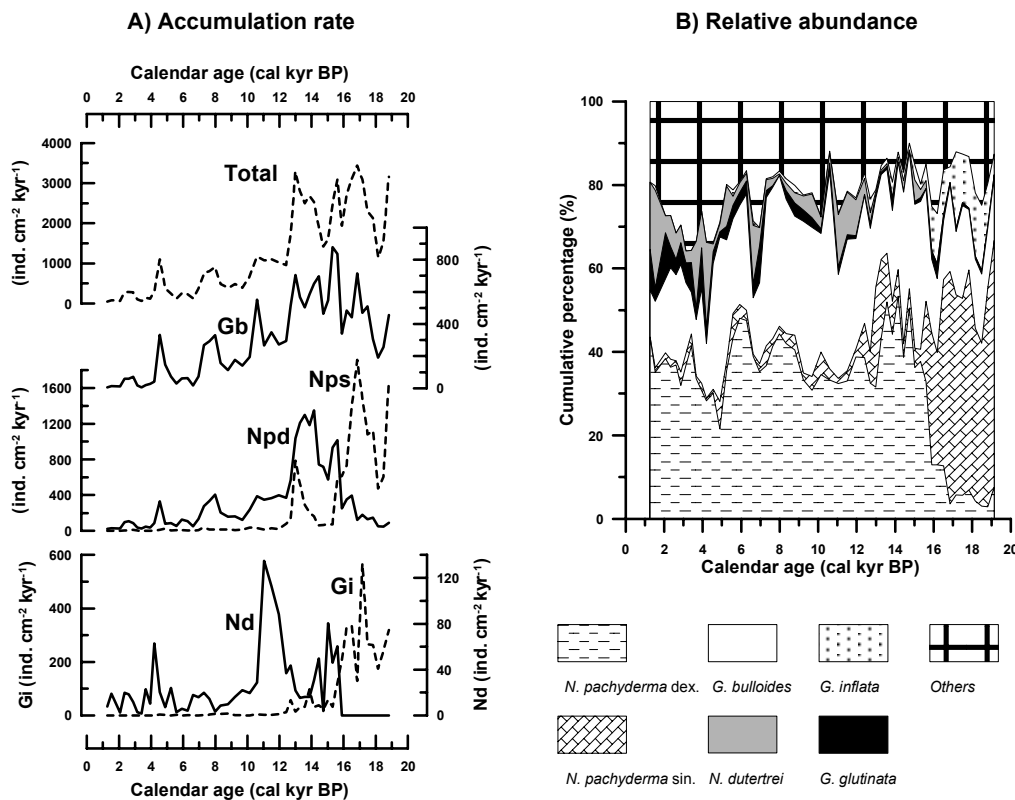


Fig. 4 Variability in the relative abundances and AR of planktic foraminifera species in core GeoB 7112-5 from 24° S off northern Chile. A) Relative abundance (%), and B) Accumulation rates (ind. cm⁻² kyr⁻¹). T: total planktic foraminifera; Gb: *G. bulloides*; Npd: *N. pachyderma* dex.; Nps: *N. pachyderma* sin.; Gi: *G. inflata*; Nd: *N. dutertrei*. Note the different scales for each panel.

4.4. Planktic foraminifera

A total of 21 species were identified in core GeoB7112-5 (Appendix). Six species account on average for approximately 80% of the total planktic foraminiferal assemblage in core GeoB 7112-5 (Fig. 4B). The dominant species are *N. pachyderma* dex. (mean = 37%) and *G.*

bulloides (mean = 27%), followed by *N. pachyderma* sin. (mean = 15%), *N. dutertrei* (mean = 4%), *G. glutinata* (mean = 3%) and *Globorotalia inflata* (mean = 3%).

4.4.1. Faunal composition

N. pachyderma dex. occurs with minimum rates <10% of the total foraminifera fauna before 16 cal kyr BP, and maximum abundances up to 50% between 16 and 13 cal kyr BP (Fig. 4B). Its relative abundance remains high (ca. 40%) between 13 and 1 cal kyr BP, intercepted by a period of relatively low levels between 5 and 3 cal kyr BP. *G. bulloides*, the second most abundant species throughout the core, is more or less evenly distributed between 16 and 5 cal kyr BP with 25-40% of the total fauna, and lower values before and after this period. *N. pachyderma* sin. correlates negatively to *N. pachyderma* dex. and shows high relative abundances up to 60% before 16 cal kyr BP, moderate levels of ~20% between 14 and 13 cal kyr BP, and a very low contribution from 13 cal kyr BP towards the Late Holocene. A similar trend is shown by *G. inflata*, with relative amounts up to 18% of total foraminifera fauna before 16 cal kyr BP, values around 4% between 14 and 13 cal kyr BP, and very low levels from 13 cal kyr BP towards the Late Holocene. *N. dutertrei* was absent prior to 16 cal kyr BP, and shows relative abundances up to 15% between 13 and 10 cal kyr BP, lower values between 7 and 5 cal kyr BP, and rapid fluctuations with maximum rates up to 20% from 5 cal kyr BP towards the present. *G. glutinata* occurs relatively independent of glacial-interglacial conditions. Yet strongly varying and gradually increasing levels from 8 cal kyr BP towards the Late Holocene are observed, with maximum rates of ~10% from 5 cal kyr BP towards the present.

4.4.2. Accumulation rates

The AR of planktic foraminifera abruptly shifts at about 13 cal kyr BP: a distinct maximum before 13 cal kyr BP, with accumulation rates between 1400 and 3300 ind. cm⁻² kyr⁻¹, drops to lower levels after 13 cal kyr BP (300-1700 ind. cm⁻² kyr⁻¹). Lowest values are recorded from 4 cal kyr BP towards the present with 40-300 ind. cm⁻² kyr⁻¹ (Fig. 4A).

N. pachyderma sin. and *G. inflata* are characterized by the highest ARs before 16 cal kyr BP, low values between 16 and 13 cal kyr BP, and extremely low rates during the Holocene (Fig. 4A). In contrast, the AR of *N. pachyderma* dex. was relatively low before 16 cal kyr BP, highest between 16 to 13 cal kyr BP, and still of moderately high levels between 13 and 5 cal kyr BP. The AR of *G. bulloides* shows a successive decrease from 16 towards 4 cal kyr BP, to reach the lowest values after 4 cal kyr BP. *N. dutertrei* was absent before 16 cal kyr BP. The AR of *N. dutertrei* is moderately high between 16 and 13 cal kyr BP, reaches highest levels

between 13 and 11 cal kyr BP, and remains low to moderate from 11 cal kyr BP towards the Late Holocene.

5. Discussion

Large downcore variations in biogenic components, in addition to the species dynamics of planktic foraminifera and the siliceous phytoplankton, indicate considerable fluctuations in the productivity and the hydrographical conditions off northern Chile at 24°S. Based on the different patterns of analyzed parameters, we divide the record into four time periods and discuss them separately.

19-16 cal kyr BP

We assume that almost glacial conditions still dominated at the core position between 19 and 16 cal kyr BP. During this early deglaciation period, highest AR of bulk components, planktic foraminifera, and diatoms indicate a highly productive environment. This statement is additionally supported by the strongest contribution of upwelling diatoms. The “sub-polar” planktic foraminifera assemblage dominated by *N. pachyderma* sin., *G. bulloides*, and *G. inflata*, is also indicative of high marine productivity and cold temperatures at 24°S off Chile. In mid-latitude coastal upwelling systems, *N. pachyderma* sin. has been associated with enhanced upwelling intensity (Marchant et al., 1998; Ufkes et al., 1998; Ivanova et al., 1999). Consequently, such setting led to increased contributions of *N. pachyderma* sin. during glacial intervals (Wells and Okada, 1996; Little et al., 1997; Hebbeln et al., 2002).

Surface samples from the Chilean continental slope (Hebbeln et al., 2000a, Mohtadi et al., submitted) as well as downcore records from north and central Chile (Marchant et al., 1999; Hebbeln et al., 2002; this study), off Peru (Feldberg and Mix, 2003), and from Eastern Equatorial Pacific (EEP, Martinez et al., 2003) indicate that higher relative abundances of *G. inflata* are associated with higher contributions of *N. pachyderma* sin., and thus, high abundances of *G. inflata* can be related to increased coastal upwelling and high productivity. Since both species presently show different flux seasonality, *N. pachyderma* sin. during austral summer (e.g. Marchant et al., 1998; King and Howard, 2003), and *G. inflata* during austral spring (e.g. King and Howard, 2003), we assume that a strong seasonality, specially during the glacial stages, might have been responsible of these mixed faunas.

However, the dominance of *N. pachyderma* sin. during the last deglaciation at 24°S is surprising since in the modern PCC the planktic foraminiferal assemblage at least from north of 44°S is dominated by *N. pachyderma* dex. (Hebbeln et al., 2000a; Feldberg and Mix,

2002), with *G. bulloides* and *N. pachyderma* sin. as accompanying species (Bandy and Rodolfo, 1964; Boltovskoy, 1976; Hebbeln et al., 2000a).

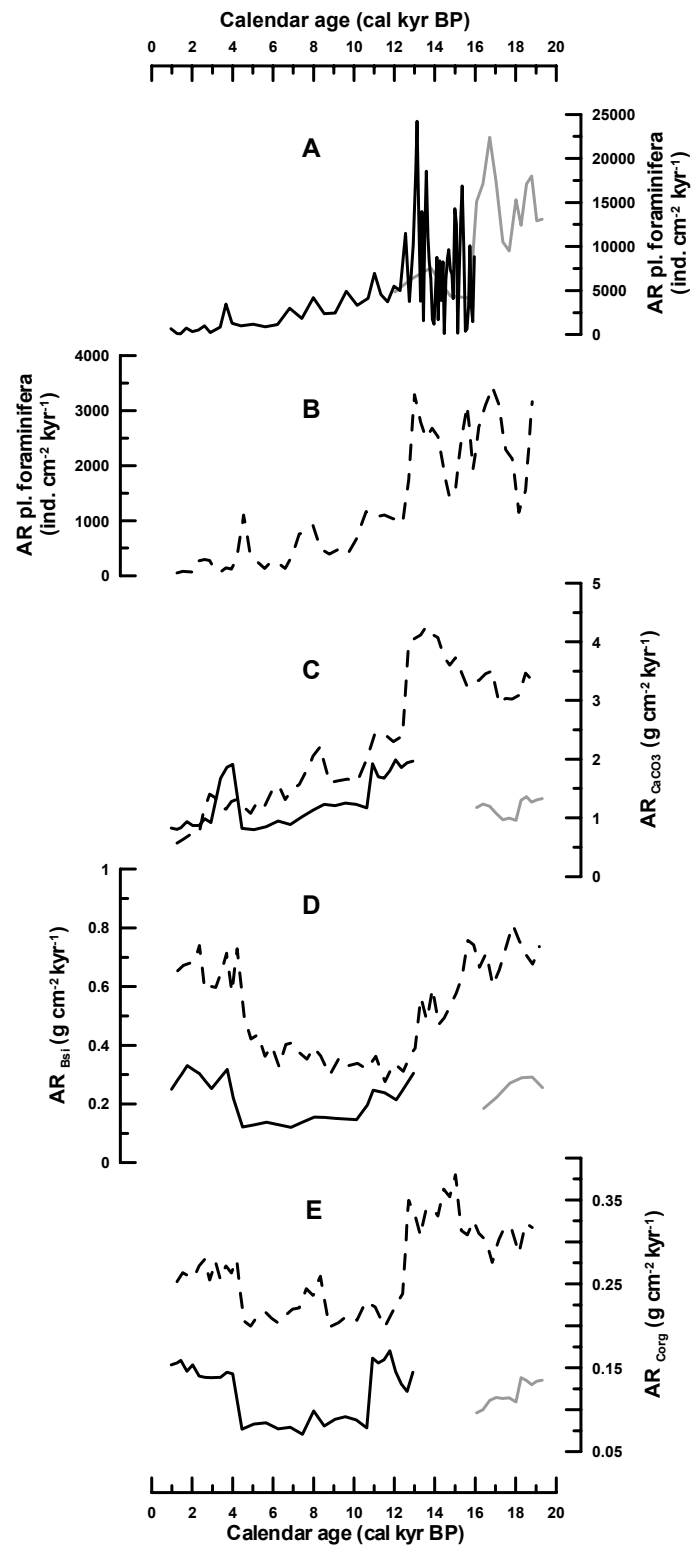


Fig. 5 Comparison of AR of planktic foraminifera (A and B), AR_{CaCO3} (C), AR_{BSI} (D), and AR_{Corg} (E) from GeoB 7112-5 at 24°S (dashed line, this study) with GeoB 3302-1 (gray solid line) / GIK 17748-2 (black solid line) at 33°S (data from Hebbeln *et al.*, 2002). The section between 16 and 13 cal kyr BP is removed from bulk geochemical data at 33°S due to resedimentation processes (see Hebbeln *et al.*, 2002).

Hebbeln et al. (2000a) found >50% *N. pachyderma* dex. in the planktic foraminifera assemblages by studying the surface sediments of the continental slope off Chile between 27° (modern Sea Surface Temperature (SST): ~ 18°C) and 42°S (modern SST: < 12°C) without particular N-S preferences. As already mentioned, Hebbeln et al. (2002) observed at 33°S also a dominance of *N. pachyderma* sin. and significantly higher productivities for the last glacial suggesting rather a regional than a local character of this signal. Based on factor analyses of planktic foraminifera, Feldberg and Mix (2002) estimated a significant cooling of SST of ~8°C during the Last Glacial Maximum (LGM) relative to modern conditions for this part of the PCC (modern SST: 20°C). However, this would match the present-day temperatures off southern Chile, where nowadays *N. pachyderma* dex. remains the dominant species. Thus, a lower temperature between 19 and 16 cal kyr BP alone will not explain the changing dominance between *N. pachyderma* dex. and *N. pachyderma* sin. Also a northward migration of 20° of latitude in the position of the boundary between subpolar and transitional planktic foraminifera assemblages appears to be unlikely (currently at least south of 44°S, Hebbeln et al., 2000a).

A likely scenario would imply the combination of several factors. As suggested by Lamy et al. (1999) and Hebbeln et al. (2002) for the region farther to the south at 33°S, a northward displacement of the climatic zonation would bring the ACC, the main nutrient source for the PCC, closer to the study site resulting in a further increase of productivity. In addition, a higher thermal gradient between pole and equator would have resulted in increased zonal and meridional wind stress (Andreasen and Ravelo, 1997) and subsequently, stronger upwelling. The ascent of the cold, nutrient-rich Antarctic intermediate waters, presently flowing northward below 400 m depth, into the surface as a result of permanently strong upwelling would have had a positive effect on the productivity. This water mass nowadays approaches the surface during periods of stronger upwelling (Strub et al., 1998). Thus, stronger winds prevailing under glacial conditions, in addition to stronger advection of nutrient-rich subpolar waters of the ACC may have resulted in a pronounced cooling and enhanced productivity. This interpretation coincides with records off Peru (Feldberg and Mix., 2002; 2003), and in the EEP (Martinez et al., 2003) suggesting stronger advection of the PCC during glacial periods. Nevertheless, the hydrographical reconstruction of the late glacial period off northern Chile remains tentative, as a modern regional analogue is missing.

16-13 cal kyr BP

This late deglaciation period is characterized by the onset of a rapid change to warmer, less-productive conditions around 16 cal kyr BP. In the planktic foraminiferal record, AR of cold-

water species dropped to much lower values, while that of warmer water species such as *N. pachyderma* dex. and *N. dutertrei* abruptly rose. The latter is most likely transported into the study area by the warm, subtropical surface waters of the PCCC (Marchant et al., 1998). A similar shift in the planktic foraminiferal fauna from a subpolar to a transitional assemblage, marked by the changing dominance from the colder species *N. pachyderma* sin. to the warmer species *N. pachyderma* dex. at 24°S off north Chile, has also been observed along the PCC at 16°S off Peru, and at 33°S off central Chile with similar timing (Hebbeln et al., 2002; Feldberg and Mix, 2003).

Integration of the data from GeoB 7112-5 with other records off Chile is problematical. Despite the lack of siliceous phytoplankton records off Chile so far, temporal resolution, lack of foraminifera data, and short overlapping time-periods make the marine records farther south at 27.5°S (9-110 cal kyr BP, Lamy et al., 1998a) and at 41°S (0-8 cal kyr BP, Lamy et al., 2001) less comparable with GeoB 7112-5. At 33°S, resedimentation processes during the deglaciation (between 16 and 13 cal kyr BP, Hebbeln et al., 2002) do not allow any significant correlation of bulk geochemical data with GeoB 7112-5 (Fig. 5C-E). However, the planktic foraminifera at 33°S are apparently unaffected by the resedimentation processes and agree well with those of GeoB 7112-5 (Fig. 5A, B). Both AR of planktic foraminifera at 24°S and 33°S show the same pattern, with much higher absolute values at 33°S. The correlation of bulk sediment ARs between both sites shows values roughly in the same order of magnitude, which is surprising considering the different planktic foraminifera ARs, and the present-day productivity pattern off Chile with higher productivities towards the south. The particular position of GeoB 7112-5 in a fore-arc basin and its specific morphology probably acted as a sediment trap, and syn-sedimentary accumulation of fine sediment particles such as C_{org} redistributed from farther upslope led to generally high values of this proxy at this site. In addition, the drop in the bulk sediment ARs appears at 33°S at ~11 cal kyr BP, 2000 yr later than recorded in the planktic foraminifera AR of both records, and the bulk sediment AR at 24°S. On-going resedimentation processes e.g. sediment focussing and redeposition probably caused this incoherency at 33°S.

The decreasing trend in the relative contribution of upwelling diatoms in our record during the late deglaciation remains roughly unchanged, while $AR_{silicofl.}$ is at its highest. Nevertheless, $AR_{diatoms}$ and $AR_{silicofl.}$ record a significant drop towards the Early Holocene. By observing Andean glaciers between 18° and 24°S, Ammann et al. (2001) found indications of increased humidity and glacier advance during the late glacial “Tauca” phase (~17-11 cal kyr BP, e.g. Clapperton et al., 1997). Evidences from lake sediments also show increased humidity (e.g.

Grosjean et al., 2001) which could have led to enhanced continental runoff and nutrient supply into the study area. This might have induced relatively high productivities during the late deglaciation. Most probably, the qualitative switch in the planktic foraminifera assemblage reflects rather changes in the oceanic system responding to global warming, while the qualitative composition of the siliceous phytoplankton-association remained unaffected due to the still on-going, relatively strong coastal upwelling, and high nutrient supply.

13--5 cal kyr BP

Lowest productivity and weakest upwelling intensity are mirrored during the Early and the Middle Holocene by reduced AR_{Corg} and AR_{Bsi} . In the foraminifera fauna, the AR of *N. dutertrei* is highest between 12 and 10 cal kyr BP, while the ARs of the other foraminifera species drop to their lowest levels towards the Late Holocene indicating a significant change in the water masses and productivity conditions, i.e. increased advection of warmer subtropical surface waters coupled with reduced upwelling intensity. The planktic foraminifera assemblage, dominated by *N. pachyderma* dex., *G. bulloides* and *N. dutertrei*, clearly evidences the warmest conditions for the last 19 cal kyr at 24°S in the PCC. In addition, increased contribution of tropical/subtropical diatoms reflects weakest upwelling conditions and warmest SST during the Early and Middle Holocene at 24°S off Northern Chile (Fig. 3B).

Previous investigations from farther south in the PCC at 33° and at 41°S have also shown decreased productivity parallel to increased onshore aridity during the Early and Middle Holocene (12 - 4 cal kyr BP, Lamy et al., 1999; 2001; Marchant et al., 1999). Hebbeln et al. (2002) proposed that decreasing productivity during Early and Middle Holocene points to a southward shift in the position of the climate zones, i.e. the Southern Westerlies and the circum-Antarctic circulation, which would also cause the observed onshore aridity during the Early and the Middle Holocene. Comparison of their record at 33°S with our core GeoB 7112-5 reveals very low AR of C_{org} and Bsi during this period, with a synchronous rise at ~ 5 cal kyr BP (Fig. 5D, E).

Palaeoclimate reconstructions for the Early and Middle Holocene between 19° and 24°S in the central Andes and the Atacama desert have been so far a matter of controversial discussions (e.g. Grosjean et al., 2003 and references therein). Using different proxies, some authors suggest more humid conditions during the Middle Holocene than today (Betancourt et al., 2000; Latorre et al., 2002; 2003), while other authors hypothesize drier conditions (Heusser, 1990; Seltzer et al., 1998; Thompson et al., 1998; Grosjean, 2001; Jenny et al., 2002; Abbott et al., 2003).

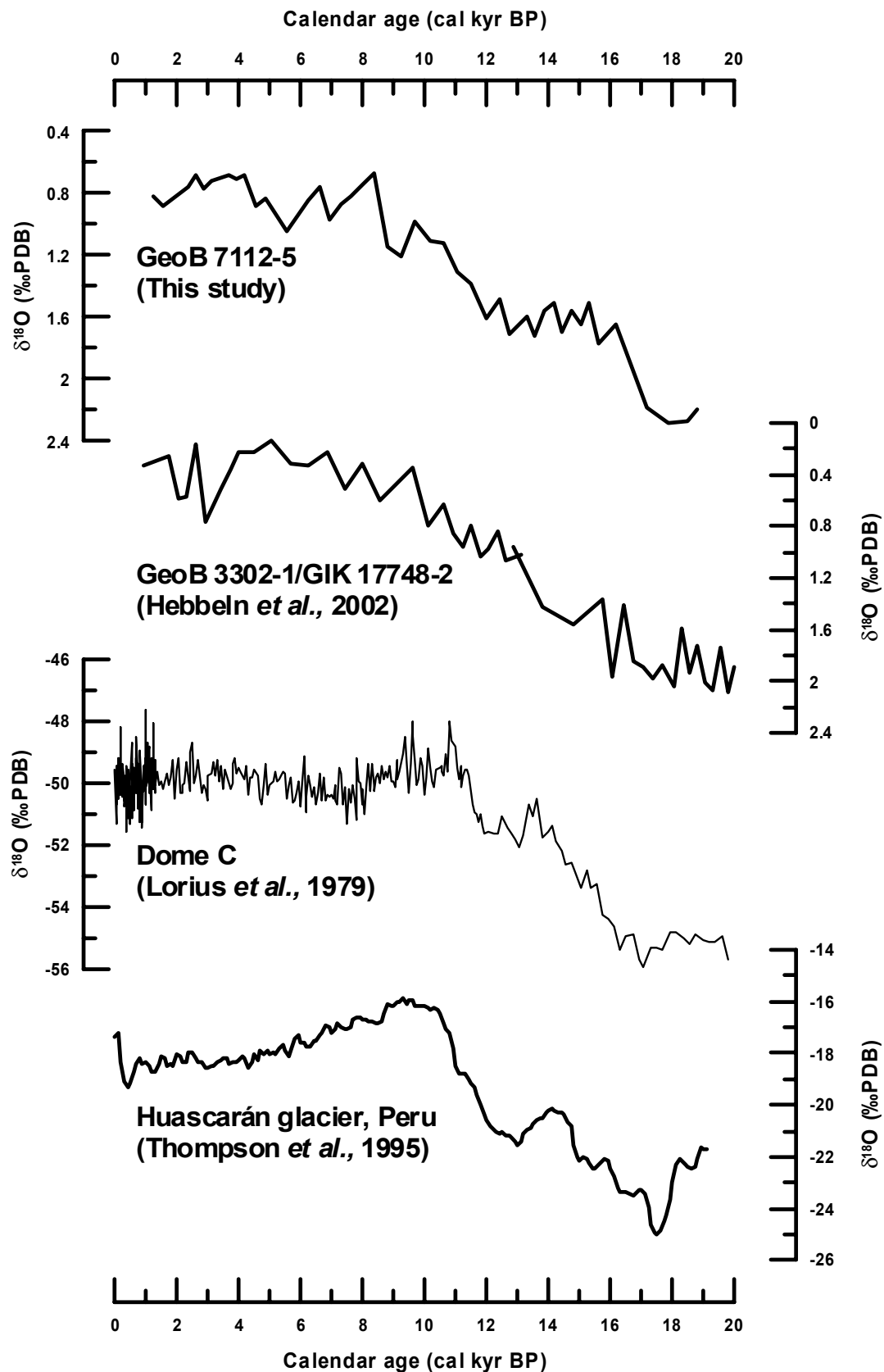


Fig. 6 Comparison of the $\delta^{18}\text{O}$ record of GeoB 7112-5 with other records from South America and Antarctica for the last 19,000 years. From top to bottom: Marine sediments GeoB 7112-5 (24°S/71°W), and GeoB 3302-1/GIK 17748-2 (33°S/72°W), ice cores from Dome C (74°S/124°E, Antarctica), and Huascarán glacier (9°S/77°W, Peru).

A multi-proxy approach suggests a very dry climate during the Middle Holocene by attributing inconsistencies between the palaeoclimate reconstructions to the different proxy records (Grosjean et al., 2003). Considering that the precipitation in southern and central Chile is strongly related to the Southern Westerlies (Aceituno, 1988), variations in humidity therefore indicate changes in the position and/or intensity of the Westerlies. However, any direct influence of the Southern Westerlies at the study area during the late Pleistocene is generally rejected (Fox and Strecker, 1991; Veit, 1992; 1996). Off northern Chile, the position and the intensity of the South Pacific subtropical gyre, with the PCC as its eastern branch, appear to control the upwelling-intensity and productivity (Andreasen and Ravelo, 1997). On the other hand, the position and the intensity of the South Pacific anticyclone seems to be strongly coupled with the position and intensity of atmospheric zonal and meridional winds (e.g. Southern Westerly belt) and oceanic currents (e.g. ACC, Andreasen and Ravelo, 1997). Markgraf (1989; 1998) states that arid periods in central and northern Chile generally occur when a stronger influence of the southeast Pacific high-pressure cell blocks the Westerly frontal system and deflects it farther south. Markgraf (1993) also suggests that between 10 and 5 cal kyr BP the Southern Westerlies shifted to higher latitudes and a seasonal latitudinal shift, e.g. as active under modern conditions, did not develop. Such an impact of the Southern Westerlies on the precipitation system has also been detected in marine sediments off central and south Chile (Lamy et al., 1998; 1999).

~5-1 cal kyr BP

The Late Holocene period shows slightly enhanced upwelling with rapid fluctuations in the hydrographical regime. The minor increase in the AR_{Corg} , AR_{Bsi} , $AR_{diatoms}$, $AR_{silicofl.}$, and the relative abundance of upwelling diatoms point to a change in the hydrographical setting, which led to slightly enhanced upwelling and productivity. Identical environmental change from an arid, less-productive Middle to a more humid, and more productive Late Holocene has also been observed in the PCC farther south at 33°S and at 41°S (Fig. 5D, E, Lamy et al., 2001; Hebbeln et al., 2002). Furthermore, glacier advances in the Andes at 29°S (Grosjean et al., 1998), paleosols in northern Chile between 27° and 33°S (Veit, 1996), as well as pollen records at 32°S (Villagrán and Varela, 1990), and at 34°S (Heusser, 1990) show a general shift to more humid conditions in northern Chile during the Late Holocene.

Analysis of the foraminiferal assemblage in the youngest part of GeoB 7112-5 reveals several rapid changes with higher relative abundances of *G. bulloides* and *N. pachyderma* sin., and diminished contributions of *N. dutertrei*, and vice versa. Although the sampling resolution is not sufficient during the Late Holocene, this pattern could point to intensified El Niño events

described for the same period farther south at 33°S (Marchant et al., 1999). The onset of such events seems to be around 7 cal kyr BP, when the rapid fluctuations in the relative contribution of planktic foraminifera started. Stronger fluctuations within the last 5 kyr probably point to an intensification of ENSO events. The timing of the onset (~7 cal kyr BP) and the intensification (~5 cal kyr BP) of ENSO in our record are consistent with records off Peru (Keefer et al., 1998), and lake sediments from Ecuador (Rodbell et al., 1999) suggesting a more regional ENSO feature rather than local events limited to northern Chile. McGlone et al. (1992) conclude that the increased continental humidity in northern Chile during the Late Holocene is related to increased frequency of ENSO. During warm phases of ENSO, the Hadley cell weakens and abnormally warm conditions prevail. This scenario induces a northward shift of the Westerly belt, which is not blocked by the high-pressure belt leading to positive rainfall anomalies in central and northern Chile (Montecinos et al., 2000). Off Peru, however, high rainfall in the arid coastal lowland results from the southward and eastward invasion of warm air masses (Aceituno, 1988). High precipitation in central and northern Chile, Peru and Ecuador during the Late Holocene seem to be provoked by intensified El Niño activities (Markgraf, 1998).

Global paleoclimatic implications

The onset of the decrease in the $\delta^{18}\text{O}$ values at 17.5 cal kyr BP at site GeoB 7112-5 is coherent with the marine record at 33°S (Hebbeln et al., 2002), the ice core records from Dome C in Antarctica (Lorius et al., 1979), and from Huascarán glacier in Peru (Thompson et al., 1995) suggesting the global nature of the onset of warming observed off northern Chile (Fig. 6). According to an alkenone-derived SST record from 33°S, deglacial warming started at ~18.5 cal kyr BP (Kim et al., 2002). This temporal difference is either due to an earlier local increase in the SST at 33°S, or to the different sensitivity of different proxies to temperature changes.

The onset of warming in the $\delta^{18}\text{O}$ record of GeoB 7112-5 starts at ~17.5 cal kyr BP, 1500 years earlier than the abrupt decrease in the AR of siliceous phytoplankton and the major change in the planktic foraminifera assemblage (Fig. 3 and 4). Siliceous phytoplankton and planktic foraminifera probably responded abruptly to increasing temperatures after the temperature surpassed a certain threshold. By investigating glaciers, and lake and marine sediments between 40° and 55°S in southern South America, McCulloch et al. (2000) recognized the same delay of ~1.5 kyr in the enhanced humidity indicated in their records following the synchronous, initial warming between 17.5 and 17.15 cal kyr BP. Since the

Southern Westerlies are the main humidity source in this region, and their position is strongly coupled with the position of the oceanic currents, the observed lagged response of the humidity pattern in southern South America can be related to the delayed southward return of the climate zones at this time. McCulloch et al. (2002) suggest that this time lag was induced by Heinrich 1 event suppressing the global thermo-haline circulation, and represents the timing of the reorganisation of the global ocean circulation. According to this hypothesis, the modern ocean circulation and the subsequent modern SSTs led to a latitudinal shift of the climate zones, and consequently, the response of the fauna observed at 24°S. The decrease in the $\delta^{18}\text{O}$ values in the marine cores continues until the Holocene climate optimum around 8 cal kyr BP, ~2 kyr longer than in the $\delta^{18}\text{O}$ signal of the ice core records (Fig. 6). This discrepancy can be explained by different signals preserved in both types of records. While the $\delta^{18}\text{O}$ signal in the ice core records is mainly affected by the temperature, the marine signal is additionally influenced by the global ice volume, which continuously decreased until ~8 cal kyr BP.

As mentioned above, changes in the position and intensity of the Southeast Pacific subtropical high and the Southern Westerlies are closely related to the ENSO intensity. During the mid-Holocene, weaker ENSO intensities in line with stronger subtropical gyre circulation, a stronger Southeast Pacific subtropical high, and a more southerly position of the Southern Westerlies led to increased aridity onshore, and decreased marine productivity (e.g. Clement et al., 2000). During the Late Holocene, the onset of modern ENSO associated with weaker subtropical gyre circulation probably caused slight northward migration of the Southern Westerlies, stronger upwelling, and higher marine productivity (e.g. Lamy et al., 1999; Rodbell et al., 1999; Kim et al., 2002).

6. Conclusions

According to the downcore dynamics of bulk sediment, siliceous plankton, and planktic foraminifera, we distinguish between four main periods with different productivity patterns for the last 19 kyr at 24°S off Chile. Highest productivity and upwelling intensity are recorded before 16 cal kyr BP, followed by decreasing productivity and upwelling intensity during the late deglaciation (16–13 cal kyr BP). It is possible that the lagged response of the organisms to the $\delta^{18}\text{O}$ -decrease during the deglaciation points to a delay in the reorganization of the oceanic thermohaline circulation caused by the Heinrich 1 event. Lowest productivity and upwelling intensity are evident during the Early and Middle Holocene (12–4 cal kyr BP). The

Late Holocene (< 4 cal kyr BP) is characterized by increasing productivity and upwelling intensity, possibly corresponding to enhanced ENSO activity.

The paleoproductivity off Chile for the last 19 kyr seems to be mainly driven by the setting of the large scale climate zonation in the Southeast Pacific region. Displacement of the ACC in the south as the main macronutrient source, directly affects the productivity off Chile on one hand, and on the other hand indirectly through latitudinal shifting in the position of the Southern Westerlies belt, which effects the precipitation on the continental hinterland and hence, nutrient supply into the upwelling region. For the nearby area of our downcore record, such displacements led to changes in the intensity and/or position of the South Pacific anticyclone, and the strength of zonal and meridional winds and, subsequently, upwelling intensity.

Acknowledgements

We thank M. Segl and B. Meyer-Schack, who performed the stable isotope measurements. C. Hayn and T. Schmidt are acknowledged for their lab work. This study was supported by the German Bundesministerium für Bildung und Forschung through funding of the project “PUCK” (03G0156A). We are also grateful to the Research Center Ocean Margin (RCOM) in Bremen for technical support. This is RCOM publication Nr. RCOM0103. The data presented in this paper are also available in digital format (www.pangaea.de/PangaVista).

Appendix

1. Diatoms

The grouping of marine diatom components is based on ecological characteristics as stated in well-known bibliographies on distribution of extant marine diatoms (Simonsen, 1974; Round et al., 1990; Hasle and Syvertsen, 1996).

A. Coastal upwelling group

Vegetative cells (VC) of *Chaetoceros debilis* Cleve 1894
 VC *C. decipiens* Cleve 1873
 VC *C. didymus* Ehrenberg 1873
 Resting spores (RS) *Chaetoceros affinis* Lauder 1864
 RS *C. cinctus* Gran 1897
 RS *C. compressus* Lauder 1864
 RS *C. constrictus* Gran 1897
 RS *C. coronatus* Gran 1897
 RS *C. debilis* Cleve 1894
 RS *C. diadema* (Ehrenberg) Gran 1897
 RS *C. didymus* Ehrenberg 1845
 RS *C. radicans* Schütt 1895
 RS *C. vanheurckii* Gran 1897
 Unidentified RS of *Chaetoceros* spp.
Thalassionema pseudonitzschioides (Schuette and Schrader) Hasle 1996

B. Tropical/subtropical group

Alveus marinus (Grunow) Kaczmarek and Fryxell 1996
Asteromphalus arachne Brébisson 1857
A. cleveanus Grunow 1874
A. flabelatus (Brébisson) Greville 1859
A. heptactis (Brébisson) Greville 1861
Azpeitia africana (Janisch ex Schmidt) G.Fryxell and T.P. Watkins 1986
A. neocrenulata (Van Landingham) G.Fryxell and T.P. Watkins 1986
A. tabularis (Grunow) G.Fryxell and P.A.Sims 1986
Bacteriastrum comosum Pavillard 1916
B. elongatum Cleve 1897
Chaetoceros bacteriastroides Karsten 1907
 RS of *Chaetoceros lorenzianus* Grunow 1863
Coscinodiscus centralis Ehrenberg 1844
C. janischii A.Schmidt 1878
C. reniformis Castracane 1886
Detonula pumila (Castracane) Gran 1900
Ditylum brightwelli (West) Grunow 1880
Fragilariopsis doliolus (Wallich) Medlin and Sims 1993
Guinardia cylindrus (Cleve) Hasle 1996
Hemidiscus cuneiformis Wallich 1860
Lioloma elongatum (Grunow) Hasle 1996
Mastogloia rostrata (Wallich) Hustedt 1956
Navicula distans Wm. Smith 1853
Neidium sp. Pfitzer 1871
Nitzschia interruptestriata (Heiden) Simonsen 1974
N. sicula (Castracane) Hustedt 1958
Odontella longicruris (Greville) Hoban 1983
Planktoniella sol (Wallich) Schütt 1892
Pleurosigma directum Grunow 1880
P. planctonicum Simonsen 1974
Proboscia alata (Brightwell) Sundström 1986

P. alata f. *indica* (Brightwell) Sundström 1986
Pseudohimmantidium pacificum Hustedt and Krasske 1941
Pseudo-nitzschia fraudulenta (Cleve) Hasle 1965
Pseudotriceratium punctatum (Wallich) Simonsen 1974
Rhizosolenia acicularis Sundström 1986
R. acumunata (H.Peragallo) H.Peragallo 1892
R. bergonii H. Peragallo 1892
R. castracanei H. Peragallo 1888
R. imbricata Brightwell 1858
R. styliformis Brightwell 1858
Roperia tessellata (Roper) Grunow ex Pelletan 1889
Stellarima stellaris (Roper) Hasle and Sims 1986
Stephanopyxis sp. (Ehrenberg) Ehrenberg 1844
Thalassionema bacillare (Heiden) Kolbe 1955
T. frauenfeldii (Grunow) Hallegraef 1986
T. nitzschioides var. *capitulata* (Castracane) Moreno-Ruiz 1996
T. nitzschioides var. *inflata* Kolbe 1928
T. nitzschioides var. *parva* (Heiden) Moreno-Ruiz 1996
Thalassiosira ferelineata Hasle and G.Fryxell 1977
T. leptopus (Grunow) Hasle and G.Fryxell 1977
T. lineata Josue 1968
T. minuscula Krasske 1941
T. nanolineata (Mann) G.Fryxell and Hasle 1977
T. oestrupii var. *oestrupii* (Ostenfeld) Hasle 1972
T. partheneia Schrader 1972
T. plicata Schrader 1974
T. sacketii f. *sacketii* G.Fryxell 1977
T. sacketii f. *plana* G.Fryxell 1977
T. subtilis (Ostenfeld) Gran 1900
T. symmetrica G.Fryxell and Hasle 1972

c. Benthic group

Actinoptychus senarius (Ehrenberg) Ehrenberg 1843
A. splendens (Shadbolt) Ralfs 1861
A. vulgaris Schumann 1867
Adoneis pacifica G.W. Andrews and P.Rivera 1987
Amphora ostrearia Brébisson 1849
Biddulphia alternans (J.W.Bailey) Van Heurck 1880
Campyloneis sp. Grunow 1862
Cocconeis britannica Naegeli 1849
C. californica var. *lengana* P.Rivera 1973
C. costata var. *costata* Gregory 1855
C. costata var. *hexagona* Grunow 1880
C. decipiens Cleve 1873
C. dirupta Gregory 1857
C. dirupta var. *triumphis* (Hanna and W.M. Grant) Freng. 1949
C. pelta A. Schmidt 1874
C. placentula Ehrenberg 1838
C. speciosa Ehrenberg 1855
C. stauroneiformis (Rabenhorst) Okuno 1957
Ctenophora sp. (Grunow) D.M. Williams and F.E. Round 1986
Cyclophora sp. Castracane 1878
Cymatosira belgica Grunow 1880
Delphineis karstenii (Pisias et al.) G.F.Fryxell 1981
D. surirella (Ehrenberg) G.W.Andrews 1981
Diplomenora sp. Blazé 1984
Diploneis bombus Ehrenberg 1844
D. pupula var. *constricta* Hustedt 1930
Grammatophora marina (Lyngbie) Kützing 1844
Opephora sp. Petit 1888

Paralia sulcata (Ehrenberg) Cleve 1873
Plagiogrammopsis vanheurckii (Grunow) Hasle, von Stosch and Syvertsen 1983
Psammodiscus sp. F.E.Round and D.G.Mann 1980
Psammodictyon panduriforme (Gregory) D.G.Mann 1990
Trachyneis aspera (Ehrenberg) Cleve 1984
Tryblionella sp. W. Smith 1853

2. Planktic foraminifera

Globigerina bulloides d'Orbigny, 1826
Globigerina falconensis Blow, 1959
Globigerinella calida (Parker), 1962
Globigerinella siphonifera (d'Orbigny), 1839
Globigerinita glutinata (Egger), 1895
Globigerinoides conglobatus (Brady), 1879
Globigerinoides ruber (d'Orbigny), 1839
Globigerinoides sacculifer (Brady), 1884
Globorotalia crassaformis (Galloway and Wissler), 1927
Globorotalia hirsuta (d'Orbigny), 1839
Globorotalia inflata (d'Orbigny), 1839
Globorotalia menardii (d'Orbigny), 1865
Globorotalia scitula (Brady), 1882
Globorotalia truncatulinoides (d'Orbigny), 1839
Hastigerina digitata (Rhumbler), 1911
Neogloboquadrina dutertrei (d'Orbigny), 1839
Neogloboquadrina pachyderma (Ehrenberg), 1861
Orbulina universa d'Orbigny, 1839
Pulleniatina obliquiloculata (Parker and Jones), 1865
Sphaerodinella dehiscens (Parker and Jones), 1865
Turborotalia quinqueloba (Natland), 1938

References

- Abbott, M.B., Wolfe, B.B., Wolfe, A.P., Seltzer, G.O., Aravena, R., Mark, B.G., Polissar, P.J., Rodbell, D.T., Rowe, H.D. and Vuille, M., 2003. Holocene paleohydrology and glacial history of the central Andes using multiproxy lake sediment studies. *Palaeogeography, Palaeoclimatology, Palaeoecology*, 194(1-3): 123-138.
- Aceituno, P., 1988. On the functioning of the Southern Oscillation in the South American Sector. Part 1: Surface Climate. *Monthly Weather Review*, 116: 505-524.
- Ammann, C., Jenny, B., Kammer, K. and Messerli, B., 2001. Late Quaternary Glacier response to humidity changes in the arid Andes of Chile (18-29°S). *Palaeogeography, Palaeoclimatology, Palaeoecology*, 172: 313-326.
- Andreasen, D.J. and Ravelo, A.C., 1997. Tropical Pacific Ocean thermocline depth reconstructions for the last glacial maximum. *Paleoceanography*, 12(3): 395-413.
- Bandy, O.L. and Rodolfo, K.S., 1964. Distribution of foraminifera and sediments, Peru-Chile trench area. *Deep-sea Research*, 11: 817-837.
- Bard, E., 1988. Correction of accelerator mass spectrometry ¹⁴C ages measured in planktonic foraminifera: Paleooceanographic implications. *Paleoceanography*, 3: 635-645.
- Berger, W.H., Fischer, K., Lai, C. and Wu, G., 1987. Ocean productivity and organic carbon flux. (Part I: Overview and maps of primary productivity and export production). University of California: San Diego: SIO ref. 87-30.
- Berger, W.H., Smetacek, V.S. and Wefer, G., 1989. Ocean productivity and paleoproductivity -an overview. In: W.H. Berger, V.S. Smetacek, and G. Wefer (Editor), *Productivity of the oceans: present and past*. John Willey & Sons, New York, pp. 1-34.
- Betancourt, J.L., Latorre, C., Rech, J.A., Quade, J. and Rylander, K.A., 2000. A 22,000-year record of monsoonal precipitation from northern Chile's Atacama desert. *Science*, 289: 1542-1546.
- Blanco, J.L., Thomas, A.C., Carr, M.-E. and Strub, P.T., 2001. Seasonal climatology of hydrographic conditions in the upwelling region off northern Chile. *Journal of Geophysical Research*, 106 (C6): 11,451-11,467.
- Boltovskoy, E., 1976. Distribution of Recent foraminifera of the South America region. In: R.H. Hedley and C.G. Adams (Editors), *Foraminifera*. Academy Press, New York, pp. 171-236.
- Brandhorst, W., 1963. Descripción de las condiciones oceanográficas en las aguas costeras entre Valparaíso y el golfo de Arauco, con especial referencia al contenido de oxígeno y su relación con la pesca (resultados de la Expedición AGRIMAR). Ministerio de Agricultura, Dirección de Agricultura y Pesca, Santiago de Chile, 55 pp.
- Broecker, W.S. and Henderson, G.M., 1998. The sequence of events surrounding Termination II and their implications for the cause of glacial-interglacial CO₂ changes. *Paleoceanography*, 13(4): 352-364.

- Clapperton, C.M., Clayton, J.D., Benn, D.I., Marden, C.J. and Argollo, J., 1997. Late Quaternary glacier advances and palaeolake highstands in the Bolivian Altiplano. *Quaternary International*, 38: 49-59.
- Clement, A.C., Seager, R. and Cane, M.A., 2000. Suppression of El Niño during the mid-Holocene by changes in the Earth's orbit. *Paleoceanography*, 15: 731-737.
- De Master, D.J., 1981. The supply and accumulation of silica in the marine environment. *Geochimica Cosmochimica Acta*, 45: 1715-1732.
- Feldberg, M.J. and Mix, A.C., 2002. Sea-surface temperature estimates in the Southeast Pacific based on planktonic foraminiferal species; modern calibration and Last Glacial Maximum. *Marine Micropaleontology*, 44(1-2): 1-29.
- Feldberg, M.J. and Mix, A.C., 2003. Planktonic foraminifera, sea surface temperatures, and mechanisms of oceanic change in the Peru and south equatorial currents, 0-150 ka BP. *Paleoceanography*, 18(1): 1016, doi: 10.1029/2001PA000740.
- Fox, A.N. and Strecker, M.R., 1991. Pleistocene and modern snowlines in the Central Andes (24-28°S). *Bamberger Geographische Schriften*, 11: 169-182.
- Garleff, K., Schäbitz, F., Stingl, H. and Veit, H., 1991. Jungquartäre Landschaftsentwicklung beiderseits der Ariden Diagonale Südamerikas. *Bamberger Geographische Schriften*, 11: 359-394.
- Grosjean, M., 1994. Paleohydrology of the Laguna Lejia (north Chilean Altiplano) and climatic implications for late-glacial times. *Palaeogeography, Palaeoclimatology, Palaeoecology*, 109: 89-100.
- Grosjean, M., Geyh, M.A., Messerli, B. and Schotterer, U., 1995. Late-glacial and early Holocene lake sediments, ground water formations and climate in the Atacama Altiplano. *Journal of Paleolimnology*, 14: 241-252.
- Grosjean, M., Nuñez, L., Cartajena, I. and Messerli, B., 1997. Mid-Holocene Climate and Culture Change in the Atacama Desert, Northern Chile. *Quaternary Research*, 48: 239-246.
- Grosjean, M., Geyh, M.A., Messerli, B., Schreier, H. and Veit, H., 1998. A late-Holocene (<2600 BP) glacial advance in the south central Andes (29°S), northern Chile. *The Holocene*, 8(4): 473-479.
- Grosjean, M., 2001. Mid-Holocene climates in the South-Central Andes: humid or dry? *Science*, 292: 2391.
- Grosjean, M., van Leeuwen, J.F.N., van der Knaap, W.O., Geyh, M.A., Ammann, B., Tanner, W., Messerli, B., Nunez, L.A., Valero-Garces, B.L. and Veit, H., 2001. A 22,000 ¹⁴C year BP sediment and pollen record of climate change from Laguna Miscanti (23°S), northern Chile. *Global and Planetary Change*, 28(1-4): 35-51.
- Grosjean, M., Cartajena, I., Geyh, M.A. and Nunez, L., 2003. From proxy data to paleoclimate interpretation: the mid-Holocene paradox of the Atacama Desert, northern Chile. *Palaeogeography, Palaeoclimatology, Palaeoecology*, 194(1-3): 247-258.

- Hasle, G.R. and Syvertsen, E., 1996. Marine diatoms. In: C. Thomas (Editor), *Identifying Marine Diatoms and Dinoflagellates*. Academic Press, San Diego, pp. 385.
- Hebbeln, D., Marchant, M., Freudenthal, T. and Wefer, G., 2000a. Surface sediment distribution along the Chilean continental slope related to upwelling and productivity. *Marine Geology*, 164(3-4): 119-137.
- Hebbeln, D., Marchant, M. and Wefer, G., 2000b. Seasonal variations of the particle flux in the Peru-Chile Current at 30°S under 'normal' and under El Niño conditions. *Deep - Sea Research II*, 47: 2101-2128.
- Hebbeln, D. et al., 2001. PUCK, report and preliminary results of R/V Sonne cruise SO 156, Valparaiso (Chile) - Talcahuano (Chile), March 29 - May 14, 2001. *Berichte aus dem Fachbereich Geowissenschaften*, 182. Universität Bremen, 195 pp.
- Hebbeln, D., Marchant, M. and Wefer, G., 2002. Paleoproductivity in the southern Peru-Chile Current through the last 33000 yr. *Marine Geology*, 186(3-4): 487-504.
- Hemleben, C., Spindler, M. and Anderson, O.R., 1989. *Modern planktonic foraminifera*. Springer, New York, 363 pp.
- Heusser, C.J., 1990. Ice age vegetation and climate of subtropical Chile. *Palaeogeography, Palaeoclimatology, Palaeoecology*, 80: 107-127.
- Imbrie, J., Hays, J.D., Martinson, D.G., McIntyre, A., Mix, A.C., Morley, J.J., Pisias, N.G., Prell, W.L. and Shackleton, N.J., 1984. The orbital theory of Pleistocene climate: Support from a revised chronology of the marine $\delta^{18}\text{O}$ record. In: B. Saltzman (Editor), *Milankovitch and Climate, Part 1*. NATO ASI Series. D. Riedel, pp. 269-305.
- Ivanova, E.M., Conan, S.M.-H., Peeters, F.J.C. and Troelstra, S.R., 1999. Living *Neogloboquadrina pachyderma* sin and its distribution in the sediments from Oman and Somalia upwelling areas. *Marine Micropaleontology*, 36(2-3): 91-107.
- Jenny, B., Valero-Garces, B.L., Villa-Martinez, R., Urrutia, R., Geyh, M. and Veit, H., 2002. Early to Mid-Holocene Aridity in Central Chile and the Southern Westerlies: The Laguna Aculeo Record (34°S). *Quaternary Research*, 58(2): 160-170.
- Keefer, D.K., deFrance, S.D., Moseley, M.E., Richardson, J.B., Satterlee, D.R. and Day-Lewis, A., 1998. Early maritime economy and El Niño events at Quebrada Tacahuay, Peru. *Science*, 281: 1833-1835.
- Kennett, J.P. and Srinivasan, M., 1983. *Neogene planktonic foraminifera - A Phylogenetic atlas*. Hutchinson Ross Publishing, Stroudsburg, 265 pp.
- Kim, J., Schneider, R.R., Hebbeln, D., Müller, P.J. and Wefer, G., 2002. Last deglacial sea-surface temperature evolution in the southeast Pacific compared to climate changes on the South American continent. *Quaternary Science Reviews*, 21: 2085-2097.
- King, A.L. and Howard, W.R., 2003. Planktonic foraminiferal flux seasonality in Subantarctic sediment traps: A test for paleoclimate reconstructions. *Paleoceanography*, 18(1): 1019, doi: 10.1029/2002PA000839.

- Klump, J., Hebbeln, D. and Wefer, G., 2001. High concentrations of biogenic barium in Pacific sediments after Termination I - A signal of changes in productivity and deep water chemistry. *Marine Geology*, 177: 1-11.
- Lamy, F., Hebbeln, D. and Wefer, G., 1998a. Late Quaternary precessional cycles of terrigenous sediment input off the Norte Chico, Chile (27.5°S) and paleoclimatic implications. *Palaeogeography, Palaeoclimatology, Palaeoecology*, 141(3-4): 233-251.
- Lamy, F., Hebbeln, D. and Wefer, G., 1999. High resolution marine record of climatic change in mid-latitude Chile during the last 28,000 years based on terrigenous sediment parameters. *Quaternary Research*, 51: 83-93.
- Lamy, F., Hebbeln, D., Rohl, U. and Wefer, G., 2001. Holocene rainfall variability in southern Chile: a marine record of latitudinal shifts of the Southern Westerlies. *Earth and Planetary Science Letters*, 185(3-4): 369-382.
- Lamy, F., Rühlemann, C., Hebbeln, D. and Wefer, G., 2002. High- and low-latitude climate control on the position of the southern Peru-Chile Current during the Holocene. *Paleoceanography*, 17(2): 1028, doi:10.1029/2001PA000727.
- Latorre, B.A., Spadaro, I. and Rioja, M.E., 2002. Occurrence of resistant strains of *Botrytis cinerea* to *Anilinopyrimidine fungicides* in table grapes in Chile. *Crop Protection*, 21(10): 957-961.
- Latorre, C., Betancourt, J.L., Rylander, K.A., Quade, J. and Matthei, O., 2003. A vegetation history from the arid prepuna of northern Chile (22-23°S) over the last 13500 years. *Palaeogeography, Palaeoclimatology, Palaeoecology*, 194(1-3): 223-246.
- Little, M.G., Schneider, R.R., Kroon, D., Price, B., Bickert, T. and Wefer, G., 1997. Rapid palaeoceanographic changes in the Benguela Upwelling System for the last 160.000 years as indicated by abundances of planktonic foraminifera. *Palaeogeography, Palaeoclimatology, Palaeoecology*, 130: 135-161.
- Lorius, C., Merlivat, L., Jouzel, J. and Pourchet, M., 1979. A 30,000 yr isotope climatic record from Antarctic ice. *Nature*, 280: 644-648.
- Marchant, M., Hebbeln, D. and Wefer, G., 1998. Seasonal flux patterns fo planctic foraminifera in the Peru-Chile Current. *Deep-Sea Research*, 45: 1161-1185.
- Marchant, M., Hebbeln, D. and Wefer, G., 1999. High resolution planktic foraminiferal record of the last 13,300 years from the upwelling area off Chile. *Marine Geology*, 161: 115-128.
- Markgraf, V., 1989. Reply to C.J. Heusser's "Southern Westerlies" during the Last Glacial Maximum. *Quaternary Research*, 31: 426-432.
- Markgraf, V., 1993. Climatic history of South America since 18,000 yr B.P.: comparison of pollen records and model simulations. In: H.E. Wright et al. (Editors), *Global climate since the Last Glacial Maximum*. University of Minnesota Press, Minneapolis, pp. 357-385.

- Markgraf, V., 1998. Past climates of South America. In: J.E. Hobbs, J.A. Lindesay and H.A. Bridgman (Editors), *Climates of the southern continents: present, past and future*. Wiley, New York, pp. 107-134.
- Martinez, I., Keigwin, L.D., Barrows, T.T., Yokoyama, Y. and Southon, J., 2003. La Niña-like conditions in the eastern equatorial Pacific and a stronger Choco jet in the northern Andes during the last glaciation. *Paleoceanography*, 18(2): 1033, doi: 10.1029/2002PA000877.
- McCulloch, R.D., Bentley, M.J., Purves, R.S., Hulton, N.R.J., Sugden, D.E. and Clapperton, C.M., 2000. Climatic inferences from glacial and palaeoecological evidence at the last glacial termination, southern South America. *Journal of Quaternary Science*, 15(4): 409-417.
- McGlone, M.S., Kershaw, A.P. and Markgraf, V., 1992. El Niño/Southern Oscillation climatic variability in Australasian and South American paleoenvironmental records. In: H.F. Diaz and V. Markgraf (Editors), *El Niño: Historical and Paleoclimatic aspects of the Southern Oscillation*. Cambridge University Press, Cambridge, pp. 435-462.
- Montecinos, A., Díaz, A. and Aceituno, P., 2000. Seasonal diagnostic and predictability of rainfall in subtropical South America based on tropical Pacific SST. *Journal of Climate*, 13: 746-758.
- Müller, P.J. and Schneider, R., 1993. An automated leaching method for the determination of opal in sediments and particulate matter. *Deep-Sea Research I*, 40(3): 425-444.
- Müller, P.J., Schneider, R. and Ruhland, G., 1994. Late Quaternary PCO₂ variations in the Angola Current: Evidence from organic carbon $\delta^{13}\text{C}$ and alkenone temperature. In: R. Zahn, T.F. Pedersen, M.A. Kaminski and L. Labeyrie (Editors), *Carbon cycling in the glacial ocean: Constraints on the ocean's role in global change*. NATO ASI Series I. Springer-Verlag, Berlin, pp. 343-366.
- Nadeau, M.J., Schleicher, M., Grootes, P.M., Erlenkeuser, H., Gotoyong, A., Mous, D.J.W., Sarnthein, J.M. and Willkomm, N., 1997. The Leibniz-Labor AMS facility at the Christian-Albrechts University, Kiel, Germany. *Nuclear Instruments and Methods in Physics Research*, 123: 22-30.
- Parker, F., 1962. Planktic foraminifera species in Pacific sediments. *Micropaleontology*, 8: 219-254.
- Pisias, N.G., Martinson, D.G., Moore, T.C., Shackleton, N.J., Prell, W., Hays, J. and Boden, G., 1984. High resolution stratigraphic correlation of benthic oxygen isotopic records spanning the last 300,000 years. *Marine Geology*, 56: 119-136.
- Rodbell, D.T., Seltzer, G.O., Anderson, D.M., Abbot, M.B., Enfield, D.B. and Newman, J.H., 1999. An 15,000-year record of El Niño-driven alluviation in Southwestern Ecuador. *Science*, 283: 516-520.
- Romero, O.E., Hebbeln, D. and Wefer, G., 2001. Temporal and spatial variability in export production in the SE Pacific Ocean: evidence from siliceous plankton fluxes and surface sediment assemblages. *Deep Sea Research I*, 48(12): 2673-2697.

- Round, F.E., Crawford, R.M. and Mann, D.G., 1990. *The Diatoms*. Cambridge University Press, Cambridge, 747 pp.
- Sarmiento, J.L. and Sundquist, E.T., 1992. Revised budget for the oceanic uptake of anthropogenic carbon dioxide. *Nature*, 356: 589-593.
- Schrader, H. and Gersonde, R., 1978. Diatoms and silicoflagellates. In: W.J. Zachariasse et al. (Editors), *Micropaleontological counting methods and techniques - an exercise on an eight meter section of the Lower Pliocene of Capo Rosello, Sicily*. Utrecht Micropaleontology Bulletin, pp. 129-176.
- Seltzer, G.O., Baker, P., Cross, S., Dunbar, R. and Fritz, S., 1998. High-resolution seismic reflection profiles from lake Titicaca, Peru-Bolivia: Evidence for Holocene aridity in the tropical Andes. *Geology*, 26: 167-170.
- Shaffer, G., Salinas, S., Pizarro, O., Vega, A. and Hormazabal, S., 1995. Currents in the deep ocean off Chile (30°S). *Deep-Sea Research*, 42: 425-436.
- Simonsen, R., 1974. The diatom plankton of the Indian Ocean expedition of RV Meteor 1964-1965. *Meteor Forschungsergebnisse*, D 19: 1-66.
- Strub, P.T., Mesías, J.M., Montecino, V., Rutllant, J. and Salinas, S., 1998. Coastal ocean circulation off western South America. In: A.R. Robinson and K.H. Brink (Editors), *The Global Coastal Ocean - Regional Studies and Synthesis*. The Sea, ideas and observations on progress in the study of the seas. John Wiley & Sons, Inc., New York, pp. 273-313.
- Stuiver, M. and Reimer, P.J., 1993. Extended ¹⁴C data base and revised CALIB 3.0 ¹⁴C age calibration program. *Radiocarbon*, 35(1): 215-230.
- Thiede, J., Suess, E. and Müller, P.J., 1982. Late quaternary fluxes of major sediment components to the sea floor at the northwest African continental slope. In: U. von Rad, K. Hinz, M. Sarntheim and E. Seibold (Editors), *Geology of the northwest African continental margin*. Springer-Verlag, Berlin, Heidelberg, pp. 605-631.
- Thomas, A.C., Huang, F., Strub, P.T. and James, C., 1994. Comparison of the seasonal and interannual variability of phytoplankton pigment concentrations in the Peru and California Current systems. *Journal of Geophysical Research*, 99(C4): 7355-7370.
- Thompson, L.G., Mosley-Thompson, E., Davis, M.E., Lin, P.N., Henderson, K.A., Cole-Dai, J., Bolzan, J.F. and Liu, K.B., 1995. Late Glacial Stage and Holocene tropical ice core records from Huascarán, Peru. *Science*, 269: 46-50.
- Thompson, L.G. et al., 1998. A 25,000 year tropical climate history from Bolivian Ice cores. *Science*, 282: 1858-1864.
- Ufkes, E., Jansen, J.H.F. and Brummer, G.A., 1998. Living planktonic foraminifera in the eastern South Atlantic during spring: indicators of water masses, upwelling and the Congo (Zaire) River plume. *Marine Micropaleontology*, 33: 27-53.
- Van Andel, T.H., Heath, G.R. and Moore, T.C., 1975. Cenozoic history and paleoceanography of the central equatorial Pacific Ocean. *Geological Society of America Memoirs*, 143: 134 pp.

- Veit, H., 1992. Jungquartäre Landschafts- und Bodenentwicklung im chilenischen Andenvorland zwischen 27-33°S. *Bonner Geographische Abhandlungen*, 85: 196-208.
- Veit, H., 1996. Southern Westerlies during the Holocene deduced from geomorphological and pedological studies in the Norte Chico, Northern Chile (27-33°S). *Palaeogeography Palaeoclimatology Palaeoecology*, 123: 107-119.
- Villagrán, C. and Varela, J., 1990. Palynological evidence for increased aridity on the Central Chilean coast during the Holocene. *Quaternary Research*, 34: 198-207.
- Vincent, E. and Berger, W.H., 1981. Planktonic foraminifera and their use in paleoceanography. In: C. Emiliani (Editor), *The oceanic Lithosphere. The Sea*. Wiley, New York, pp. 1025-1119.
- Wells, P. and Okada, H., 1996. Holocene and Pleistocene glacial paleoceanography off southeastern Australia, based on foraminifers and nannofossils in Verna cored hole V18-222. *Australian Journal of Earth Sciences*, 43: 509-523.

Mechanisms and variations of the paleoproductivity off northern Chile (24°S - 33°S) during the last 40,000 years

Mohtadi, M., and Hebbeln, D.

Department of Geosciences, University of Bremen, Bremen, Germany

Submitted to Paleoceanography

Abstract

A multiparameter investigation including organic carbon, carbonate, opal, and planktic foraminifera was carried out on five sediment cores from the coastal upwelling area between 24°S and 33°S along the Peru-Chile Current to reconstruct the history of the paleoproductivity and its driving mechanisms during the last 40,000 years. We suggest that the Antarctic Circumpolar Current (ACC) as the main nutrient source in this region mainly drives the productivity by its latitudinal shifts associated with climate change. Simplified, its northerly position during the last glacial led to enhanced productivities, and its southerly position during the Holocene caused lower productivities. At 33°S, the paleoproductivity was additionally affected by the southern westerlies and records highest levels during the Last Glacial Maximum (LGM). North of 33°S, several factors e.g. position and strength of the South Pacific anticyclone, hemispheric wind stress, and El Niño Southern Oscillation (ENSO) events supplementary influenced upwelling and paleoproductivity, where maximum values occurred prior to the LGM and during the deglaciation.

INDEX TERMS: 4267 Oceanography: General: Paleoceanography; 4279 Oceanography: General: Upwelling and convergences; 4516: Oceanography: Physical: Eastern boundary currents; 3030 Marine geology and geophysics: Micropaleontology; 1050 Geochemistry: Marine geochemistry (4835, 4850); *KEYWORDS:* SE Pacific, paleoceanography, paleoclimate, Chile, planktic foraminifera.

1. Introduction

Strong coastal upwelling in Eastern Boundary Currents (EBCs) makes these to the most important productivity regions beside the equatorial and subpolar divergence zones, altogether contributing about 50% of global marine productivity (Berger et al., 1989). The EBCs play a key role in the global carbon cycle as sources and sinks of CO₂ (e.g. Broecker and Peng, 1982) and thus, they are of greatest interest for the reconstruction of the role of the ocean in changing atmospheric CO₂ levels on glacial/interglacial and shorter time scales as e.g. those recorded in ice core records. Among the EBCs, the Peru-Chile Current (PCC, or Humboldt Current) stands out with the longest N–S extension (over 40° of latitude), and a strong continuous upwelling regime resulting in a very high biological productivity (>200 g C m⁻² yr⁻¹) (Berger et al., 1987).

Recent paleoceanographic studies focus on the southern part (>33°S) of the PCC, where paleotemperature (Kim et al., 2002) and paleoproductivity (Marchant et al., 1999; Klump et al., 2001; Hebbeln et al., 2002) estimations in line with continental rainfall reconstructions (Lamy et al., 1998a; 1999; 2001) show significant differences between the last glacial and the Holocene. During the LGM, lower water temperatures and higher marine productivities paralleled enhanced precipitation onshore pointing to the coupling of the oceanic (PCC/ACC) and atmospheric (Southern Westerlies) circulation systems off central and southern Chile. To date, the database off northern Chile is rather scarce, and the records from 24°S (Mohtadi et al., in press), and 27.5°S (Lamy et al., 1998a), are hardly comparable due to different temporal resolutions and a short overlapping time-period.

Continental paleoclimatic investigations in Chile are based on pollen (e.g. Heusser, 1990; Markgraf, 1993; Markgraf et al., 1992; Villagrán, 1993; McCulloch et al., 2000), lake sediments (e.g. Grosjean, 1994; Grosjean et al., 1995; 2001; Jenny et al., 2002), glaciers (e.g. Messerli et al., 1992; Seltzer, 1992; 1994; Clayton and Clapperton, 1997; Ammann et al., 2001), as well as soils and paleosols (Veit, 1992; 1996). Nonetheless, most of the continental records cover only the Holocene, and paleoclimatic reconstructions for the last glacial in northern Chile are rare (e.g. Grosjean 1994; Grosjean et al., 1995; 2001; Veit, 1996). Consensus exists about a humid late-glacial period with an observed paleolake level rise in northern Chile and Bolivia between 17,000 and 11,000 cal yr BP (e.g. Clayton and Clapperton, 1997; Sylvestre et al., 1999). Information about the conditions during the LGM, Early and Middle Holocene are controversial (e.g. Grosjean et al., 2003 and references therein), and data on the pre-LGM humid ‘Minchin phase’ between 40,000 and 25,000 cal yr BP are uncertain (Clapperton, 1993). Finally, the paleoclimate reconstructions inferred from

continental records for the LGM and the last deglaciation do not agree well with that from the marine record at 27.5°S (e.g. Clapperton et al., 1997; Lamy et al., 1998a; Ammann et al., 2001).

Here we show results of a multiproxy approach including contents and accumulation rates of bulk biogenic compounds (organic carbon, calcium carbonate, and opal), and the flux of planktic foraminifera and their faunal composition. It is applied to five marine sediment records in order to assess the paleoproductivity and its driving mechanisms in the Southeastern Pacific during the last 40,000 yr.

2. Study Area

Shaffer et al. (1995) and Strub et al. (1998) have described the modern oceanography off Chile. According to these authors, the ACC splits, after approaching the South American continent between 40°S and 45°S, into the poleward flowing Cape Horn Current, and the equatorward flowing PCC (Fig. 1). The PCC can be divided into a coastal (PCC_{coast}, or Chile Coastal Current: CCC) branch extending to ~100 km off the coast, and an oceanic (PCC_{ocean}, or Humboldt Current) branch separated 100-300 offshore by the poleward flowing, subtropical surface waters of the Peru-Chile Counter Current (PCCC). A significant admixture of low salinity surface waters derived from the Chilean fjord region characterizes the coastal branch of the PCC. Close to the coast and beneath these surface water masses, equatorial subsurface waters of the Gunther Undercurrent (GUC) flow poleward, mainly located between 100 and 400 m water depth over the shelf and the continental slope. Between 400 and 1200 m water depth Antarctic Intermediate Water (AAIW) flows equatorward, underlain by sluggishly southward flowing Pacific Deep Water (PDW). The deepest parts of the Peru-Chile trench are filled with the equatorward flowing Antarctic Bottom Water (AABW) (Ingle et al., 1980).

The continental climate can be subdivided into two sectors: South of the study area, the continental climate is characterized by Mediterranean-type semi-arid conditions controlled by the seasonal influence of the Southern Westerlies, with precipitation values up to 1000 mm/a (Miller, 1976). The sediments on the continental slope within this area are mainly supplied by rivers, without significant eolian sediment input (Lamy et al., 1999). The hyper-arid region of the Atacama desert north of 27°S, on the other hand, represents one of the driest areas world wide with precipitations <50 mm/a (Garleff et al., 1991). Hence, a significant portion of the terrigenous content of the sediments from the continental slope in this region is of eolian origin, i.e., dust of the Atacama Desert (Lamy et al., 1998a; b).

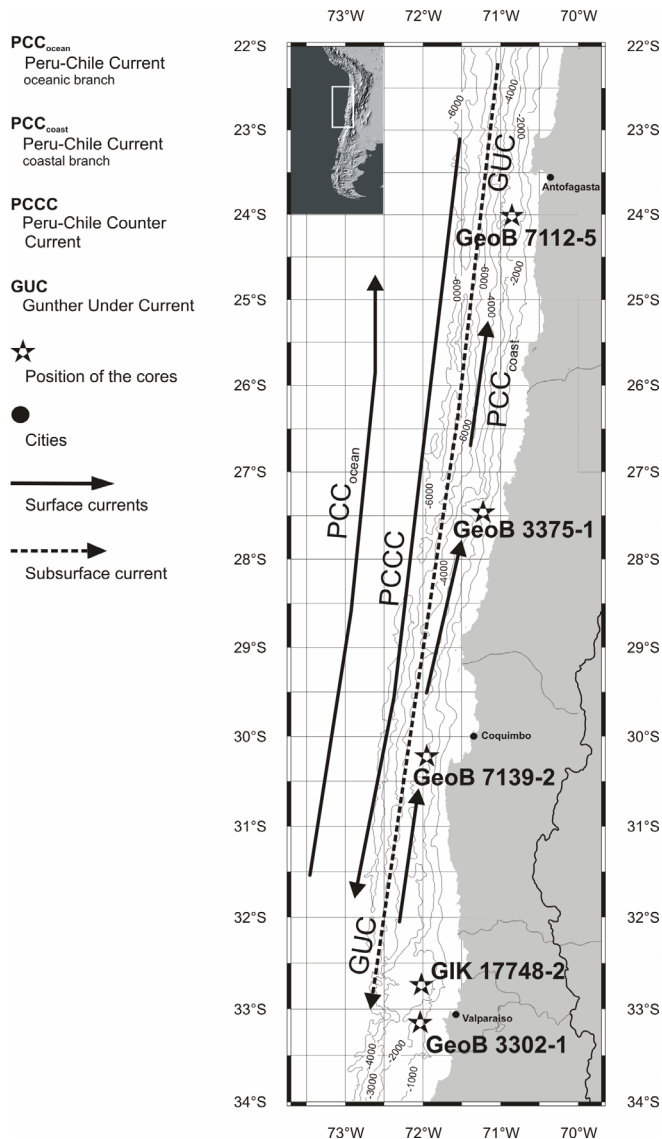


Fig. 1 Map showing the position of the investigated cores (stars), and the modern oceanographic features off central and northern Chile after Strub et al. (1998).

3. Material and Methods

3.1. Sampling

Sediment cores GeoB 3375-1 and GeoB 3302-1 (Table 1, Fig. 1) were retrieved during cruises SONNE-102 (Hebbeln et al., 1995). GeoB 3375-1 was taken at 27.5°S from the landward edge of a terrace-shaped sector on the continental slope off Copiapó. GeoB 3302-1 was obtained at 33°S from the moderately

inclined ($\sim 3^\circ$) upper continental slope, about 20 km north of the San Antonio canyon, a major submarine canyon off the mouth of the Maipo river. Sediment cores GeoB 7112-5 and GeoB 7139-2 (Table 1, Fig. 1) were collected during cruise SONNE-156 (Hebbeln et al., 2001). GeoB 7112-5 was taken at 24°S from a fore-arc basin off Antofagasta, filled with several tens of meters sediment discordant overlying older, well-layered strata. GeoB 7139-2 was retrieved at 30°S from a relatively flat lower continental slope off Coquimbo. Core GIK 17748-2 at 33°S (Table 1, Fig. 1) was obtained during cruise SONNE-80 (Stoffers et al., 1992) from the southern part of the Valparaiso basin, a 50 * 50 km wide, flat area located between 2400 and 600 m water depth on the Chilean continental margin.

All cores consist mainly of brown-olive to light-olive clayey silts and silty clays of terrigenous origin, and were deposited under hemipelagic processes. Nonetheless, at GIK 17748-2 and GeoB 3302-1, other processes such as resedimentation and winnowing have been observed and discussed by Lamy et al. (1999), Marchant et al. (1999), and Hebbeln et al. (2002). From each core, two sample-series of approx. 10 cm³ were taken at 5-cm intervals, one set for geochemical analyses, another set for stable isotopic and micropaleontological analyses. Archived

core materials are kept at the Department of Geosciences, University of Bremen, Germany.

Core name	Latitude	Longitude	Water depth (m)	Length (cm)
GeoB 7112-5	24°01.99'S	70°49.41'W	2507	324
GeoB 3375-1	27°28.00'S	71°15.10'W	1947	489
GeoB 7139-2	30°12.00'S	71°58.99'W	3267	841
GIK 17748-2	32°45.00'S	72°02.00'W	2545	383
GeoB 3302-1	33°13.10'S	72°05.40'W	1498	412

Table 1 Location of sediment cores used in this study.

3.2. Bulk Geochemical Analyses

The sediment sample set for bulk analyses was freeze-dried and homogenized prior to processing. After decalcification of the samples by 6 N HCl, total organic carbon (TOC) was obtained by combustion at 1050°C using a Heraeus CHN-O-Rapid elemental analyzer as described by Müller et al. (1994). Carbonate was calculated from the difference between total carbon (TC), measured with the CHN analyzer on untreated samples, and TOC, as:

$$\text{CaCO}_3 = (\text{TC} - \text{TOC}) * 8.33 \quad (1)$$

All samples for analysis of biogenic silica (opal) were freeze-dried and ground in an agate mortar. Opal was determined at 10 cm resolution (except for GeoB 7112-5 at 5 cm resolution) with a sequential leaching technique proposed by De Master (1981), and modified by Müller and Schneider (1993).

3.3. Planktic Foraminifera Analyses

The sediment sample set for foraminiferal analyses was freeze-dried, weighed and washed through a 150µm sieve. A minimum of 300 specimens per sample was counted, except for GeoB 3302-1 and GIK 17748-2, with approx. 200 individuals per each sample (Marchant et al., 1999; Hebbeln et al., 2002). All specimens were individually picked and identified following the taxonomy of planktic foraminifera proposed by Parker (1962), Kennett and Srinivasan (1983), and Hemleben et al. (1989). For *Neogloboquadrina pachyderma*, the relative abundances of right (dex) and left (sin) coiling individuals were determined, and the

two forms were treated as individual species. *Neogloboquadrina dutertrei* was distinguished from *N. pachyderma* primarily by the presence of an umbilical tooth, presence of more than four chambers, and a more pitted texture based on the description of Parker (1962). Accumulation rates (AR) of foraminifera are expressed as ind. cm⁻² kyr⁻¹ (individuals per square cm per thousand years).

3.4. Stable Oxygen Isotope Measurements

A Finnigan MAT 251 mass spectrometer was used to measure the stable oxygen isotope composition of the planktic foraminifera *N. pachyderma* sin (GeoB 3375-1, GeoB 7139-2), and *N. pachyderma* dex (GeoB 7112-5, GeoB 7139-2, GIK 17748-2, GeoB 3302-1). Twenty individual tests >150µm were picked for each measurement. The isotopic composition of the carbonate sample was measured on the CO₂ gas evolved by treatment with phosphoric acid at a constant temperature of 75°C. For all stable oxygen isotope measurements a working standard (Burgbrohl CO₂ gas) was used, which has been calibrated against PDB by using the NBS 18, 19 and 20 standards. Consequently, all δ¹⁸O data given here are relative to the PDB standard. Analytical standard deviation is about ± 0.07‰ (Isotope Laboratory, Department of Geosciences, University of Bremen).

3.5. AMS ¹⁴C Dating

Accelerator mass spectrometry (AMS) dating were determined at the Leibniz Laboratory for Age Determinations and Isotope Research at the University of Kiel (Nadeau et al., 1997), and at the Center for Isotope Research in Groningen, the Netherlands (GIK 17748-2). ¹⁴C AMS dates were obtained on approx. 10 mg calcium carbonate (only tests of mixed planktic foraminifera). All ages are corrected for ¹³C and a mean ocean reservoir age of 400 years (Bard, 1988). The ¹⁴C ages were converted to calendar years using the CALPAL software and are reported as cal yr BP (Jöris and Weninger, 1998, updated 2003). Consequently, those age-control points published earlier (GeoB 7112-5 (Mohtadi et al., in press), GeoB 3375-1 (Lamy et al., 1998a), GIK 17748-2 (Marchant et al., 1999), and GeoB 3302-1 (Lamy et al., 1999; Hebbeln et al., 2002)) have been recalibrated here to have all records on a common stratigraphic base (Table 2).

4. Results

The data sets from cores GeoB 7112-5 (Mohtadi et al., in press), GIK 17748-2 (Lamy et al., 1999; Marchant et al., 1999, Hebbeln et al., 2002) and GeoB 3302-1 (Lamy et al., 1999, Hebbeln et al., 2002) shown here have been published elsewhere, however, here the data are for the first time compiled to a latitudinal transect. In addition, they are accompanied by new

data obtained on cores GeoB 7139-2 and GeoB 3375-1, with only the $\delta^{18}\text{O}$ data of GeoB 3375-1 having been published before (Lamy et al., 1998a).

Core (cm)	^{14}C AMS age (yr BP)	\pm Err. (yr)	Calibrated age (cal yr BP)	\pm Err. (yr)
GeoB 7112-5				
23	2680 ¹⁾	30	2260	70
128	7855 ¹⁾	55	8270	60
178	11,010 ¹⁾	55	12,590	120
253	13,970 ¹⁾	80	15,930	220
308	16,260 ¹⁾	110	18,330	180
GeoB 3375-1				
13	10,160 ²⁾	100	11,060	180
33	13,340 ²⁾	80	15,350	90
78	16,840 ²⁾	110	18,950	250
118	20,460 ²⁾	325	23,500	510
133	22,350 ²⁾	205	25,410	280
163	26,090 ²⁾	325	29,380	910
183	34,860 ²⁾	1144	38,680	1810
GeoB 7139-2				
13	2645	40	2250	70
88	9650	80	10,420	120
153	12,960	80	14,710	340
238	16,490	80	18,540	190
353	21,630	120	24,760	320
443	25,470	220	28,500	900
553	30,600	420	34,120	510
598	36,160	1210	39,250	1890
GeoB 3302-1				
18	11,430 ³⁾	160	12,940	120
33	13,760 ³⁾	90	15,740	190
68	15,600 ³⁾	130	17,850	120
103	17,060 ³⁾	150	19,250	320
133	17,850 ³⁾	170	20,520	480
178	18,990 ³⁾	180	21,880	240
233	20,100 ³⁾	210	23,070	430
308	23,130 ³⁾	235	25,960	250
403	28,360 ³⁾	186	31,980	460
GIK 17748-2				
69	4160 ⁴⁾	40	4120	80
101	7290 ⁴⁾	40	7720	40
128	9650 ⁴⁾	70	10,410	110
156	10,920 ⁴⁾	50	12,450	170
185	11,600 ⁴⁾	50	13,020	70

¹⁾ Mohtadi et al. (in press)

²⁾ Lamy et al. (1998a)

³⁾ Lamy et al. (1999); Hebbeln et al. (2002)

⁴⁾ Marchant et al. (1999)

Table 2 AMS ^{14}C dates and converted calendar ages used for the age models of the investigated cores. The ^{14}C ages were corrected for a reservoir effect of 400 years (Bard, 1988). Data points marked by ^{x)} have been published earlier, but are re-calibrated here using the CALPAL program (Jöris and Weninger, 1998, updated 2003).

4.1. Stratigraphy

In all the cores the AMS datings line up without any reversals and consequently, the age models for the cores are based on linear interpolation between the calibrated ^{14}C AMS dates. For the stratigraphically rather long cores GeoB 3375-1 and GeoB 7139-2, we here consider only the core sections down to the oldest ^{14}C control points. Following Lamy et al. (1999) and Hebbeln et al. (2002), we treat and discuss in this study the two near-by cores GeoB 3302-1 and GIK 17748-2 as a single record for 33°S. This joint record covers the time span between ~33,000 and 1000 cal yr BP, core GeoB 7112-5 between ~19,000 and 1000 cal yr BP, core GeoB 3375-1 between ~40,000 and 9000 cal yr BP, and core GeoB 7139-2 between ~40,000 and 1000 cal yr BP (Fig. 2). These interpretations are nicely corroborated by the $\delta^{18}\text{O}$ data, which show a well expressed Last Glacial Maximum, an obvious deglaciation and typical Holocene records (Fig. 2).

Inspection of the general trend of the estimated sedimentation rates (SR) resulting from these stratigraphic interpretations reveals similar patterns (Fig. 3a): Increasing SR towards marine isotope stage (MIS) 2, highest values during MIS 2, followed by lower levels during the Holocene. Sedimentation rates are on average higher in the south (GeoB 3302-1: ~25 cm kyr⁻¹) than in the north (e.g. GeoB 3375-1: ~8 cm kyr⁻¹), reflecting different sedimentation regimes (fluvial vs. eolian) in either parts of the investigation area.

4.2. Bulk components

The contents of bulk sedimentary data show a quite similar pattern in all cores (Fig. 3b-d). The TOC (or C_{org}) contents range between 0.5 and 2.5 wt%. They are high prior to ~26,000 cal yr BP, and low between 26,000 and ~16,000 cal yr BP. In the southern cores at 30°S and 33°S, the C_{org} contents are high during Early and Middle Holocene, whereas they diminish at 24°S (Fig. 3b). CaCO_3 contents range between 4 and 27 wt% (Fig. 3c). Their contents decrease towards MIS 2, and increase during deglaciation. During the Holocene, the contents drop continuously towards the present. At 33°S, however, the values remain high until Late Holocene, followed by a significant drop at about 4000 cal yr BP. The opal contents range between 0.2 and 7 wt% (Fig. 3d). Relatively high values around ~30,000 cal yr BP detached the low values prior to it. After a continuous decrease until 15,000 – 13,000 cal yr BP, the opal contents start to increase towards the present.

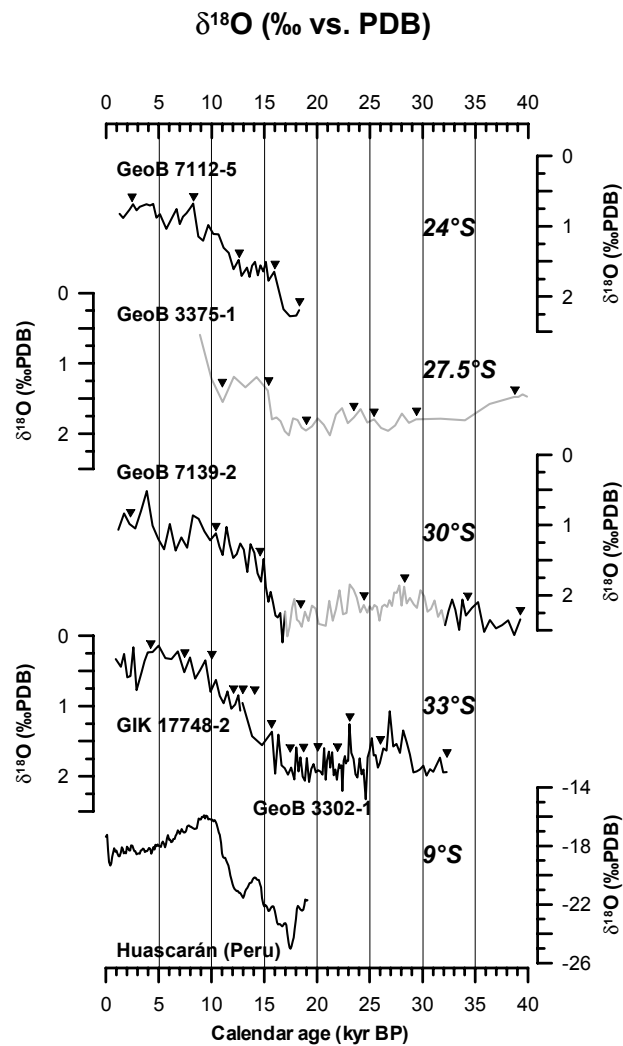


Fig. 2 Oxygen isotope record of the investigated cores from the Chilean continental slope using *N. pachyderma* dex (black lines) and/or *N. pachyderma* sin (grey lines), from north (Murray et al.) to south (bottom). The chronology is based on the AMS ^{14}C dates (triangles) and interpolation between these age control points. Bottom panel shows the $\delta^{18}\text{O}$ record of the Huascarán glacier (9°S, 77°W) in Peru (Thompson et al., 1995).

4.3. Planktic foraminifera

Absolute abundances of planktic foraminifera vary between 0 and ~ 1800 ind. g^{-1} , with much higher values found in pre-Holocene sediments (200 – 1800 ind. g^{-1}) than in Holocene sediments (0 – 650 ind. g^{-1}). Their absolute number decreases towards the north of the study area: e.g., average numbers at 24°S are only 165 ind. g^{-1} prior to the Holocene and 40 ind. g^{-1} during the Holocene. The planktic foraminiferal assemblage is dominated by six species, which account on average for 80% - 95% of the total planktic foraminifera fauna in the records (Fig. 4a). The dominant species are *N. pachyderma* dex, *N. pachyderma* sin, and *Globigerina bulloides*, followed by *N. dutertrei*, *Globigerinita glutinata*, and *Globorotalia inflata*. Species-specific dissolution can be excluded due to high abundances and good

preservation of species with delicate tests, such as *G. bulloides* and *G. glutinata*. The most prominent feature in the planktic foraminiferal fauna through the last 40,000 years in all cores is the changing dominance between *N. pachyderma* sin and *N. pachyderma* dex. The latter is dominant before ~32,000 cal yr BP, and from ~16,000 cal yr BP until present (for the present-day distribution pattern off Chile see Hebbeln et al., 2000a), with contributions up to 65% of the total fauna. Between 32,000 and 16,000 cal yr BP, *N. pachyderma* sin was the dominant species, with relative abundances up to 70% (Fig. 4a).

Additional features are the appearance of *N. dutertrei*, and the decreasing abundance of *G. inflata* at ~16,000 cal yr BP. *N. dutertrei* contributes between 2% and 28% of the total fauna since this time towards the present, with increased relative abundances recorded between ~4000 cal yr BP (at 30°S: ~6000 cal yr BP) and 1000 cal yr BP. Highest contributions of *G. inflata* coincide with the same period when *N. pachyderma* sin was the dominant species (between 32,000 and 16,000 cal yr BP), with relative abundances between 4% and 33%. During the Holocene, its contribution to the total fauna drops below 2%. The contribution of *G. bulloides* is relatively continuous (20% – 35% to the total fauna) through the last 40,000 yr. Between 15,000 and 1000 cal yr BP, however, slightly higher relative abundances of *G. bulloides* can be observed. Furthermore, at 33°S, lower values between 29,000 and 24,000 cal yr BP (6% - 20%) are recorded. *G. glutinata* contributes on average between 2% and 3% to the total fauna, except for the core GeoB 3302-1, where an average of ~10% is observed.

5. Discussion

Stable oxygen isotopes

In the study area, a southward increase in the glacial-interglacial difference of the $\delta^{18}\text{O}$ values can be observed (Fig. 2). The difference between the onset of Termination I and Holocene climatic optimum is about 1.5‰ PDB at 24°S, 1.7‰ PDB at 30°S, and 1.9‰ PDB at 33°S (at 27.5°S, there is no record <9000 cal yr BP). This coincides with the concept of generally higher glacial-interglacial temperature-difference towards higher latitudes. The onset of Termination I in our $\delta^{18}\text{O}$ records occurs at about 17,500 cal yr BP, which corresponds well with $\delta^{18}\text{O}$ record from Huascarán glacier (Thompson et al., 1995) (Fig. 2), and pollen records from southern South America (Denton et al., 1999; McCulloch et al., 2000).

The absolute $\delta^{18}\text{O}$ values at 30°S are on average higher both during Holocene (~1‰ PDB) and last glacial (~2.2‰ PDB) than at 33°S (~0.4‰ PDB during the Holocene and ~1.9‰ PDB during the last glacial, Fig. 2). This implies lower salinity caused by higher precipitation and/or increased fluvial input at 33°S throughout the last 40,000 years.

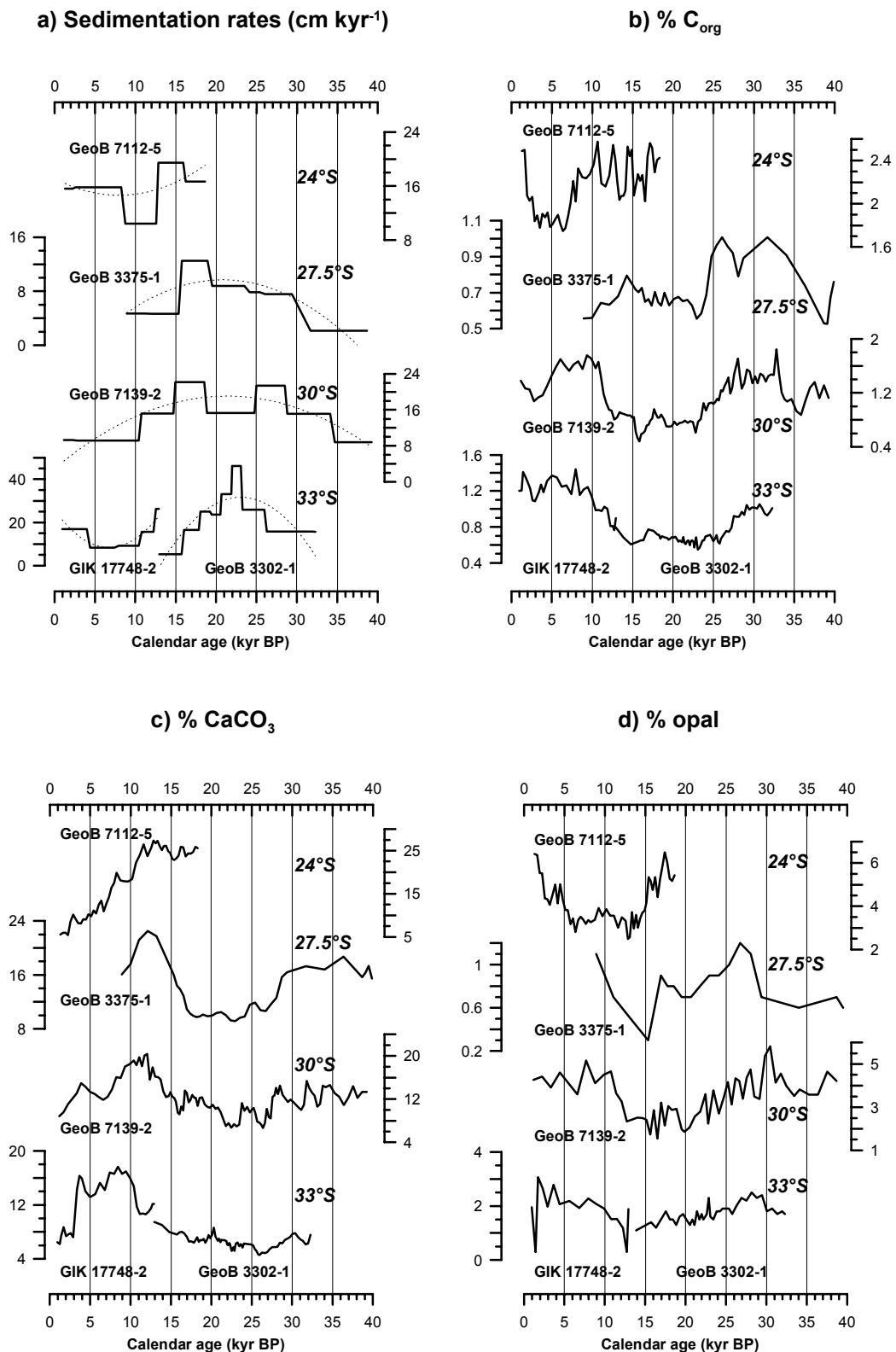


Fig. 3 Sediment data from the continental slope of Chile: a) Estimated sedimentation rates with their polynomial fit (dashed lines), b) Organic carbon (C_{org}) contents, c) Calcium carbonate (CaCO₃) contents, and d) Opal contents of the investigated cores. Note the different scales for each panel.

In the study area, however, lowest average $\delta^{18}\text{O}$ during the last glacial are recorded at 27.5°S (~1.8‰ PDB) while average values are higher northward and southward. As this core has the lowest temporal resolution of all the studied cores, this observation might be due bioturbation effects smoothing the original record. Finally, a strong evidence of a Younger Dryas signal in the $\delta^{18}\text{O}$ records off northern Chile cannot be observed.

Bulk sediment proxies

Assuming that post-sedimentary processes did not significantly affect the contents of biogenic compounds in the sediment, the calculated ARs of biogenic compounds in the bulk sediment should be reliable proxies for the ocean paleoproductivity. In our study area, carbonate dissolution starts below the lysocline, at ~3700 m water depth (Hebbeln et al., 2000a). All cores in this study were retrieved from shallower depths, and visual observations of the tests of planktic foraminifera do not show indications of significant carbonate dissolution. At 33°S, the ARs of biogenic compounds in bulk sediment were relatively low between 33,000 and 23,000 cal yr BP (Fig. 5b-d). Highest ARs of C_{org} (0.2-0.3 g cm⁻² kyr⁻¹), CaCO_3 (2-3 g cm⁻² kyr⁻¹), and opal (0.4-1.1 g cm⁻² kyr⁻¹) are recorded between 23,000 and 21,000 cal yr BP indicating highest paleoproductivity during the LGM. During the Early and Middle Holocene, the ARs were lowest (C_{org} : ~0.1 g cm⁻² kyr⁻¹, CaCO_3 : ~1 g cm⁻² kyr⁻¹, opal: ~0.2 g cm⁻² kyr⁻¹), and subsequently increased during the Late Holocene reaching about twofold higher values than during the Early and Middle Holocene. Resedimentation processes most likely affected extremely low values between 16,000 and 13,000 cal yr BP at 33°S (Lamy et al., 1999; Hebbeln et al., 2002).

North of 33°S, however, highest ARs of C_{org} , CaCO_3 and opal occur before and after the LGM, between ~30,000 and 25,000 cal yr BP, and 19,000 and 16,000 cal yr BP, respectively, with slightly lower values during the LGM (Fig. 5b-d). During the deglaciation and the Holocene the general patterns were similar, with only some minor discrepancies as e.g. the rather late shift to lower ARs at 24°S and 30°S at 13,000 cal yr BP, and 11,000 cal yr BP, respectively.

Unexpectedly high average sedimentation rates (with respect to the observed north to south gradient in sedimentation rates along the Chilean continental slope) and relatively high ARs of biogenic compounds (Fig. 5) together with low ARs of planktic foraminifera (Fig. 6) at 24°S may suggest resedimentation of fine material at this site. However, the patterns of biogenic compounds at 24°S during the Holocene show some similar trends with the records from further south, e.g. higher ARs of C_{org} and opal during the Late Holocene, and decreasing

AR of CaCO_3 throughout the Holocene (Fig. 5). Assuming the rather low ARs of planktic foraminifera as the original signal (as hard to affect by resedimentation due to the size of the individual shells and as being in line with the overall trend) and considering the shape of the fore-arc basin at 24°S acting as a sediment trap, syn-sedimentary processes such as sediment focussing could have led to the comparable high sedimentation rates of fine material at this site. In addition, such syn-sedimentary focusing of contemporary sediments would explain why their temporal pattern fits to the general trend observed further south. (Fig 6).

Planktic foraminifera

Under present-day conditions along the PCC, a general N-S annual temperature difference of $\sim 8^\circ\text{C}$ between 20°S ($\sim 20^\circ\text{C}$) and 45°S ($< 12^\circ\text{C}$) is observed. In spite of such temperature gradient, observations of surface sediment samples beneath the PCC between 22°S and 44°S show *N. pachyderma* dex as the most common planktic foraminifera species with relative abundances $> 50\%$ without any N-S preferences (Hebbeln et al., 2000a; Mohtadi et al., submitted). Hence, the changing dominance of *N. pachyderma* dex and *N. pachyderma* sin off Chile at 16,000 cal. yr BP (Fig. 4b) could not be simply driven by changes in temperature. Results from sediment traps at 33°S off Chile (Marchant et al., 1998) as well as sediment traps and plankton tows off Somalia and Oman (Ivanova et al., 1999) indicate that the occurrence of *N. pachyderma* sin is strongly related to upwelling. In addition, data from the comparable Benguela Current system have shown *N. pachyderma* sin as an indicator of high (paleo) productivity and/or upwelling intensity (Wefer et al., 1996; Little et al., 1997). Applying this tool by using the ratio between *N. pachyderma* sin and *N. pachyderma* dex ($N. \text{pas}/N. \text{pad}$) to distinguish between periods of higher and lower productivity, we find a quite similar pattern off northern Chile with highest productivities indicated between 32,000 and 16,000 cal yr BP (Fig. 4b). Interestingly, during the high productivity period the $N. \text{pas}/N. \text{pad}$ ratio is always $\sim 9:1$ in all records, pointing to an ecological threshold defining the $N. \text{pas}/N. \text{pad}$ ratio.

A conspicuous feature during this high productivity period are the variations in the contributions of *G. inflata*, which has been associated with increased coastal upwelling and productivity off Chile (Marchant et al., 1998; Hebbeln et al., 2000a, 2002). Using the *G. inflata* to *G. bulloides* ratio ($G. \text{inf}/G. \text{bul}$ ratio) provides another productivity proxy that seems to be unaffected by the $N. \text{pas}/N. \text{pad}$ ecological threshold (Fig. 4c) and, therefore, might be more sensitive to productivity changes during the high productivity period prior to 16,000 cal yr BP.

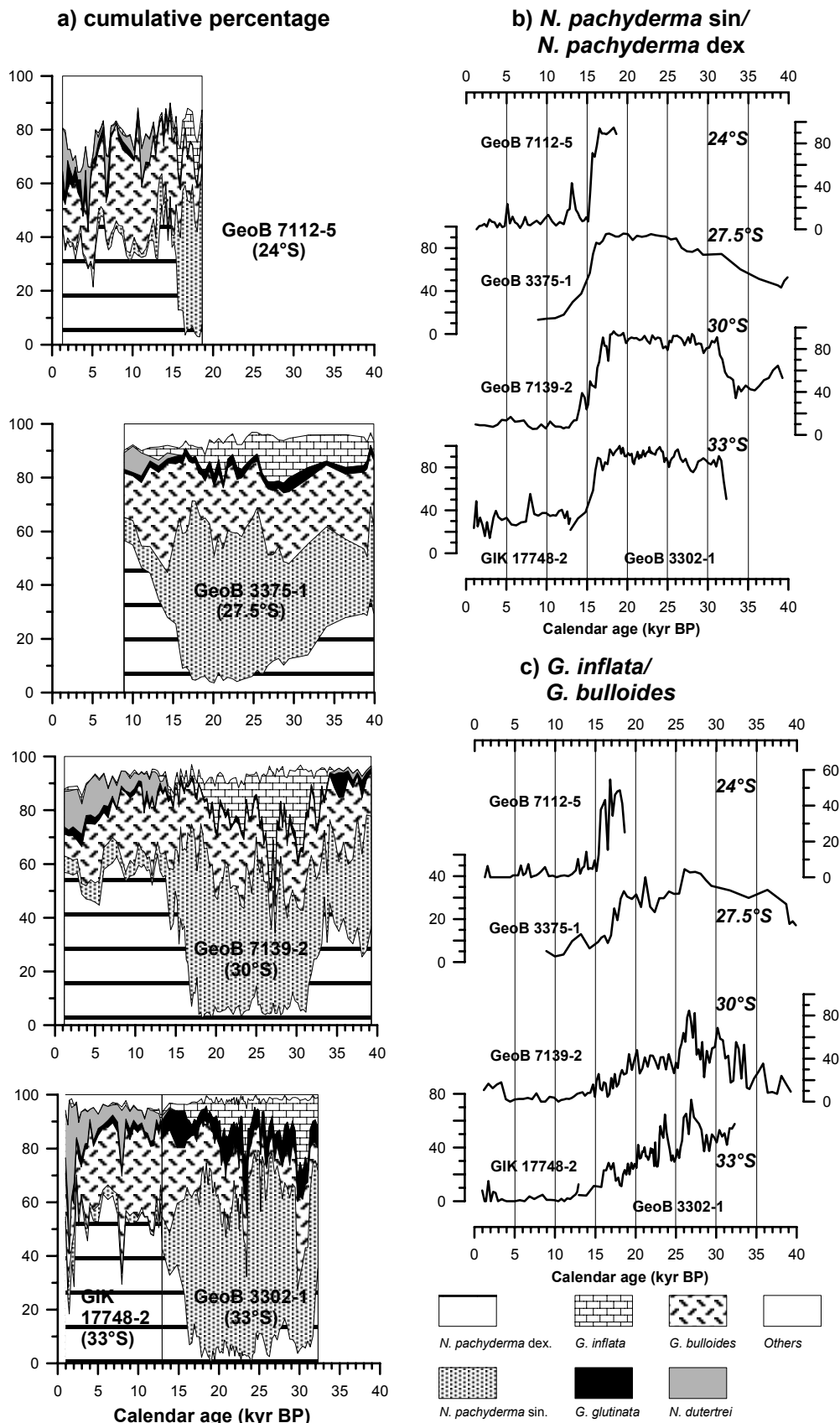


Fig. 4 Planktic foraminiferal data from the Chilean continental slope: a) Time series record of planktic foraminiferal species composition in the investigated cores, displayed as cumulative percentages, from north (Murray et al.) to south (bottom). In the lowermost panel, the solid line at 13 kyr separates GeoB 3302-1 and GIK 17748-2. b) Ratio between *N. pachyderma* sin and *N. pachyderma* dex (ratio = $N. \text{pas} / (N. \text{pas} + N. \text{pad}) * 100$) c) Ratio between *G. inflata* and *G. bulloides* (ratio = $G. \text{inf} / (G. \text{inf} + G. \text{bul}) * 100$). Note the different scales for each panel.

High *G. inf/G. bul* ratios at ~33,000 cal yr BP (30°S); 31-30,000 cal yr BP; 28-26,000 cal yr BP; 24-23,000 cal yr BP (33°S); and 21-20,000 cal yr BP thus might reflect enhanced coastal upwelling (Fig. 4c). Such changes in productivity can be induced either by major changes in upwelling intensity or by displacements of the respective upwelling cells leaving the sites in a more marginal or central position. Most likely, roughly isochronal events at 31-30,000 cal yr BP, 28-26,000 cal yr BP, and 21-20,000 cal yr BP indicate enhanced upwelling-intensities on a regional scale, whilst solitary events reflect changes in the local upwelling cells (Fig. 4c).

The appearance of *N. dutertrei* after 16,000 cal yr BP supports the interpretation of lower productivities associated with higher temperatures since this time. *N. dutertrei* is most likely transported to the study area by subtropical surface waters of the PCCC, and hence, the occurrence of this species indicates stronger advection of warm waters from the north. In addition, higher fluxes of *N. dutertrei* during the Late Holocene might be related to stronger El Niño activities during this period (Marchant et al., 1998).

There are some significant differences to be recognized between the planktic foraminiferal fauna in the records. First, at 33°S, the contributions of *G. glutinata* prior to the Holocene are much higher than in the other records. Second, relative abundances of “other species” increase from south (<5% at 33°S) to north (15-30% at 24°S, Fig. 4a) reflecting higher biodiversity caused by stronger advection of subtropical waters and higher SST throughout the last 40,000 years. And third, the last maximum of the joint relative contributions of *N. pachyderma* sin and *N. pachyderma* dex occurred at 33°S between 21,000 and 18,000 cal yr BP (LGM), while farther north at 30°S and 27.5°S, this peak emerges between 19,000 and 16,000 cal yr BP (Fig 4a).

During the last glacial as well as during the Holocene the AR of total planktic foraminifera increases significantly southward (Fig. 6). This coincides well with the present-day productivity pattern off Chile. The temporal pattern of the total AR of planktic foraminifera shows substantially higher values during the last glacial than during the Holocene (Fig. 6). This indicates generally higher productivities during the last glacial, as shown also by the ARs of biogenic compounds. Comparison of the AR of all planktic foraminifera reveals a considerable difference between the record at 33°S and the records farther north. At 33°S, the highest AR occurs between ~23,000 and 20,000 cal yr BP. North of 33°S, however, such a maximum cannot be observed. Instead, highest ARs are recorded between 19,000 and 16,000 cal yr BP. Between 16,000 and 14,000 cal yr BP, the ARs of planktic foraminifera dropped into much lower levels in all records. Very high (for the respective latitude) ARs of planktic foraminifera occurred also between 14,000 and 13,000 cal yr BP at 24°S, and between 13,000

and 11,000 cal yr BP at 27.5°S. During the Holocene, decreasing ARs of planktic foraminifera towards the present are seen at all sites pointing to lowest productivities.

The AR of *G. bulloides* and *G. glutinata* show an almost identical pattern as the AR of all planktic foraminifera (Fig. 6). Both are ubiquitous species not limited by the physical properties of the global water masses (Bé and Tolderlund, 1971; Hemleben et al., 1989), and referred to as the principal upwelling indicators under coastal upwelling conditions (Thiede, 1975; Marchant et al., 1998). It seems that the ARs of these two species reflect the general pattern of the upwelling-history and paleoproductivity. *N. pachyderma* sin and *G. inflata* have their highest fluxes between ~32,000 and 16,000 cal yr BP, when *N. pachyderma* sin contributed the main part of the peaks in the AR of planktic foraminifera. Highest fluxes of *N. pachyderma* sin north of 33°S are recorded during the last deglaciation, whilst at 33°S, its highest flux occurred during the LGM (Fig. 6). Highest AR of *N. pachyderma* dex occurred before ~32,000 cal yr BP, and during the last deglaciation. ARs of *N. dutertrei* record a marked peak between 13,000 and 11,000 cal yr BP, which occurred earlier in the south (~13,000 cal yr BP) than in the north (~11,000 cal yr BP) of the study area (Fig. 6). Considering that *N. dutertrei* requires higher water temperatures (Bé, 1977), and should have been transported from north to south in this region (Marchant et al., 1998), the interpretation of these peaks is puzzling.

Synthesis of the proxy-records

Comparison of our data show both temporal and spatial variability in the development of the paleoproductivity off northern Chile for the last 40,000 yr. Generally, higher productivities occurred prior to the Holocene. This pattern is indicated both in ARs of biogenic compounds and of planktic foraminifera, as well as in the planktic foraminiferal assemblages of all records (Fig. 4, 5, 6). In addition, at 24°S and 33°S, the ARs of bulk biogenic compounds suggest slightly increased productivity during the late Holocene (Fig. 5). On a spatial scale, a general southward increase of the paleoproductivity in the study area can be inferred from the N-S gradient in the ARs of planktic foraminifera and the bulk biogenic compounds (here with the exception of site GeoB 7112-1, where resedimentation processes are assumed to result in enhanced deposition of fine materials). At 33°S, highest productivity occurred around the LGM, mirrored in highest ARs of planktic foraminifera, *N. pachyderma* sin, and the bulk biogenic compounds. North of 33°S, high paleoproductivity occurred prior to 24,000 cal yr BP, decreased during the LGM to lower values, and increased again during the post glacial (18,000 – max. 11,000 cal yr BP).

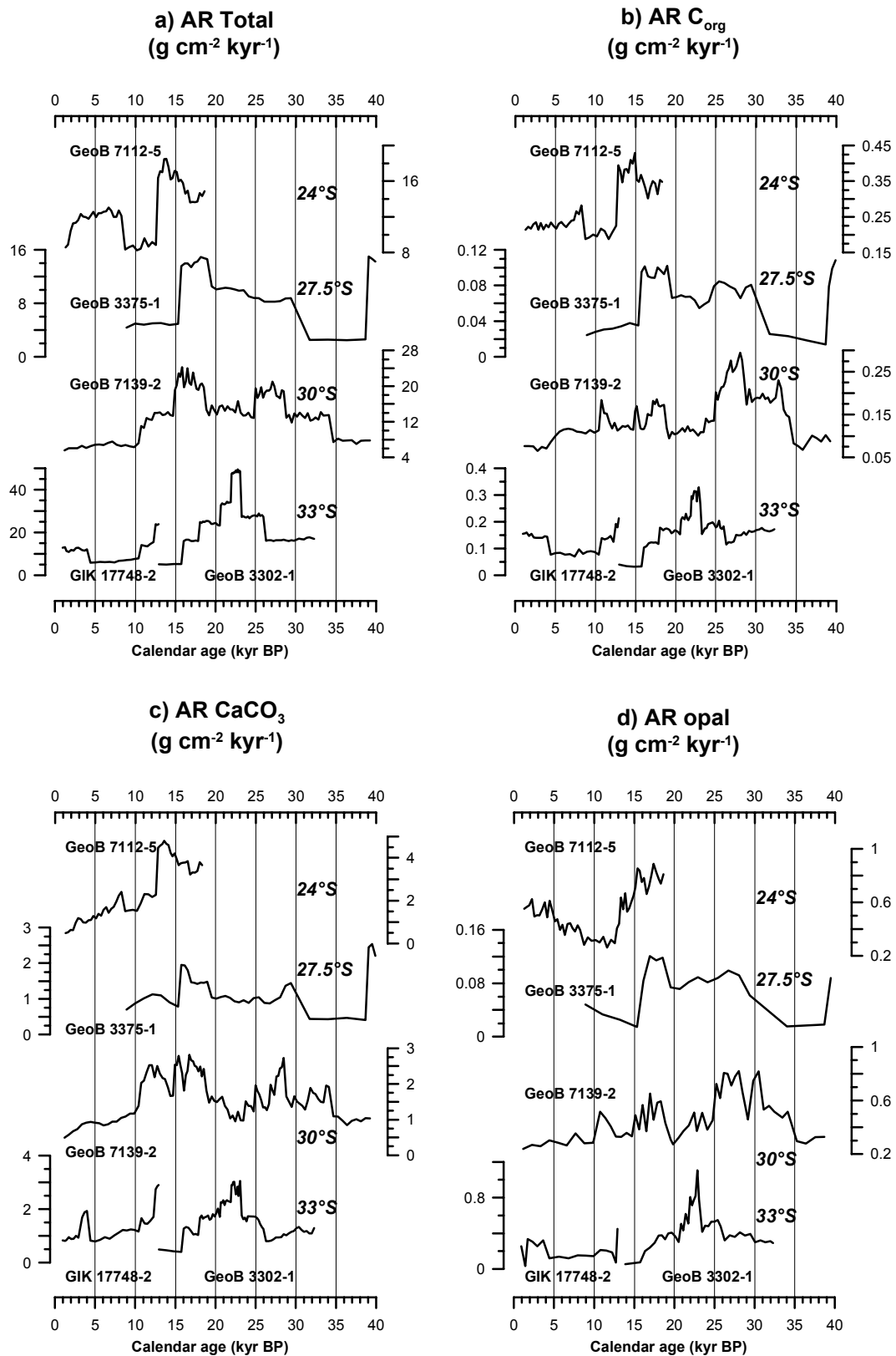


Fig. 5 Accumulation rates (AR) of a) Bulk sediment (Total), b) Organic carbon (C_{org}), c) Calcium carbonate (CaCO_3), and d) Opal in the investigated cores from the Chilean continental slope. All values are in $\text{g cm}^{-2} \text{ kyr}^{-1}$. Note the different scales for each panel.

In addition, this two-peak pattern is documented in the ARs of planktic foraminifera, the ARs of *N. pachyderma* sin, and in the ARs of biogenic compounds (Fig. 5, 6).

Paleoceanographic and paleoclimatic history

Sediment data from off northern Chile confirm the picture of regional late Pleistocene and Holocene productivity variations driven by changes in the paleoceanographic and paleoclimatic regimes. During the last glacial, paleoproductivity was highest at 33°S. Lamy et al. (1999) and Hebbeln et al. (2002) referred this peak in the paleoproductivity to the northward displacement of the climate zones induced by a northward shift of the main regional atmospheric and oceanographic circulation systems, namely the ACC and the Southern Westerlies. According to these authors, a northward shift of the ACC brings the main macronutrient-source (particularly phosphate and nitrate) (Levitus et al., 1994), closer to the study area, thereby providing more nutrients and hence, increasing productivity. In addition, a northward movement of the Southern Westerlies, as the main precipitation source onshore, causes more continental run-off and consequently, a higher supply of micronutrients (in particular iron) contributing to higher productivities. This scenario can be observed nowadays south of 40°S at the position of the southern westerlies, where marine productivity is highest although coastal upwelling does not occur (Hebbeln et al., 2000a). Subsequently, the southward displacement of these circulation systems during the deglaciation caused a decrease in paleoproductivity at 33°S (Lamy et al., 1999; Hebbeln et al., 2002).

This interpretation, however, does not fit with the data obtained north of 33°S, where highest productivities are indicated for the deglaciation (Fig. 5, 6).

Lamy et al. (1998a) investigated illite/chlorite and smectite/illite ratios, as well as the crystallinity of smectite and illite clay minerals at 27.5°S (GeoB 3375-1) and found evidences for increased humidity onshore during precession maxima, and postulated it for the period between 18,000 and 29,000 cal yr BP, as a period of precession maximum. However, the expression of the precession cycles in their data is weak or even absent between 40,000 and 10,000 yr (Lamy et al., 1998a), and a higher frequency temporal observation of their data implies increased humidity before and after the LGM, as shown in our data. Comparisons of our $\delta^{18}\text{O}$ records, planktic foraminifera, as well as bulk sediment data suggest that probably the discharge of the river Copiapó close to the core site caused lower salinities with a minor impact on the marine paleoproductivity (Fig. 4, 5, 6). Yet the link of this increased humidity onshore to the Southern Westerlies (Lamy et al., 1998a) remains speculative since the source areas of the observed clay minerals as well as the catchment areas of the river Copiapó during

the LGM are not easy to define. Numerous investigations on land north of 29°S do not support any influence of the Southern Westerlies during the LGM (Fox and Strecker, 1991; Veit, 1992; 1996). Moreover, observations by Grosjean et al. (2001) on pollen, spores and algae in lake sediments at 23°S evidence extremely dry conditions during the LGM. Ammann et al. (2001) could not find indications for a shift in the position of the Southern Westerlies during the LGM by their glacier-reconstruction between 18°S and 29°S, since the northern limit of the glacier growth due to precipitation from the Westerlies, presently at 27°S, did not change at all.

The modern moisture-source for the Atacama and the central Andes is currently (and for the late Pleistocene) the tropical Atlantic. The moisture is transported via tropical easterlies over the Amazonian basin into the Altiplano (e.g. Grosjean, 1994; Grosjean et al., 1995; Thompson et al., 1995; 1998; Aravena et al., 1999). A late glacial humid phase prevailed approx. between 17,500 and 11,000 cal yr BP (Servant et al., 1995; Clapperton et al., 1997) leading to large glacier extension in the dry Andes around 15,000 cal yr BP (Messerli et al., 1992; Seltzer, 1992; 1994; Clayton and Clapperton, 1997), and maximum lake levels between 13,000 and 11,000 cal yr BP (Grosjean, 1994). This period of increased humidity onshore coincides well with the very high marine productivities recorded north of 33°S. Whether and how exactly this precipitation source affected the marine paleoproductivity remains unsolved. Nevertheless, it is tempting to suggest that this humid phase affected the paleoproductivity through enhanced river borne nutrient supply into the upwelling area. Furthermore, the flooding of the exposed continental shelf during the postglacial sea level rise may have provided additional nutrients contributing to the productivity maximum during the deglaciation.

North of 33°S, the subtropical high-pressure belt is one of the most important controlling factors of the regional climate, and the main reason for high aridity nowadays in this region. A weaker subtropical high-pressure belt coincides with stronger winds and enhanced upwelling of coastal waters and hence, higher productivity. In any case, the marine productivity off the hyper-arid areas of northern Chile appears to be affected rather by the strength and the position of the South Pacific anticyclone than by the position of the Southern Westerlies. In addition, the strength of the high-pressure cell over the SE-Pacific also affects the migration of the frontal systems of the Southern Westerlies (Villagrán, 1990), however without significant effects north of 33°S.

Yet the question is what drove the generally high productivities in the study area during the last glacial? It can be explained relatively simply by the position of the ACC.

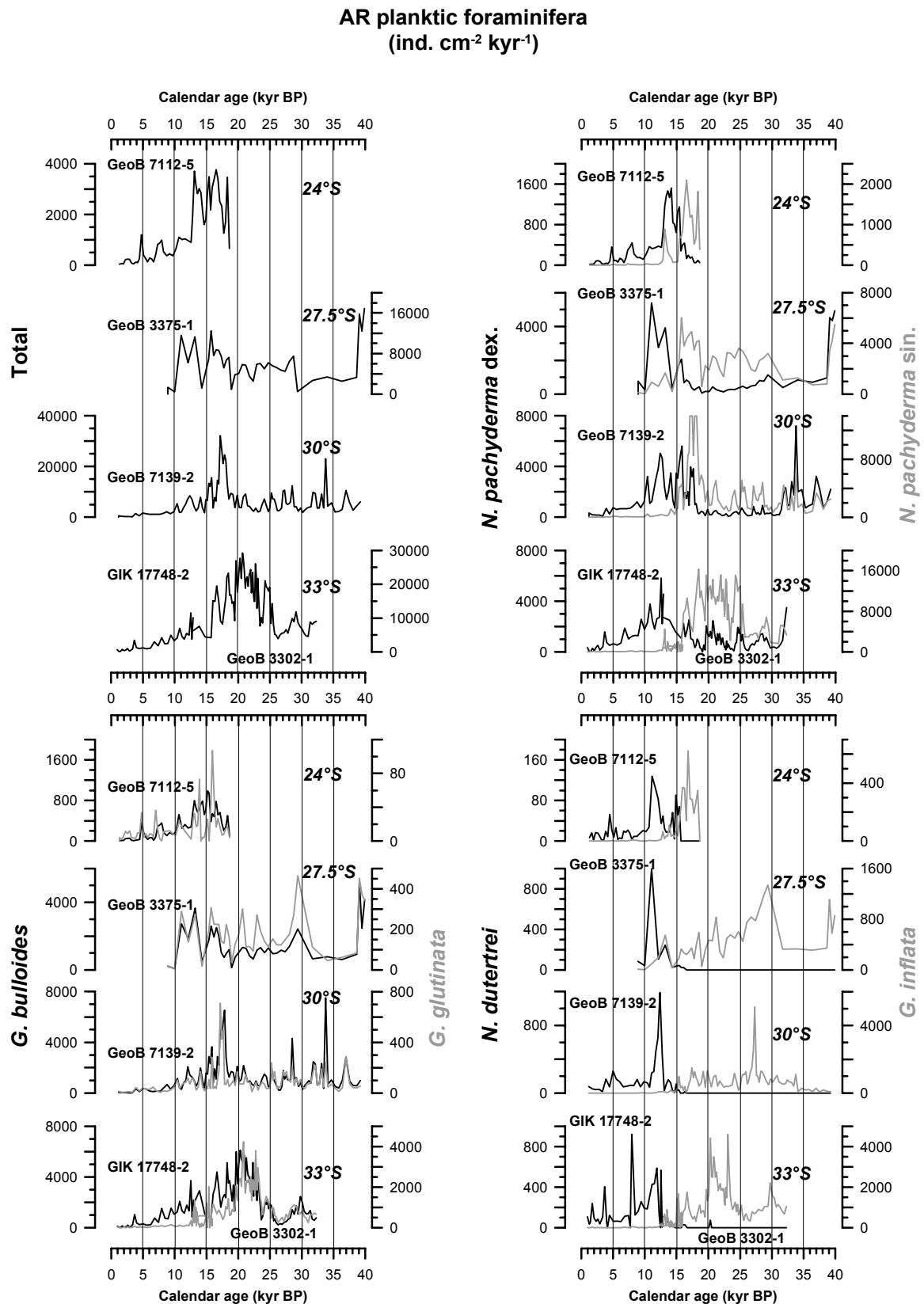


Fig. 6 Accumulation rates of all planktic foraminifera (upper left), and of the most important planktic foraminifera species in the investigated cores from the Chilean continental slope, given in individuals (ind.) cm⁻² kyr⁻¹. Note the different scales for each panel.

In this scenario, the ACC was situated farther north and supplied more nutrients into the study area during the last glacial. Boosted by enhanced precipitation caused by the Southern Westerlies, at 33°S these conditions led the paleoproductivity culminating to its highest levels during the LGM (combination of stronger advection of the ACC and stronger Southern Westerlies). North of 33°S, a higher hemispheric thermal gradient caused stronger winds leading to stronger upwelling and higher productivities (combination of stronger advection of the ACC and stronger upwelling). Stronger advection of the PCC during the glacial periods has been proposed also by investigations north of the study area, off Peru (Feldberg and Mix, 2002; 2003), off Galapagos (Le et al., 1995), and in the Eastern Equatorial Pacific (Pisias and Mix, 1997; Mix et al., 1999). Investigations onshore also show that optimum conditions for lake development occur neither during full glacial conditions (extremely dry and cold) nor during interglacial conditions (high evaporation) (e.g. Messerli et al., 1992; Clapperton et al., 1997; Clayton and Clapperton, 1997).

Dry conditions in north Chile and the accompanied reduced continental runoff during the LGM explain relatively lower productivities during the LGM, while high productivities during the deglaciation possibly occurred through a combination of a still northerly position of the ACC (supply of macronutrients), relatively strong winds (strong upwelling), enhanced precipitation onshore and flooding of the shelf (supply of micronutrients). A rather southward position of the ACC (and the Southern Westerlies) and reduced precipitation during the Early and Middle Holocene probably resulted in the lowest observed productivities off Chile during the last 40 kyr.

Another prominent feature in our records is the lagged response of the planktic foraminiferal fauna to the onset of the deglaciation signal in the planktic foraminifera $\delta^{18}\text{O}$ records. The decrease in the $\delta^{18}\text{O}$ values started nearly synchronous at ~17,500 cal yr BP reflecting the onset of Termination I (e.g. Denton et al., 1999; Denton, 2000) (Fig. 2). However, the planktic foraminifera community responded about 1500 yr later, at ~16,000 cal yr BP (Fig. 4a,b), when the shift from *N. pachyderma* sin to *N. pachyderma* dex occurred simultaneously between 24°S and 33°S, without being related to the different productivity patterns north and south of 32°S. McCulloch et al. (2000) referred to pollen records from between 40°S and 55°S in the Chilean lake district and in the Strait of Magellan and described a similar delay in the response of the vegetation to the hemispheric onset of the deglaciation. They related the observed offset (1600 yr) to the reorganization of the oceanic thermohaline circulation following its earlier suppression during the Heinrich 1 event (Denton, 2000). If this hypothesis is correct then it points to the lagged return of the ACC (and the Southern

Westerlies) to its (their) Holocene-position farther south. Following this hypothesis, the start of the modern thermohaline circulation only after Heinrich 1 should have been the most important reason that delayed the postglacial reorganization of the major circulation systems in the SE-Pacific.

6. Conclusions

1. During the last 40,000 yr, paleoproductivity off northern Chile was generally higher during the last glacial than during the Holocene. Between 24°S and 33°S, a generally southward increase of the paleoproductivity can be observed.
2. Two different atmospheric phenomena induced changes in the paleoproductivity in the upwelling areas off central and north Chile. At 33°S, paleoproductivity was highest around the LGM caused by the northward migration and intensification of the Southern Westerlies and the ACC resulting in higher precipitation onshore and enhanced nutrient supply into the upwelling region. North of 33°S, evidences from $\delta^{18}\text{O}$ records, biogenic compounds, and planktic foraminifera suggest that the paleoproductivity remained unaffected by the southern westerlies throughout the last 40,000 yr. It increased during the deglaciation induced by the strengthening of the upwelling parallel to enhanced micronutrient supply probably caused by increased precipitation in northern Chile between 17,500 and 11,000 cal yr BP, and flooding of the continental shelf.
3. The main macronutrient source for the upwelling region off Chile is the ACC. Our data suggest that changes in its position and intensity affected the entire upwelling regimes and caused changes in the paleoproductivity.

Acknowledgments

We thank M. Segl and B. Meyer-Schack, who performed the stable isotope measurements. This study was supported by the German Bundesministerium für Bildung und Forschung through funding of the projects “CHIPAL” and “PUCK”. The Research Center Ocean Margins at the University of Bremen provided technical support. The data presented in this paper are also available in digital format (www.pangaea.de/PangaVista). This is a RCOM publication Nr.

References

- Ammann, C., Jenny, B., Kammer, K. and Messerli, B., 2001. Late Quaternary Glacier response to humidity changes in the arid Andes of Chile (18-29°S). *Palaeogeography, Palaeoclimatology, Palaeoecology*, 172: 313-326.
- Aravena, R., Suzuki, O., Peña, H., Pollastri, A., Fuenzalida, H. and Gilli, A., 1999. Isotopic composition and origin of the precipitation in Northern Chile. *Appl. Geochem.*, 14: 411-422.
- Bard, E., 1988. Correction of accelerator mass spectrometry ^{14}C ages measured in planktonic foraminifera: Paleoceanographic implications. *Paleoceanography*, 3: 635-645.
- Bé, A.W.H. and Tolderlund, D.S., 1971. Distribution and ecology of living planktonic foraminifera in surface water of the Atlantic and Indian Oceans. In: B.M. Turnell and W.R. Riedel (Editors), *The Micropaleontology of the Ocean*. Cambridge University Press, pp. 105-149.
- Bé, A.W.H., 1977. An ecological, zoogeographic and taxonomic review of recent planktonic foraminifera. In: A.T.S. Ramsey (Editor), *Oceanic Micropaleontology*. Academic Press, London.
- Berger, W.H., Fischer, K., Lai, C. and Wu, G., 1987. Ocean productivity and organic carbon flux. Part I. Overview and maps of primary production and export productivity. University of California, San Diego.
- Berger, W.H., Smetacek, V.S. and Wefer, G., 1989. Ocean productivity and paleoproductivity -an overview. In: W.H. Berger, V.S. Smetacek, and G. Wefer (Editor), *Productivity of the oceans: present and past*. John Willey & Sons, New York, pp. 1-34.
- Broecker, W.S. and Peng, T.H., 1982. *Tracers in the Sea*. Lamont Doherty Geol. Obs. Publications, New York, 689 pp.
- Clapperton, C., 1993. *Quaternary geology and geomorphology of South America*. Elsevier Science Publishers, Amsterdam, The Netherlands, 779 pp.
- Clapperton, C.M., Clayton, J.D., Benn, D.I., Marden, C.J. and Argollo, J., 1997. Late Quaternary glacier advances and palaeolake highstands in the Bolivian Altiplano. *Quaternary International*, 38: 49-59.
- Clayton, J.D. and Clapperton, C.M., 1997. Broad synchrony of a Late Glacial glacier advance and the highstand of paleolake Tauca in the Bolivian Altiplano. *Journal of Quaternary Science*, 12: 169-182.
- De Master, D.J., 1981. The supply and accumulation of silica in the marine environment. *Geochimica Cosmochimica Acta*, 45: 1715-1732.
- Denton, G.H., Heusser, C.J., Lowell, T.V., Moreno, P.J., Andersen, B.G., Heusser, L.E., Schlüchter, C. and Marchant, D.R., 1999. Interhemispheric linkage of paleoclimate during the last glaciation. *Geografiska Annaler*, 81 A: 107-153.

- Denton, G.H., 2000. Does an asymmetric thermohaline-ice-sheet oscillator drive 100,000-yr glacial cycles? *Journal of Quaternary Science*, 15(4): 301-318.
- Feldberg, M.J. and Mix, A.C., 2002. Sea-surface temperature estimates in the Southeast Pacific based on planktonic foraminiferal species; modern calibration and Last Glacial Maximum. *Marine Micropaleontology*, 44(1-2): 1-29.
- Feldberg, M.J. and Mix, A.C., 2003. Planktonic foraminifera, sea surface temperatures, and mechanisms of oceanic change in the Peru and south equatorial currents, 0-150 ka BP. *Paleoceanography*, 18(1): 1016, doi: 10.1029/2001PA000740.
- Fox, A.N. and Strecker, M.R., 1991. Pleistocene and modern snowlines in the Central Andes (24-28°S). *Bamberger Geographische Schriften*, 11: 169-182.
- Garleff, K., Schäbitz, F., Stingl, H. and Veit, H., 1991. Jungquartäre Landschaftsentwicklung beiderseits der Ariden Diagonale Südamerikas. *Bamberger Geographische Schriften*, 11: 359-394.
- Grosjean, M., 1994. Paleohydrology of the Laguna Lejia (north Chilean Altiplano) and climatic implications for late-glacial times. *Palaeogeography, Palaeoclimatology, Palaeoecology*, 109: 89-100.
- Grosjean, M., Geyh, M.A., Messerli, B. and Schotterer, U., 1995. Late-glacial and early Holocene lake sediments, ground water formations and climate in the Atacama Altiplano. *Journal of Paleolimnology*, 14: 241-252.
- Grosjean, M., van Leeuwen, J.F.N., van der Knaap, W.O., Geyh, M.A., Ammann, B., Tanner, W., Messerli, B., Nunez, L.A., Valero-Garces, B.L. and Veit, H., 2001. A 22,000 ¹⁴C year BP sediment and pollen record of climate change from Laguna Miscanti (23°S), northern Chile. *Global and Planetary Change*, 28(1-4): 35-51.
- Grosjean, M., Cartajena, I., Geyh, M.A. and Nunez, L., 2003. From proxy data to paleoclimate interpretation: the mid-Holocene paradox of the Atacama Desert, northern Chile. *Palaeogeography, Palaeoclimatology, Palaeoecology*, 194(1-3): 247-258.
- Hebbeln, D., Wefer, G. and cruise participants, 1995. Cruise Report of R/V SONNE Cruise 102, Valparaiso-Valparaiso, 9.5.-28.6.95. *Berichte aus dem Fachbereich Geowissenschaften*, 68. Universität Bremen, Bremen, 126 pp.
- Hebbeln, D., Marchant, M., Freudenthal, T. and Wefer, G., 2000a. Surface sediment distribution along the Chilean continental slope related to upwelling and productivity. *Marine Geology*, 164(3-4): 119-137.
- Hebbeln, D. et al., 2001. PUCK, report and preliminary results of R/V Sonne cruise SO 156, Valparaiso (Chile) - Talcahuano (Chile), March 29 - May 14, 2001. *Berichte aus dem Fachbereich Geowissenschaften*, 182. Universität Bremen, 195 pp.
- Hebbeln, D., Marchant, M. and Wefer, G., 2002. Paleoproductivity in the southern Peru-Chile Current through the last 33000 yr. *Marine Geology*, 186(3-4): 487-504.
- Hemleben, C., Spindler, M. and Anderson, O.R., 1989. *Modern planktonic foraminifera*. Springer, New York, 363 pp.

- Heusser, C.J., 1990. Ice age vegetation and climate of subtropical Chile. *Palaeogeography, Palaeoclimatology, Palaeoecology*, 80: 107-127.
- Ingle, J.C., Keller, G. and Kolpack, R.L., 1980. Benthic foraminiferal biofacies, sediments and water masses of the southern Peru-Chile Trench area, southeastern Pacific Ocean. *Micropaleontology*, 26: 113-150.
- Ivanova, E.M., Conan, S.M.-H., Peeters, F.J.C. and Troelstra, S.R., 1999. Living *Neogloboquadrina pachyderma* sin and its distribution in the sediments from Oman and Somalia upwelling areas. *Marine Micropaleontology*, 36(2-3): 91-107.
- Jenny, B., Valero-Garces, B.L., Villa-Martinez, R., Urrutia, R., Geyh, M. and Veit, H., 2002. Early to Mid-Holocene Aridity in Central Chile and the Southern Westerlies: The Laguna Aculeo Record (34°S). *Quaternary Research*, 58(2): 160-170.
- Jöris, O. and Weninger, B., 1998. Extension of the ^{14}C calibration curve to ca. 40,000 cal BC by synchronizing Greenland $^{18}\text{O}/^{16}\text{O}$ ice core records and North Atlantic foraminifera profiles: A comparison with U/Th coral data. *Radiocarbon*, 40(1): 495-504.
- Kennett, J.P. and Srinivasan, M., 1983. Neogene planktonic foraminifera - A Phylogenetic atlas. Hutchinson Ross Publishing, Stroudsburg, 265 pp.
- Kim, J., Schneider, R.R., Hebbeln, D., Müller, P.J. and Wefer, G., 2002. Last deglacial sea-surface temperature evolution in the southeast Pacific compared to climate changes on the South American continent. *Quaternary Science Reviews*, 21: 2085-2097.
- Klump, J., Hebbeln, D. and Wefer, G., 2001. High concentrations of biogenic barium in Pacific sediments after Termination I - A signal of changes in productivity and deep water chemistry. *Marine Geology*, 177: 1-11.
- Lamy, F., Hebbeln, D. and Wefer, G., 1998a. Late Quaternary precessional cycles of terrigenous sediment input off the Norte Chico, Chile (27.5°S) and paleoclimatic implications. *Palaeogeography, Palaeoclimatology, Palaeoecology*, 141(3-4): 233-251.
- Lamy, F., Hebbeln, D. and Wefer, G., 1999. High resolution marine record of climatic change in mid-latitude Chile during the last 28,000 years based on terrigenous sediment parameters. *Quaternary Research*, 51: 83-93.
- Lamy, F., Hebbeln, D., Rohl, U. and Wefer, G., 2001. Holocene rainfall variability in southern Chile: a marine record of latitudinal shifts of the Southern Westerlies. *Earth and Planetary Science Letters*, 185(3-4): 369-382.
- Le, J., Mix, A.C. and Shackleton, N.J., 1995. Late Quaternary paleoceanography in the Eastern Equatorial Pacific Ocean from planktonic foraminifers: A high-resolution record from ODP Site 846. In: N.G. Pisias, L.A. Mayer, T.R. Janecek, A. Palmer-Jelson and T.H. van Andel (Editors), *Proceedings of the Ocean Drilling Program, Scientific Results*. Ocean Drilling Program, College Station, pp. 675-693.
- Levitus, S., Burgett, R. and Boyer, T.B., 1994. *World Ocean Atlas 1994*, 3: Nutrients. NOAA, US Department of Commerce, Washington, DC.
- Little, M.G., Schneider, R.R., Kroon, D., Price, B., Bickert, T. and Wefer, G., 1997. Rapid paleoceanographic changes in the Benguela Upwelling System for the last 160,000

- years as indicated by abundances of planktonic foraminifera. *Palaeogeography, Palaeoclimatology, Palaeoecology*, 130: 135-161.
- Marchant, M., Hebbeln, D. and Wefer, G., 1998. Seasonal flux patterns of planktic foraminifera in the Peru-Chile Current. *Deep-Sea Research I*, 45: 1161-1185.
- Marchant, M., Hebbeln, D. and Wefer, G., 1999. High resolution planktic foraminiferal record of the last 13,300 years from the upwelling area off Chile. *Marine Geology*, 161: 115-128.
- Markgraf, V., Dodson, J.R., Kershaw, P.A., McGlone, M.S. and Nicholls, N., 1992. Evolution of late Pleistocene and Holocene climates in the circum-South Pacific land areas. *Climate Dynamics*, 6: 193-211.
- Markgraf, V., 1993. Climatic history of South America since 18,000 yr B.P.: comparison of pollen records and model simulations. In: H.E. Wright et al. (Editors), *Global climate since the Last Glacial Maximum*. University of Minnesota Press, Minneapolis, pp. 357-385.
- McCulloch, R.D., Bentley, M.J., Purves, R.S., Hulton, N.R.J., Sugden, D.E. and Clapperton, C.M., 2000. Climatic inferences from glacial and palaeoecological evidence at the last glacial termination, southern South America. *Journal of Quaternary Science*, 15(4): 409-417.
- Messerli, B., Grosjean, M., Graf, K., Schotterer, U., Schreier, H. and Vuille, M., 1992. Die Veränderungen von Klima und Umwelt in der Region Atacama (Nordchile) seit der letzten Kaltzeit. *Erdkunde*, 46: 257-272.
- Miller, A., 1976. The climate of Chile. In: W. Schwerdtfeger (Editor), *World Survey of Climatology Vol. 12*. Elsevier, Amsterdam, pp. 113-145.
- Mix, A.C., Morey, A.E., Pisias, N.G. and Hostetler, S.W., 1999. Foraminiferal fauna estimates of paleotemperature: Circumventing the no-analog problem yields cool ice age tropics. *Paleoceanography*, 14(3): 350-359.
- Mohtadi, M., Romero, O.E. and Hebbeln, D., in press. Changing marine productivity off northern Chile during the last 19,000 years: a multiparameter approach. *Journal of Quaternary Science*.
- Müller, P.J. and Schneider, R., 1993. An automated leaching method for the determination of opal in sediments and particulate matter. *Deep-Sea Research I*, 40(3): 425-444.
- Müller, P.J., Schneider, R. and Ruhland, G., 1994. Late Quaternary PCO₂ variations in the Angola Current: Evidence from organic carbon $\delta^{13}\text{C}$ and alkenone temperature. In: R. Zahn, T.F. Pedersen, M.A. Kaminski and L. Labeyrie (Editors), *Carbon cycling in the glacial ocean: Constraints on the ocean's role in global change*. NATO ASI Series I. Springer-Verlag, Berlin, pp. 343-366.
- Murray, J.W., Jannasch, H.W., Honjo, S., Anderson, R.F., Reburgh, W.S., Top, Z., Friedrich, G.E., Codispoti, L.A. and Izdar, E., 1989. Unexpected changes in the oxic/anoxic interface in the Black Sea. *Nature*, 338: 411-413.

- Nadeau, M.J., Schleicher, M., Grootes, P.M., Erlenkeuser, H., Gottolong, A., Mous, D.J.W., Sarnthein, J.M. and Willkomm, N., 1997. The Leibniz-Labor AMS facility at the Christian-Albrechts University, Kiel, Germany. *Nuclear Instruments and Methods in Physics Research*, 123: 22-30.
- Parker, F., 1962. Planktic foraminifera species in Pacific sediments. *Micropaleontology*, 8: 219-254.
- Pisias, N.G. and Mix, A.C., 1997. Spatial and temporal oceanographic variability of the eastern equatorial Pacific during the late Pleistocene: evidence from radiolaria microfossils. *Paleoceanography*, 12(3): 381-393.
- Seltzer, G.O., 1992. Late Quaternary glaciation of the Cordillera Real, Bolivia. *Journal of Quaternary Science*, 7: 87-98.
- Seltzer, G.O., 1994. Andean snowline evidence for cooler subtropics at the last glacial maximum. In: J.C. Duplessy and Spyridakis (Editors), *Long-Term Climatic Variations*. Nato ASI Series. Springer-Verlag, Berlin, Heidelberg, pp. 374-378.
- Servant, M., Fournier, M., Argollo, J., Servant-Vildary, S., Sylvestre, F., Wirrmann, D. and Ybert, J.P., 1995. La dernière transition glaciaire/interglaciaire des Andes tropical sud (Bolivie) d'après l'étude des variations des niveaux lacustres et des fluctuations glaciaires. *Comptes Rendues de l'Academie des Sciences de Paris*, 320: 729-736.
- Shaffer, G., Salinas, S., Pizarro, O., Vega, A. and Hormazabal, S., 1995. Currents in the deep ocean off Chile (30°S). *Deep-Sea Research*, 42: 425-436.
- Stoffers, P., Hekinian, R. and Cruise Participants, 1992. Cruise report Sonne 80a - Midplate III oceanic volcanism in the Southeast Pacific. *Berichte*. Universität Kiel, Kiel, 128 pp.
- Strub, P.T., Mesías, J.M., Montecino, V., Rutllant, J. and Salinas, S., 1998. Coastal ocean circulation off western South America. In: A.R. Robinson and K.H. Brink (Editors), *The Global Coastal Ocean - Regional Studies and Synthesis*. The Sea, ideas and observations on progress in the study of the seas. John Wiley & Sons, Inc., New York, pp. 273-313.
- Sylvestre, F., Servant, M., Servant-Vildary, S., Causse, C., Fournier, M. and Ybert, J.-P., 1999. Lake-level chronology on the southern Bolivian Altiplano (18°-23°S) during the late-glacial time and the early Holocene. *Quaternary Research*, 51: 54-66.
- Thiede, J., 1975. Distribution of foraminifera in surface waters of a coastal upwelling area. *Nature*, 253: 712-714.
- Thompson, L.G., Mosley-Thompson, E., Davis, M.E., Lin, P.-N., Hendersen, K.A., Cole-Dai, J., Bolzan, J.F. and Liu, K.-b., 1995. Late Glacial Stage and Holocene Tropical Ice Core Records from Huascarán, Peru. *Science*, 269: 46-50.
- Thompson, L.G. et al., 1998. A 25,000 year tropical climate history from the Bolivian ice cores. *Science*, 282: 1858-1864.
- Veit, H., 1992. Jungquartäre Landschafts- und Bodenentwicklung im chilenischen Andenvorland zwischen 27-33°S. *Bonner Geographische Abhandlungen*, 85: 196-208.

- Veit, H., 1996. Southern Westerlies during the Holocene deduced from geomorphological and pedological studies in the Norte Chico, Northern Chile (27-33°S). *Palaeogeography Palaeoclimatology Palaeoecology*, 123: 107-119.
- Villagrán, C., 1990. Glacial climates and their effects on the history of the vegetation of Chile: A synthesis based on palynological evidence from Isla de Chiloé. *Review of Palaeobotany and Palynology*, 65: 17-24.
- Villagrán, C., 1993. Una interpretación climática del registro palinológico del último ciclo glacial-postglacial en Sudamérica. *Bull. Inst. fr. études andines*, 22(1): 243-258.
- Wefer, G. et al., 1996. Late Quaternary surface circulation of the South Atlantic: The stable isotope record and implications for heat transport and productivity. In: G. Wefer, W.H. Berger, G. Siedler and D.J. Webb (Editors), *The South Atlantic: present and past circulation*. Springer, Berlin Heidelberg, pp. 461-502.

Conclusions and perspectives

Previous paleoceanographic studies have shown significant variations of marine productivity off Chile on glacial – interglacial timescales, and a strong coupling of atmospheric and oceanic circulations especially off south and central Chile (Lamy et al., 1998a; 1999; 2001; 2002; Marchant et al., 1999; Klump et al., 2001; Hebbeln et al., 2002; Kim et al., 2002). The focus of this PhD thesis was to apply different geochemical and micropaleontological proxies for a better estimation of temporal and spatial productivity variations along the Chilean continental margin. This study was based upon two main sections: First, observations on surface sediments in order to improve the knowledge of the present-day regional productivity gradients and to evaluate the potential of the applied proxies for paleoproductivity reconstructions in the investigation area. Second, generating age models for different sediment cores and application of the proxies' qualitative and quantitative variations for paleoclimatic reconstructions on a regional scale.

A distinct latitudinal distribution pattern was observed both in the isotopic and faunal compositions of planktic foraminifera in the surface sediments beneath the PCC. From the analyses, it is evident that two main oceanographic processes control the present-day biological production off Chile. South of 39°S, enhanced onshore humidity brought by the Southern Westerlies results in increased precipitation, continental runoff and supply of micronutrients to the coastal regions. This setting, in addition to the supply of macronutrients by the ACC causes highest productivities recorded off Chile. North of 39°S, coastal upwelling promotes high marine production, especially in the upwelling centers at 30° - 33°S and north of 25°S.

The same atmospheric and oceanographic circulation systems appear to be responsible for productivity variations within the last 40,000 years. A northerly position of the ACC during the last glacial led to higher productivities off Chile compared to the Holocene. At 33°S and south of it, productivity was boosted additionally through enhanced nutrient supply into the coastal regions, as a result of northward displacement of the Southern Westerly belt. During the Late Holocene, productivity increased in the study area due to a northward shift in the position of the zonal systems. In addition, an intensification of ENSO events occurred in the last 7000 years. These findings are so far consistent with the previous studies off central and south Chile (Lamy et al., 1998a; 1999; 2001; 2002; Marchant et al., 1999; Hebbeln et al., 2002).

North of 33°S, productivity was additionally controlled by upwelling intensity. Variations in the upwelling intensity are in turn a result of changing hemispheric thermal gradient and the intensity of the South Pacific extra-tropical anticyclone, and ENSO events. Paleoproductivity recorded in marine cores north of 33°S, however, seems to be unaffected by the Southern Westerlies throughout the last 40,000 years. These findings support a rather minor northward migration in line with an intensification of the zonal systems during the last glacial, as proposed by Ammann et al. (2001) and Grosjean et al. (2001).

The present-day distribution pattern of *G. inflata* off Chile seems to be controlled by nutrient availability without any latitudinal preferences. Higher abundances of this species closer to the coast, where productivity and upwelling intensity are highest, support this idea (manuscript 1). In addition, this species is most abundant during cold intervals (glacial periods) and high productivities off Chile (manuscripts 2 and 3, Hebbeln et al., 2002) and in the East Pacific (Le et al., 1995; Feldberg and Mix, 2003). Although not been described before, the temporal and spatial distribution patterns of *G. inflata* suggest this species to be an excellent productivity indicator (beside *N. pachyderma* and *G. bulloides*) in this part of the world ocean.

High spatial resolution of marine records off Chile is obligatory for a better understanding of oceanic and atmospheric dynamics mirrored in marine productivity, and for investigations of regional and global climate variations on glacial – interglacial, and on millennial – decadal time scales. Marine sediments off southern Chile reveal very high sedimentation rates (Mohtadi et al, unpublished data) and are therefore suitable for high-resolution paleoclimate studies. Furthermore, palynological studies on the same material could result in a better correlation of marine and terrestrial data sets, and help to establish a better dating of the continental records. Next to sediment core analyses, more sediment trap and plankton tow studies are needed, especially between 36°S and 39°S where no planktic foraminiferal data from surface sediments exist, to understand the present-day variations and dynamics of marine plankton in this part of the world ocean.

References

- Ammann, C., Jenny, B., Kammer, K. and Messerli, B., 2001. Late Quaternary Glacier response to humidity changes in the arid Andes of Chile (18-29°S). *Palaeogeography, Palaeoclimatology, Palaeoecology*, 172: 313-326.
- Feldberg, M.J. and Mix, A.C., 2003. Planktonic foraminifera, sea surface temperatures, and mechanisms of oceanic change in the Peru and south equatorial currents, 0-150 ka BP. *Paleoceanography*, 18(1): 1016, doi: 10.1029/2001PA000740.
- Grosjean, M., van Leeuwen, J.F.N., van der Knaap, W.O., Geyh, M.A., Ammann, B., Tanner, W., Messerli, B., Nunez, L.A., Valero-Garces, B.L. and Veit, H., 2001. A 22,000 ¹⁴C year BP sediment and pollen record of climate change from Laguna Miscanti (23°S), northern Chile. *Global and Planetary Change*, 28(1-4): 35-51.
- Hebbeln, D., Marchant, M. and Wefer, G., 2002. Paleoproductivity in the southern Peru-Chile Current through the last 33000 yr. *Marine Geology*, 186(3-4): 487-504.
- Kim, J., Schneider, R.R., Hebbeln, D., Müller, P.J. and Wefer, G., 2002. Last deglacial sea-surface temperature evolution in the southeast Pacific compared to climate changes on the South American continent. *Quaternary Science Reviews*, 21: 2085-2097.
- Klump, J., Hebbeln, D. and Wefer, G., 2001. High concentrations of biogenic barium in Pacific sediments after Termination I - A signal of changes in productivity and deep water chemistry. *Marine Geology*, 177: 1-11.
- Lamy, F., Hebbeln, D. and Wefer, G., 1998a. Late Quaternary precessional cycles of terrigenous sediment input off the Norte Chico, Chile (27.5°S) and paleoclimatic implications. *Palaeogeography, Palaeoclimatology, Palaeoecology*, 141(3-4): 233-251.
- Lamy, F., Hebbeln, D. and Wefer, G., 1999. High resolution marine record of climatic change in mid-latitude Chile during the last 28,000 years based on terrigenous sediment parameters. *Quaternary Research*, 51: 83-93.
- Lamy, F., Hebbeln, D., Rohl, U. and Wefer, G., 2001. Holocene rainfall variability in southern Chile: a marine record of latitudinal shifts of the Southern Westerlies. *Earth and Planetary Science Letters*, 185(3-4): 369-382.
- Lamy, F., Rühlemann, C., Hebbeln, D. and Wefer, G., 2002. High- and low-latitude climate control on the position of the southern Peru-Chile Current during the Holocene. *Paleoceanography*, 17(2): 1028, doi:10.1029/2001PA000727.
- Le, J., Mix, A.C. and Shackleton, N.J., 1995. Late Quaternary paleoceanography in the Eastern Equatorial Pacific Ocean from planktonic foraminifera: A high-resolution record from ODP Site 846. In: N.G. Pisias, L.A. Mayer, T.R. Janecek, A. Palmer-Jelson and T.H. van Andel (Editors), *Proceedings of the Ocean Drilling Program, Scientific Results*. Ocean Drilling Program, College Station, pp. 675-693.
- Marchant, M., Hebbeln, D. and Wefer, G., 1999. High resolution planktic foraminiferal record of the last 13,300 years from the upwelling area off Chile. *Marine Geology*, 161: 115-128.

Danksagung

Für die Vergabe der Arbeit und die beispielhafte Betreuung bei der Durchführung bedanke ich mich ganz herzlich bei Priv. Doz. Dr. Dierk Hebbeln. Prof. Dr. Gerhard Bohrmann danke ich für die Übernahme des Zweitgutachtens.

Für die wertvollen Diskussionen zu den Manuskripten und die vielfältige Unterstützung danke ich ganz besonders Dr. Oscar Romero. Meinem Zimmerkollegen Dr. Jan-Berend Stuut danke ich für die zahlreichen Ratschläge. Prof. Dr. Gerold Wefer danke ich für die Schaffung einer hervorragenden wissenschaftlichen Arbeitsbedingung und seine außergewöhnliche Hilfsbereitschaft.

Für die Unterstützung im Labor bedanke ich mich herzlich bei Dr. Monika Segl, Birgit Meyer-Schack, Christina Hayn, Volker Diekamp, Alexius Wülbers, Hella Buschoff und Marco Klann. Gisela Boelen und Carmen Murken danke ich für ihre zahlreiche und hervorragende administrative Hilfeleistungen.

Besonderen Dank gilt meinen Kolleginnen und Kollegen der Arbeitsgruppe „Allgemeine Geologie“ für die angenehme Arbeitsatmosphäre und den intensiven wissenschaftlichen Austausch. Ganz besonders Dr. Boris Dorschel, Peer Helmke, Holger Kuhlmann, Alexandra Jurkiw und Nicolas Nowald für die interessanten, nicht immer wissenschaftlichen Diskussionen am Mittagstisch seien gedankt.

Insbesondere möchte ich mich bei Prof. Dr. Carina Lange, Dr. Margarita Marchant und allen anderen Kolleginnen und Kollegen an der Universität Concepción für die ausgezeichnete Unterstützung und die wunderbare Zeit während meines Aufenthalts in Chile bedanken.

Nicht zuletzt möchte ich mich bei meiner Familie für die jahrelange Unterstützung ganz herzlich bedanken. Sie war und ist mir ein ganz großer Rückhalt.

Das Bundesministerium für Bildung und Forschung (BMBF) hat die vorliegende Arbeit im Rahmen des Projekts „*PUCK: Paläoumweltbedingungen am Chilenischen Kontinentalhang*“ finanziell gefördert.